Scheduling in Wireless Networks with Physical Interference Constraints

FU, Liqun

A Thesis Submitted in Partial Fulfilment
of the Requirements for the Degree of
Doctor of Philosophy
in
Information Engineering

The Chinese University of Hong Kong
August 2010

ProQuest LLC.
789 East Eisenhower Parkway
P.O. Box 1346
Ann Arbor, MI 48106 - 1346

Abstract of thesis entitled:

Scheduling in Wireless Networks with Physical Interference Constraints

Submitted by FU, Liqun

for the degree of Doctor of Philosophy

at The Chinese University of Hong Kong in August 2010

This thesis studies the wireless link scheduling problem under the *physical interference model*. Such problem is more realistic than the widely studied wireless scheduling problem under the *protocol interference model*. However, it is a challenging problem because the physical interference model considers the cumulative effect of the interference powers from all the other concurrent transmitters. This thesis covers the complexity analysis and algorithm design (both centralized and distributed) for such a challenging problem.

We first give a rigorous NP-completeness proof for the power-controlled scheduling with consecutive transmission constraint under the physical interference model. We then present a centralized scheduling algorithm based on a column generation method which finds the optimal schedules and transmit powers. We further consider an integer constraint that requires the number of time slots allocated to a link to be an integer. Building upon the column generation method, we propose a branch-and-price method which can find the optimal integer solution. By simplifying the pricing problem and designing a new branching rule, we significantly improve the efficiency of both the column generation and the branch-and-price methods. For example, the av-

erage runtime is reduced by 99.86% in 18-link networks compared with the traditional column generation method.

Due to the inherent complexity of the power-controlled scheduling problem, finding optimal schedules and power allocations for large-size networks will still consume extraordinary large amounts of time despite the performance of our method. We therefore propose an approximation algorithm, called the Guaranteed and Greedy Scheduling (GGS), which can find near optimal solutions within a short runtime. GGS is a polynomial time algorithm with a provable upper bound for the approximation ratio relative to the optimal solution.

For the distributed scheduling algorithm design, we focus on the CSMA (Carrier-Sense Multiple-Access) network, which is the most widely used distributed wireless network in practice. We establish a rigorous conceptual framework, upon which effective solutions to interference-safe transmissions can be constructed under the physical interference model. Specifically, we propose to use the concept of "safe carrier sensing range", which guarantees interference-safe transmissions under the physical interference model. We further propose a novel carrier-sensing mechanism, called Incremental-Power Carrier-Sensing (IPCS), which implements the safe carrier-sensing range concept in a simple way. Extensive simulation results show that IPCS can boost spatial reuse and network throughput by more than 60% relative to the conventional carrier-sensing mechanism.

論文題目： 物理干擾模型下的無線鏈路調度

作者 ： 付立群

學校 ： 香港中文大學

學系 ： 信息工程學系

修讀學位： 哲學博士

摘要 ：

本論文研究了物理干擾模型下的鏈路調度問題。這類問題比廣泛研究的協議干擾模型下的鏈路調度問題更具實際意義。但是，這是一個富有挑戰的問題，因為物理干擾模型考慮了來自所有其它同時工作的發射機的干擾功率的累積效應。本文對這個富有挑戰的問題進行了複雜性分析和算法設計（包括集中式和分佈式兩類算法）。

首先， 我們對物理干擾模型下帶有連續傳輸約束的功率控制調度問題進行了嚴格的 NP 完全性（NP-completeness）證明。然後我們提出了一種基於列生成（column generation）方法的集中式調度算法，利用該方法可以找到最優的調度方案以及發射功率。進一步，我們考慮了整數約束，即分配給一個鏈路的時隙數目必須是一個整數。針對該問題，我們在列生成的方法基礎上提出了一種分支-定價（branch-and-price）算法，該算法可以找到最優整數解。之後，我們通過簡化定價問題并設計一種新的分支方法，大大提高了列生成算法和分支-定價算法的運行效率。舉例說明，在一個由 18 條鏈路組成的網絡中，跟傳統的列生成算法相比，上述算法的平均運行時間縮短了 99.86%。

然而，儘管我們的算法跟傳統算法相比效率已經有了大幅度的提高，但是由於功率控制調度問題固有的高複雜度，對於大規模網絡而言，找到最優的調度和功率分配方案仍然需要花費異常多的時間。因此我們提出一種稱為保證和貪婪調度（GGS：Guaranteed and Greedy）的近似算法，該算法可以在短時間內找到次優解。GGS 算法是一種多項式時間算法，並且可以證明，通過該算法獲得的次優解與最優解的偏離程度，即最壞性能比，有常數上界。

另一方面，對於分佈式調度算法的設計，我們主要針對 CSMA（Carrier-Sense Multiple）網絡進行研究，因為該網絡是在實際中應用最廣泛的分佈式無線網絡。我們建立了一個嚴謹的概念架構，并基於此架構提出了物理干擾模型下有效的無干擾傳輸解決方案。具體來說，我們首先提出了“安全載波偵聽範圍”的概念，採用此“安全載波偵聽範圍”的 CSMA 網絡可以保證物理干擾模型下的無干擾傳輸。進一步，我們提出了一種新穎的功率增量載波偵聽（IPCS：Incremental-Power Carrier-Sensing）機制，該機制用一種簡單的方式實現了“安全載波偵聽範圍”的概念，因此可以在 CSMA 網絡中實現物理干擾模型下的無干擾傳輸。最後，我們進行了大量的仿真實驗，仿真結果表明 IPCS 機制相對於傳統的載波偵聽機制可以使空間複用率和網絡吞吐量提高超過 60%。

Acknowledgements

The last four years as a Ph.D student have been an unforgotten experience in my life. Looking back now, I am glad that I made the decision of taking the Ph.D program four years ago.

Many people contribute to this thesis. I thank them all. First and foremost, I would like to thank my supervisor, Professor Soung Chang Liew. He is really patient in advising students so that they can finally develop and improve themselves. He taught me to continually look for the big picture and let curiosity guide in doing research. I would also like to thank my co-supervisor, Professor Jianwei Huang. He is an enthusiastic person and always encourages me to give a try on the targets that I thought were impossible till I achieved them. Professor Liew and Professor Huang are really hands-on supervisors so that I am not alone during the long journey of research in my Ph.D study.

I would also like to thank Professor Ying Jun (Angela) Zhang and Professor Wing Shing Wong. The technical discussions with them made me get a deeper understanding of wireless communications. I would also like to thank my lab members in CUHK, Dr. Patrick P. Lam, Dr. Shengli Zhang, Dr. Hongning Dai, Dr. Fen Hou, Dr. Junhua Zhu, Caihong Kai, Jialiang Zhang, An (Jack) Chan, Lu Lu, Yuanyuan Cui, Shuqin (Helen) Li, Janice Law, Lingjie Duan, Kam Wong (Scotty) Leung, Kwan Fong (Erica) Leung, Guosen Feng, and Xu Chen, for all the great time that we spent together.

I also want to thank Professor Mung Chiang, for hosting and advising me during the pleasant and productive visit in Princeton University. I also want to thank Dr. Hongseok Kim, Ioannis Kamitsos, Tian Lan, and Wenjie Jiang, for many discussions and having a good time together in Princeton.

Last but not least, I am grateful to my husband, Wei Xie, and my parents, Guangwu Fu and Cuie Wang, for their love and unconditional support. They are always there for me. I would not have been where I am now without their encouragement and understanding.

Dedicated to my dear husband and parents, for your love and support!

Contents

List of Figures

List of Tables

Chapter 1

Introduction

1.1 Motivation and Overview

Wireless networks have found important applications in many facets of life. The cellular networks are so popular that almost everybody in the cities around the world subscribes to cell phone service [1]. The wireless local area networks (WLANs) have also enjoyed great popularity - many companies and homes are connected to the Internet via WLANs [2]. The wireless ad hoc networks, although not as widely deployed as the first two types of networks yet, have many potential applications, such as emergency/rescue operations, disaster relief efforts, and military communications [3, 4].

As wireless network deployments grow, we are witnessing an increasing level of mutual interference among the wireless links operating on the same channel, due to the broadcast nature of wireless signals. To avoid detrimental interference, an effective solution is to perform proper *link scheduling*. For wireless links that are near each other and thus mutually interfere, we can schedule their transmissions in different time slots to ensure successful transmissions; for wireless links that are far apart and thus do not mutually

interfere, we can schedule their transmissions into the same time slot to increase network throughput. In short, the issue is how to increase spatial reuse while avoiding mutual interferences.

The "interference model" that attempts to capture how wireless links interfere with each other is crucial to the study of scheduling. In the literature, most studies on wireless scheduling are based on the *protocol interference model* or its variations [5–35]. In the protocol interference model, the interference range of a receiver is assumed to be limited, and any other transmitter beyond that range does not interfere with the receiver. However, the protocol interference model over-simplifies the physical properties of wireless signals since it does not model the cumulative effect of the interference powers from multiple transmitters. As a result, the analytical results and the scheduling algorithms building upon the protocol interference model may be overly optimistic and may not work in practice [36–39].

This thesis focuses on the wireless scheduling problem under a more realistic interference model, called the *physical interference model* [40]. Under the physical interference model, a receiver decodes its signal successfully if the signal-to-interference-plus-noise ratio (SINR) at the receiver is above a certain threshold. Here, the interference is the sum of the powers it receives from all the concurrent transmitters other than its own. While the physical interference model is more realistic than the protocol interference model in terms of modeling interference, the analysis and the scheduling algorithm design are considerably more challenging under the physical interference model.

This thesis analyzes the complexity of the wireless scheduling problems under the physical interference model. In addition, it investigates centralized as well as distributed scheduling algorithm designs under the physical interference model.

For the centralized scheduling, we focus on joint power control and scheduling in a Spatial-reuse Time Division Multiple Access (STDMA) system. STDMA scheduling assigns each link a set of time slots within a frame to meet its traffic demand. For the links that are scheduled to transmit simultaneously, the SINR requirements at all receivers involved should be satisfied. The system objective is to minimize the frame length such that the traffic demands of all links are satisfied. We find that the wireless scheduling problems under the physical interference model typically have high complexity. If we want to guarantee solution optimality, the column generation and the branch-and-price methods proposed in this thesis are much more efficient than the state-of-the-art algorithms in the literature. For modest-size networks (e.g., less than 30 links), the column generation and the branch-and-price methods are computationally efficient. However, for large-size networks, finding the optimal scheduling solution is very time-consuming. Fortunately, the column generation and branch-and-price algorithms can be modified to serve as fast heuristic algorithms that provide approximate solutions. We also propose a polynomial time heuristic algorithm, called the Guaranteed and Greedy Scheduling (GGS) algorithm, for the joint power control and scheduling problem. We find that these heuristic algorithms have a short execution time with reasonably good solutions. For example, the GGS algorithm has a provable bounded approximation ratio relative to the optimal scheduling algorithm, and the average cost penalties of the column generation and branch-and-price based heuristic algorithms are small (i.e., below 10%) for networks tested in our simulations.

For distributed scheduling, we move to CSMA (Carrier-Sense Multiple-Access) networks. Specifically, we propose to use the concept of "safe carrier-sensing range" for the analysis and operation of CSMA networks in an

interference-safe manner (also called hidden-node free design) under the physical interference model. With this concept, we can then study how much spatial reuse is possible in CSMA networks, and how to set the carrier-sensing range to optimize spatial reuse while ensuring interference-safe operation (also called hidden-node free design [32]). Importantly, we find that the carrier-sensing range determined using the protocol interference model does not guarantee interference-safe operation under realistic cumulative interferences. We derive a tight safe carrier-sensing range that will guarantee the transmissions are interference-safe under the physical interference model. The concept of a safe carrier-sensing range, although is amenable to elegant analytical results, is inherently not compatible with the conventional power-threshold carrier-sensing mechanism currently used in IEEE 802.11 standard. We propose a simple carrier-sensing mechanism, called Incremental-Power Carrier-Sensing (IPCS), which fills this gap. Our extensive simulation results indicate that IPCS can boost spatial reuse and network throughput by more than 60% relative to the conventional carrier-sensing mechanism.

On the big picture, this thesis provides a better understanding of the scheduling problem under the broadcast wireless medium. The scheduling problem with the simple objective of minimizing the frame length is already NP-complete if we insist on finding the optimal solution. Although by exploiting the special structure of our problem, we manage to improve the speed for finding the optimal solution by several order of magnitude, for large network, finding the optimal solution still takes an extraordinarily long time. Another finding in this thesis is that the heuristic algorithms work well in practice. The proposed heuristic algorithms can find close to optimal solutions in very short runtime. Therefore, we find that doing a perfect job is difficult, but doing a good job is achievable.

This thesis also gives some guidelines to the design of practical CSMA wireless systems. For example, it gives the carrier-sensing power threshold setting to prevent hidden-node collisions in wireless networks. Furthermore, our IPCS mechanism is a better carrier sensing mechanism in that it improves network throughput and spatial reuse significantly.

1.2 Thesis Outline

This thesis is organized in six chapters. In Chapter 2, we analyze the complexity of the scheduling problem under the physical interference model. Specifically, we present the first NP-completeness proof of the joint power control and scheduling problem with consecutive transmission constraint.

In Chapter 3, we propose the column generation and branch-and-price centralized scheduling algorithms that can find the optimal solutions for the joint power control and scheduling problem. We further suggest efficient heuristic algorithms based on the structure of the optimal algorithms.

In Chapter 4, we propose the centralized scheduling algorithm for the power-controlled scheduling problem with consecutive transmission constraint, in which the time slots allocated to a link must be consecutive within a TDMA frame. The polynomial time algorithm we proposed is called the Guaranteed and Greedy Scheduling (GGS) algorithm.

In Chapter 5, we present the framework of interference-safe transmissions in CSMA networks under the physical interference model. We first derive a tight safe carrier-sensing range that will guarantee the transmissions are interference-safe under the physical interference model. We then present the Incremental-Power Carrier-Sensing (IPCS) mechanism, which can implement the safe carrier-sensing range in a simple way. We also demonstrate the

benefits of the IPCS mechanism as compared to the carrier sensing mechanism used in the current 802.11 protocol through extensive simulations.

Finally, we conclude the thesis in Chapter 6 with an outlook of some future work.

Chapter 2

Complexity Analysis

2.1 Introduction

In this chapter, we focus on the complexity study of the scheduling problem under the physical interference model. In the literature, there have been various NP-completeness proofs for the scheduling problems under the protocol interference model (e.g., [6–12]). Since the interferences among links are pairwise relationships (i.e., a link can either interfere with another link or not), the interference relations can be represented by graphs (e.g., [12]). Graph theory is a powerful tool in these NP-completeness proofs. The proofs typically involve reducing the vertex-cover problem or the clique problem that are known to be NP-complete in graph theory [6] to the corresponding wireless scheduling problems. The pairwise relation of the protocol interference model is essential for graph theory to be applicable.

The physical interference model, on the other hand, requires each link to calculate the cumulative interferences from all the other transmitters. Graph based techniques are no longer valid. There are only a few papers that studied the complexity of the scheduling problems under the physical interference

model (e.g., [41,42]). In [42], the minimum-frame-length scheduling problem under the physical interference model but *without* power control was proven to be NP-complete. Assuming equal transmission power for all links, [42] showed that the cumulative interferences to each link can be calculated, and the Partition Problem (which is known to be NP-complete) can be reduced to the scheduling problem. However, [42] does not consider power control.

The complexity study of the wireless scheduling problems become more complicated when power control is considered. Since we have the freedom to choose the transmit power of each transmitter, determining whether a set of links can be active simultaneously is not trivial [43]. The complexity of joint power control and minimum-frame-length scheduling under the physical interference model but *without* consecutive transmission constraints has been examined in [41]. The authors in [41] introduced a problem called "MAX-SIR-MATCHING", and showed that *if* this problem is NP-hard, then computing the minimum frame length is also NP-hard. However, no proof is given about the NP-hardness of "MAX-SIR-MATCHING". Thus, the complexity issue has not been fully addressed.

In this chapter, we present the NP-completeness proof for the power controlled scheduling problem *with* consecutive transmission constraint. The requirement of consecutive transmission is motivated by several practical considerations. First, in an STDMA frame, each time slot must include a guard time period which corresponds to the maximum differential propagation delay between pairs of nodes in the network. The overhead introduced by the guard time periods can be significant for a network with large propagation delays. In consecutive scheduling, the guard time periods of all time slots allocated to the same link (other than the first guard time period) can be used for data transmissions. Second, it is possible to compress the header

information of consecutive slots when they belong to the same traffic source. That is, one header is all that is needed for the transmission in consecutive time slots. Third, significant energy is spent by wireless nodes in switching between transmission and reception modes [44]. Consecutive scheduling can improve energy efficiency, a crucial consideration in wireless sensor networks. Fourth, and perhaps the most important practical consideration, is that in the emerging IEEE 802.16 family of standards [45], only consecutive scheduling is supported. To the best of our knowledge, this is the first NP-completeness proof for the power controlled scheduling problem with consecutive transmission constraint.

In section 2.2, we define the network and the physical interference model and formulate the Joint Power control and Scheduling problem with Consecutive transmission Constraints (JPS-CC). The complexity analysis is presented in section 2.3. A summary of this chapter is given in section 2.4.

2.2 System Model

2.2.1 Network and Physical Interference Model

A wireless network is represented by a set of directed links $\mathcal{L} = \{l_i, 1 \leq i \leq |\mathcal{L}|\}$ with positive traffic demands on all links. Let $\mathcal{T} = \{T_i, 1 \leq i \leq |\mathcal{L}|\}$ and $\mathcal{R} = \{R_i, 1 \leq i \leq |\mathcal{L}|\}$ denote the set of transmitting nodes and the set of receiving nodes, respectively. In a general wireless network, set $\mathcal{T}$ and set $\mathcal{R}$ may have nodes in common. We can use an $|\mathcal{L}| \times |\mathcal{L}|$ incidence matrix $\mathbf{C}$ to denote whether two links $l_i, l_j \in \mathcal{L}$ share a common node or not, where the

element c_{ij} of $\mathbf{C}$ is

$$c_{ij} = \begin{cases} 1, & \text{if } i \neq j \text{ and nodes } T_i, R_i, T_j, R_j \\ & \text{have at least one node in common,} \\ 0, & \text{otherwise.} \end{cases} \tag{2.1}$$

We assume a simple transceiver structure satisfying the following primary constraints:

Definition 1 (Primary constraints) *A node can not transmit and receive simultaneously. A node is not allowed to transmit to or receive from more than one node simultaneously.*

A set of transmission links satisfying the primary constraints is a matching, defined as follows:

Definition 2 (Matching) *A matching $\mathcal{M} \subset \mathcal{L}$ is a subset of the link set $\mathcal{L}$ such that no two links in $\mathcal{M}$ share the same node, i.e., if links $l_i, l_j \in \mathcal{M}$, then $c_{ij} = 0$.*

Let $\mathcal{T}_\mathcal{M}$ and $\mathcal{R}_\mathcal{M}$ denote the sets of transmitting nodes and receiving nodes of the links in $\mathcal{M}$, respectively. Sets $\mathcal{T}_\mathcal{M}$ and $\mathcal{R}_\mathcal{M}$ are disjoint according to the definition of matching.

Definition 3 (Sub-matching) *A sub-matching of a matching $\mathcal{M}$ is a subset of $\mathcal{M}$.*

Besides the primary constraints, links that are simultaneously active must satisfy the SINR constraints at each receiving node. A matching which satisfies the SINR constraints is called a feasible matching, defined as follows:

Definition 4 (Feasible matching) *A matching $\mathcal{M}$ is feasible if there exists a positive power vector $\mathbf{p} = (p_i : \forall i \text{ s.t. } l_i \in \mathcal{M})^T$ such that the SINR constraints at the receivers are satisfied, i.e.,*

$$\frac{p_i G(T_i, R_i)}{\eta_i + \sum_{l_j \in \mathcal{M}, j \neq i} p_j G(T_j, R_i)} \geq \gamma_0, \quad \forall l_i \in \mathcal{M}, \tag{2.2}$$

where p_i is the transmit power of T_i, η_i is the average noise power at R_i, and $G(T_j, R_i)$ is the channel gain from T_j to R_i. The SINR threshold value γ_0 is assumed to be common among all links.

We assume that radio signal propagation follows the log-distance path model with path loss exponent α.The channel gain $G(T_i, R_j)$ from transmitter T_i to receiver R_j is:

$$G(T_i, R_j) = G(d_0) \cdot \left(\frac{d(T_i, R_j)}{d_0} \right)^{-\alpha},$$

where $d(T_i, R_j)$ is the Euclidean distance between nodes T_i and R_j, and $G(d_0)$ is the reference channel gain at the reference distance d_0 [46]. Without loss of generality, we assume $d_0 = 1m$ and use G_0 to denote the reference channel gain at $d_0 = 1m$. So the channel gain $G(T_i, R_j)$ is

$$G(T_i, R_j) = G_0 \cdot d(T_i, R_j)^{-\alpha}.$$

The log-distance path model has been used extensively in the literature (e.g., [42, 47, 48]). We assume the common situation where $\alpha > 2$ [40].

Consider a matching $\mathcal{M} \subseteq \mathcal{L}$, we define an $|\mathcal{M}| \times |\mathcal{M}|$ nonnegative relative-channel-gain matrix $\mathbf{B}_{\mathcal{M}}$ with entries as follows:

$$b_{ij} = \begin{cases} 0, & \text{if } i = j, \\ \frac{G(T_j, R_i)}{G(T_i, R_i)}, & \text{if } i \neq j. \end{cases} \tag{2.3}$$

and let $\rho(\mathbf{B}_{\mathcal{M}})$ denote the largest real eigenvalue of $\mathbf{B}_{\mathcal{M}}$ (also called Perron-Frobenius eigenvalue or spectral radius). Note that all the elements on the main diagonal of $\mathbf{B}_{\mathcal{M}}$ are 0, and all the other elements are positive. Thus, $\mathbf{B}_{\mathcal{M}}$ is an irreducible non-negative matrix [49,50]. By Perron-Frobenius theorem [50], $\rho(\mathbf{B}_{\mathcal{M}})$ is positive and the corresponding eigenvector is positive componentwise. Ref. [49,51] provided the necessary and sufficient condition for a matching to be feasible in the noiseless case, and Ref. [43] extended the results in [49,51] to the case of non-zero noise. Given a matching is feasible, Ref. [52] further provided the component-wise minimum power solution of each transmitter. Proposition 1 is a compilation of the propositions given in [43,49,51,52].

Proposition 1 *A necessary and sufficient condition for the matching to be feasible is*

$$\rho\left(\mathbf{B}_{\mathcal{M}}\right) < \frac{1}{\gamma_0}. \tag{2.4}$$

The minimum power vector $\mathbf{p}$ *which achieves an SINR of* γ_0 *at all receivers is given by*

$$\mathbf{p} = \left(\mathbf{I} - \gamma_0 \mathbf{B}_{\mathcal{M}}\right)^{-1} \mathbf{v}_{\mathcal{M}}, \tag{2.5}$$

where $\mathbf{I}$ *is the* $|\mathcal{M}| \times |\mathcal{M}|$ *identity matrix, and vector* $\mathbf{v}_{\mathcal{M}} = \left(\frac{\gamma_0 \eta_i}{G(T_i, R_i)} : \forall i \text{ s.t. } l_i \in \mathcal{M}\right)^T$ *is the average noise power vector normalized by the link gain and the SINR requirement.*

Condition (2.4) provides a way to check the feasibility of a matching. If condition (2.4) is satisfied, the minimum transmit power vector can be set according to (2.5); otherwise, no matter how we tune the transmit powers, the links in the matching can not be active simultaneously.

Proposition 2 (*[43]*) *Any sub-matching of a feasible matching is also feasible.*

Definition 5 (Maximal feasible matching) *A feasible matching is maximal if it is not a strict subset of any other feasible matching.*

The proposition below provides bounds on the Perron-Frobenius eigenvalue of a non-negative matrix [50]:

Proposition 3 (*[50]*) *Let* $\mathbf{B}$ *be an* $n \times n$ *non-negative matrix. The elements of matrix* $\mathbf{B}$ *are denoted by* b_{ij}*, where* i *is the row index and* j *is the column index. Then*

$$\min_{1 \le i \le n} \sum_{j=1}^{n} b_{ij} \le \rho(\mathbf{B}) \le \max_{1 \le i \le n} \sum_{j=1}^{n} b_{ij}$$

and

$$\min_{1 \le j \le n} \sum_{i=1}^{n} b_{ij} \le \rho(\mathbf{B}) \le \max_{1 \le j \le n} \sum_{i=1}^{n} b_{ij}.$$

2.2.2 Problem Statement

Consider the wireless link set $\mathcal{L} = \{l_i, 1 \le i \le |\mathcal{L}|\}$. We assume that the network topology is given and there is only one common channel in the network. Time is divided into time slots of equal length. Denote the traffic demands of the links by $\mathbf{f} = \{f_i, 1 \le i \le |\mathcal{L}|\}$, where f_i is the number of time slots to be assigned to link l_i in each frame. We assume that when a node starts to transmit in a frame, it sends all its traffic in consecutive time slots. This is referred to as the "consecutive transmission constraints". Our objective is to find a frame with minimum length.

Let $\mathcal{S}(t)$ denote the set of links which are scheduled in time slot t. The transmit powers of the links in $\mathcal{S}(t)$ are represented by vector $\mathbf{p}(t) = (p_i(t) : \forall i \ s.t. \ l_i \in \mathcal{S}(t))^{\dagger}$, where $p_i(t)$ is the transmit power of link i in time

†Link set $\mathcal{S}(t)$ is a subset of $\mathcal{L}$ We specify that the order in vector $\mathbf{p}(t)$ is in an increasing order of i.

slot t. A schedule of length V can be represented by the set of power vectors $\mathcal{SCH} = \{\mathbf{p}(t), 1 \leq t \leq V\}$.

Problem (JPS-CC): The Joint Power control and Scheduling problem with Consecutive transmission Constraints (JPS-CC) under the physical interference model is to find a schedule $\mathcal{SCH}$ of minimum length V such that (i) the set of active links in each time slot is a feasible matching, (ii) the traffic demand of each link is satisfied in consecutive slots.

The key notations of this thesis are listed in Table 2.1. We use lowercase boldface symbols, e.g., $\mathbf{p}$, to denote vectors, with p_i denoting the ith component. We use uppercase boldface symbols, e.g., $\mathbf{Q}$, to denote matrices, with q_{ij} denoting the (i,j)th component and Q_j denoting the jth column. We use calligraphic symbols, e.g., $\mathcal{L}$, to denote sets. The vector inequalities denoted by $\succeq$ and $\preceq$ are component-wise inequalities.

2.3 Complexity Analysis

In this section, we prove that the JPS-CC problem is NP-complete. We first show that the JPS-CC problem belongs to the class NP. Then we show that a known NP-complete problem, the Partition Problem, can be reduced to the JPS-CC problem in polynomial time.

We note that NP-completeness applies not to optimization problems, but to decision problems to which the answer is either "yes" or "no". There is a convenient conversion between optimization problems and decision problems [53]. The decision problem corresponding to the JPS-CC problem is defined as follows:

Definition 6 (Decision Problem of JPS-CC) *Given a wireless network with a set $\mathcal{L} = \{l_i, 1 \leq i \leq |\mathcal{L}|\}$ of directed link, the relative channel gain*

Table 2.1: Key Notations

Notation	Physical Meaning
$\mathcal{L}$	the set of all links
$\mathcal{M}$	matching (Definition 2)
$\mathcal{T}$	the set of transmitters
$\mathcal{R}$	the set of receivers
$G(T_i, R_j)$	the channel gain between nodes T_i and R_j
G_0	the channel gain at the reference distance $d_0 = 1m$
$d(T_i, R_j)$	the Euclidean distance between nodes T_i and R_j
η_i	the average noise power at receiver R_i
$v_i = \gamma_0 \eta_i / G(T_i, R_i)$	the normalized noise power of link l_i
α	the path loss exponent
$\mathbf{B}$	relative channel gain matrix
$\rho(\mathbf{B})$	the Perron-Frobenius eigenvalue of matrix $\mathbf{B}$
$\mathbf{f}$	traffic demand vector of the links in set $\mathcal{L}$
U	fixed frame length
V	the airtime length to satisfy the traffic demands
$\mathcal{S}(t)$	the set of links scheduled in time slot t
$\mathbf{p}(t)$	transmit power vector in time slot t
$\mathbf{D}(\cdot)$	diagonal matrix operator

matrix, the traffic demands $\mathbf{f}$*, and an integer* V^**, whether there exists an STDMA schedule* $\mathcal{SCH}$ *consisting of at most* V^* *time slots such that (i) the set of active links in each time slot is a feasible matching, (ii) the traffic demand of each link is satisfied in consecutive slots.*

Lemma 1 *The JPS-CC is in the complexity class NP.*

Proof: To show that the JPS-CC is in NP, we show that a solution to an instance of the JPS-CC problem can be verified in polynomial time. Consider an instance of the JPS-CC problem. a wireless network with directed link set $\mathcal{L} = \{l_i, 1 \leq i \leq |\mathcal{L}|\}$, the relative channel gain matrix and the traffic demands $\mathbf{f}$. Suppose we are given a schedule $\mathcal{SCH} = \{\mathbf{p}(t), 1 \leq t \leq V\}$. To verify if the schedule is a solution to the decision problem of JPS-CC, we need to check (i) whether V is less than or equal to V^*; (ii) for each link l_i, $1 \leq i \leq |\mathcal{L}|$, whether it is assigned no less than f_i consecutive time slots; and (iii) in each time slot $t, 1 \leq t \leq V$, whether the set of active links form a feasible matching. Verifying (i) and (ii) requires one operation and $O(|\mathcal{L}|)$ operations, respectively. Verifying (iii) requires $O(|\mathcal{L}|^2)$ operations because of the computation of SINR. The whole verification can be performed in $O(|\mathcal{L}|^2)$ time. Thus a solution to an instance of the JPS-CC problem can be verified in polynomial time. □

Next we need to show that a known NP-complete problem can be reduced to the JPS-CC problem. Here we choose the Partition Problem [53] which can be formulated as follows: given a set $\mathcal{A} = \{a_1, \cdots, a_n\}$ of n integers, is there a way to partition $\mathcal{A}$ into two disjoint subsets $\mathcal{A}_1$ and $\mathcal{A}_2$ such that the sum of the numbers in $\mathcal{A}_1$ equals the sum of the numbers in $\mathcal{A}_2$?

Proposition 4 *The Partition Problem can be reduced to the JPS-CC problem in polynomial time.*

Proof: To show that the Partition Problem can be reduced to the JPS-CC Problem in polynomial time, we need to reduce *any* instance in the Partition Problem to an instance in the JPS-CC Problem in polynomial time. When power control is considered, determining whether a set of links can be active simultaneously is equivalent to checking the Perron-Frobenius eigenvalue of the corresponding relative channel gain matrix. This is quite complicated for a general network.

The reduction begins with an instance of the Partition Problem consisting of a set of integers $\mathcal{A} = \{a_1, \cdots, a_n\}$. We will construct an instance of the JPS-CC Problem to which there is a feasible schedule if and only if the set $\mathcal{A}$ can be partitioned into two subsets of equal sum. The instance of the JPS-CC Problem is constructed as follows. The network consists of n directed links $\mathcal{L} = \{l_1, \cdots, l_n\}$. All the n links are of equal length D. With reference to Fig. 2.1, we place the transmitters and receivers of the n links on two concentric circles with center O, with the transmitters on the outer circle and the receivers on the inner circle. The radius of the inner circle r satisfies $r < (\frac{\sqrt[\alpha]{2}-1}{2})D$, where α is the path loss exponent. The radius of the outer circle is $r + D$. We arbitrarily draw n radial straight lines $\{g_1, \cdots, g_n\}$ from center O. The transmitter T_i of link l_i is placed at the intersect of line g_i with the outer circle; and the receiver R_i of link l_i is placed at the intersect of line g_i with the inner circle. The SINR threshold γ_0 is set to 1. The traffic demand on link l_i is set to a_i, the ith element in set $\mathcal{A}$. Let $S_{\mathcal{A}}$ denote the sum of the elements in set $\mathcal{A}$, $S_{\mathcal{A}} = \sum_{i=1}^{n} a_i$. We set $V^* = \lfloor \frac{S_{\mathcal{A}}}{2} \rfloor$. It is straightforward to perform such mapping from an instance in the Partition Problem to an instance in the JPS-CC Problem in polynomial time.

Link set $\mathcal{L}$ is a matching according to Definition 2. Given the SINR threshold $\gamma_0 = 1$, we can show that any two links in the link set $\mathcal{L}$ form

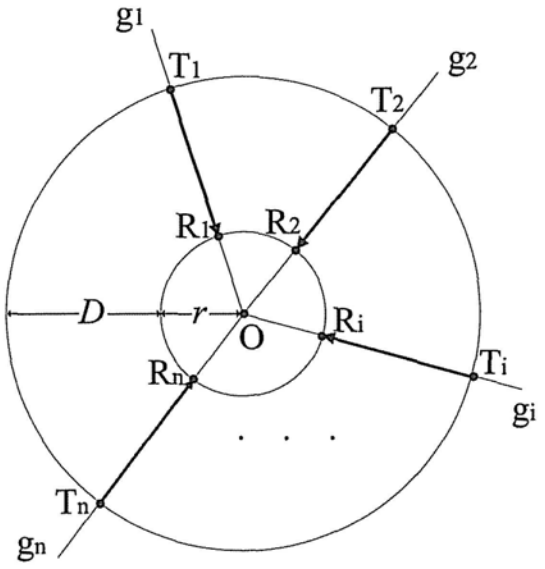

Figure 2.1: The topology of the JPS-CC problem in the reduction

a feasible sub-matching; however, any three links in the link set $\mathcal{L}$ can not form a feasible sub-matching. That is, for any two links in the link set $\mathcal{L}$, there exists positive power allocation such that these two links can be active simultaneously; but for any three links in the link set $\mathcal{L}$, no matter how we tune the transmit powers, the three links cannot be active simultaneously.

According to the topology setting shown in Figure 2.1, we can find that

$$D < d(T_i, R_j) \leqslant (D + 2r), \quad \forall i \neq j. \tag{2.6}$$

Since the radius of the inner circle r satisfies $r < (\frac{\sqrt[\alpha]{2}-1}{2})D$, we can find that

$$D < d(T_i, R_j) < \sqrt[\alpha]{2}D, \quad \forall i \neq j. \tag{2.7}$$

First, consider any two links l_i and l_j in the link set $\mathcal{L}$. The relative channel gain matrix of links l_i and l_j is:

$$\mathbf{B}_2 = \begin{pmatrix} 0 & \frac{d^{-\alpha}(T_j,R_i)}{D^{-\alpha}} \\ \frac{d^{-\alpha}(T_i,R_j)}{D^{-\alpha}} & 0 \end{pmatrix}$$

The Perron-Frobenius eigenvalue of matrix $\mathbf{B}_2$ can be calculated directly,

$$\rho(\mathbf{B}_2) = \sqrt{\frac{d(T_i, R_j)^{-\alpha} \cdot d(T_j, R_i)^{-\alpha}}{D^{-2\alpha}}}.$$

Because inequality (2.7) holds, we find that

$$\rho(\mathbf{B}_2) < 1.$$

So condition (2.4) is satisfied.

Next, consider any three links l_i, l_j and l_k in the link set $\mathcal{L}$. The relative channel gain matrix is

$$\mathbf{B}_3 = \begin{pmatrix} 0 & \frac{d^{-\alpha}(T_j,R_i)}{D^{-\alpha}} & \frac{d^{-\alpha}(T_k,R_i)}{D^{-\alpha}} \\ \frac{d^{-\alpha}(T_i,R_j)}{D^{-\alpha}} & 0 & \frac{d^{-\alpha}(T_k,R_j)}{D^{-\alpha}} \\ \frac{d^{-\alpha}(T_i,R_k)}{D^{-\alpha}} & \frac{d^{-\alpha}(T_j,R_k)}{D^{-\alpha}} & 0 \end{pmatrix}$$

Because inequality (2.7) holds, we can find that for any row, the row sum S_{row} satisfies the following inequality:

$$S_{row} = \frac{d^{-\alpha}(T_j, R_i) + d^{-\alpha}(T_k, R_i)}{D^{-\alpha}} \tag{2.8}$$

$$> \frac{(\sqrt[\alpha]{2}D)^{-\alpha} + (\sqrt[\alpha]{2}D)^{-\alpha}}{D^{-\alpha}} \tag{2.9}$$

$$= 1. \tag{2.10}$$

According to Proposition 3 we can find that

$$\rho(\mathbf{B}_3) \geq \min(S_{row}) > 1.$$

So for any three links in the link set $\mathcal{L}$, condition (2.4) can not be satisfied.

We now show that there exists a schedule which consists at most $V^* = \lfloor \frac{S_A}{2} \rfloor$ number of time slots to these n links $\mathcal{L} = \{l_1, \cdots, l_n\}$ if and only if the set $\mathcal{A} = \{a_1, \cdots, a_n\}$ can be partitioned into two subsets $\mathcal{A}_1$ and $\mathcal{A}_2$ of equal sum.

First, suppose that the set $\mathcal{A} = \{a_1, \cdots, a_n\}$ can be partitioned into two subsets $\mathcal{A}_1$ and $\mathcal{A}_2$ of equal sum. Because each element in $\mathcal{A}$ is an integer, we can easily find that $\lfloor \frac{S_A}{2} \rfloor = \frac{S_A}{2}$. We can form a schedule to the links in set $\mathcal{L} = \{l_1, \cdots, l_n\}$ as follows. Divide the links in set $\mathcal{L}$ into two subsets $\mathcal{L}_1$ and $\mathcal{L}_2$. Link subset $\mathcal{L}_1$ contains the links which have the traffic demands in the subset $\mathcal{A}_1$ and link subset $\mathcal{L}_2$ contains the links which have the traffic demands in the subset $\mathcal{A}_2$, respectively. The total traffic demands of the links in subset $\mathcal{L}_1$ are equal to the total traffic demands of the links in subset $\mathcal{L}_2$, which is $\frac{S_A}{2}$. The links belong to the same subset are activated one by one, which means the next link is activated until the previous link has sent all its packets. Since any two links in set $\mathcal{L}$ can be active simultaneously, we find that link subsets $\mathcal{L}_1$ and $\mathcal{L}_2$ can share the same time duration $\frac{S_A}{2}$. So

there exists a schedule to the link set $\mathcal{L} = \{l_1, \cdots, l_n\}$ which consists at most $V^* = \lfloor \frac{S_A}{2} \rfloor$ time slots such that the links which are active simultaneously form a feasible matching, and the traffic demands on each link in set $\mathcal{L}$ is satisfied in consecutive time slots.

Conversely, suppose that the links in set $\mathcal{L} = \{l_1, \cdots, l_n\}$ can be scheduled in at most $\lfloor \frac{S_A}{2} \rfloor$ time slots such that the links which are active simultaneously form a feasible matching, and the traffic demands on each link in set $\mathcal{L}$ is satisfied in consecutive time slots. Since at most two links in set $\mathcal{L}$ can be active simultaneously, the links in set $\mathcal{L}$ can not be scheduled in V time slots, where $V < \lfloor \frac{S_A}{2} \rfloor$. So the links in set $\mathcal{L}$ are scheduled exactly in $\lfloor \frac{S_A}{2} \rfloor$ time slots. So in each time slot, exactly two links are active and $\frac{S_A}{2} = \lfloor \frac{S_A}{2} \rfloor$. Because the traffic demands on each link in set $\mathcal{L}$ is satisfied in successive time slots, we can find that the links in set $\mathcal{L}$ can be partitioned into two subsets which has equal sum of the traffic demands. This means that the integers in set $\mathcal{A} = \{a_1, \cdots, a_n\}$ can be partitioned into two subsets of equal sum. □

Theorem 1 *The JPS-CC problem is NP-complete.*

Proof: The proof follows from Lemma 1 and Proposition 4. □

2.4 Summary

In this chapter, we present the NP-completeness proof of the power controlled scheduling *with* consecutive transmission constraint under the physical interference model. To our best knowledge, the complexity of the power controlled scheduling but without consecutive transmission constraint is still an open problem. Although the complexity study of the class of scheduling problems under the physical interference model is not complete, most researchers

believe that they have high complexity. In the following chapters, we will focus on the algorithm designs of the scheduling problems under the physical interference model which cover both centralized and distributed scheduling algorithms.

Chapter 3

Centralized Optimal Algorithm

3.1 Introduction

In this chapter, we propose a column generation based algorithm that finds the optimal schedules and transmit powers for the power controlled scheduling problem under the physical interference model. We consider the general power controlled scheduling problem in which the consecutive transmission constraint is not imposed. The system objective is to minimize the frame length such that the traffic demands of all links in the network are satisfied. The column generation method decomposes the original problem into a master problem and a pricing problem. In each iteration, the pricing problem finds a better set of simultaneously active links only if the objective function can be further improved. Furthermore, we consider the realistic case where the number of time slots allocated to a link should be an integer instead of any real number. Building upon the column generation method, we further propose a branch-and-price method that combines the column generation method with the branch-and-bound method to provide optimal integer solutions. We note that column generation has previously been considered in [54–56]. In

this work, we significantly improve the efficiency of both the column generation and the branch-and-price methods by exploiting the special structure of our problem. Our key contributions are as follows:

1. *Simplification of the Pricing Problem* : We integrate the Perron-Frobenius eigenvalue condition ([49, 57]) into the formulation of the pricing problem. This integration eliminates the continuous variables and also reduces the number of the constraints, and thus reduces the computational complexity of solving the pricing problem.

2. *Efficient Algorithm to Solve the Pricing Problem*: We propose a Smart Enumerating (SE) algorithm that solves the pricing problem to optimality. Instead of relegating the pricing problem to a general optimization solver, we design smart search policies that eliminate the infeasible solutions and the non-optimal solutions in an efficient way.

3. *New Branching Rule that Controls the Pricing Problem Size*: We develop a new branching rule in the branch-and-price method. Our new branching rule maintains the size of the pricing problem after each branching, and thus improves the overall efficiency of the branch-and-price method.

In recent works using column generation method (e.g., [54–56]) , the pricing problem is formulated as a Mixed Integer Programming problem that contains both continuous and integer variables. Due to its high complexity, most of the runtime of the column generation method is spent on solving the pricing problem to optimality. Our new pricing problem formulation, together with the SE algorithm, reduces the runtime spent on the pricing problem. As a result, the efficiency of the column generation method can be significantly improved. Take 18-link networks as an example. Simulations show that using our new pricing problem formulation and the proposed SE algorithm, it takes

only 2.031 seconds on average for the column generation method to find optimal solutions. However, using the column generation approach in [54–56], an average runtime of 1461.3 seconds is required. Our column generation method reduces the runtime by 99.86%.

For cases where reaching a close to optimal solution in a short time is more attractive than reaching the precise optimal solution, we propose a fast heuristic algorithm, Combined Sum Criterion Removal (CSCR), for the pricing problem. If we just use the CSCR algorithm to solve the pricing problem, this makes both the column generation and the branch-and-price methods fast heuristic algorithms. Simulations show that these heuristic algorithms outperform the ISPA (Integrated Scheduling and Power control Algorithm) proposed in [58], a state-of-the-art heuristic algorithm for this problem in the existing literature.

In section 3.2, we present the problem formulation. In section 3.3, we introduce the column generation method with emphasis on the new formulation of the pricing problem, and propose the Smart Enumerating (SE) algorithm to solve the pricing problem to optimality. In section 3.4, we introduce the branch-and-price method and propose the new branching rule. In section 3.5, we discuss the column generation and branch-and-price based heuristics. The simulation results are shown in section 3.6. A summary of this chapter is given in section 3.7.

3.2 Problem Formulation

We consider a time-slotted system with a fixed frame length U. Each link in set $\mathcal{L}$ has a fixed traffic demand in a frame, representing a fixed average rate requirement from the corresponding upper-layer applications. Each link

$l_i \in \mathcal{L}$ requires a throughput th_i. Let f_i denote the required active airtime of link l_i in a frame. The achievable data rate r_i per unit time of link l_i depends on the SINR threshold γ_i[†] at its receiver R_i. The relation between th_i and f_i is $th_i = r_i \frac{f_i}{U}$. Therefore, the throughput demand th_i is equal to the active airtime demand $f_i = \frac{th_i U}{r_i}$ in each frame.

Our focus is to minimize the length of airtime V needed to satisfy all the traffic demands in each frame, so that the maximum airtime $U - V$ can be left for other traffic (e.g., best-effort traffic). A minimum value of V greater than U indicates that the total traffic demands (and the corresponding average rate requirements) exceed the system capacity and can not be satisfied.

Now let us formulate the optimization problem formally. Let $\mathcal{E} = \{\mathcal{E}_k : 1 \leq k \leq |\mathcal{E}|\}$ denote the set of all the feasible matchings of link set $\mathcal{L}$. The transmit power vector of the feasible matching $\mathcal{E}_k$ is denoted by $\mathbf{p}_k$. We can also use an $|\mathcal{L}| \times |\mathcal{E}|$ incidence matrix $\mathbf{Q}$ to represent $\mathcal{E}$, where the element q_{ik} of $\mathbf{Q}$ is

$$q_{ik} = \begin{cases} 1, & \text{if link } l_i \text{ is in the feasible matching } \mathcal{E}_k, \\ 0, & \text{otherwise.} \end{cases} \tag{3.1}$$

We denote the kth column in $\mathbf{Q}$ by $Q_k, 1 \leq k \leq |\mathcal{E}|$, which represents a feasible matching $\mathcal{E}_k$.

Our objective is to minimize the airtime length V required. If the incidence matrix $\mathbf{Q}$ and all the associated transmit power vectors can be obtained a priori, the joint power control and minimum-airtime scheduling problem can

[†]In this chapter, the SINR requirements of links in $\mathcal{L}$ can be different. γ_i is the link-dependent threshold depending on various considerations such as the desired bit error rate and the modulation schemes.

be formulated as follows:

$$\begin{aligned} \text{minimize} \quad & V = \mathbf{e}^T \mathbf{u} \\ \text{subject to} \quad & \mathbf{Q}\mathbf{u} \succeq \mathbf{f}, \\ \text{variables} \quad & \mathbf{u} \succeq 0, \end{aligned} \tag{P1}$$

where $\mathbf{e}$ is the $|\mathcal{E}| \times 1$ all-one vector and $\mathbf{f} = (f_1, f_2, \cdots, f_{|\mathcal{L}|})^T$. The variables $\mathbf{u} = (u_k : 1 \leq k \leq |\mathcal{E}|)^T$ indicate the chosen feasible matchings to be scheduled in the frame. In particular, each variable u_k denotes the airtime allocated to the feasible matching $\mathcal{E}_k$ in the frame.

Problem (P1) is a Linear Program (LP). In a real wireless system, a slot is the smallest time unit in the time allocation process. Thus, the joint power control and scheduling problem should be formulated with additional integer constraints on the variables $\mathbf{u} = (u_k : 1 \leq k \leq |\mathcal{E}|)^T$. We denote (P1) with integer constraints on $\mathbf{u}$ by $(\text{P1})_{\text{INT}}$, which is an Integer Linear Program (ILP).

There are two difficulties in (P1) and $(\text{P1})_{\text{INT}}$. First, there is no known polynomial-time algorithm for finding all the feasible matchings and the corresponding transmit power vectors. Thus, completely characterizing the coefficient matrix $\mathbf{Q}$ in advance is difficult. Second, even if all the feasible matchings could be found, the size of the set $\mathcal{E}$ can be huge and in general increases exponentially with the number of links [41]. This means that (P1) and $(\text{P1})_{\text{INT}}$ can be too large to be tackled directly. We circumvent these difficulties using iterative methods that generate feasible matchings on-the-fly rather than a priori. Specifically, we propose a column generation method to solve (P1). Building upon it, we use a branch-and-price method to solve $(\text{P1})_{\text{INT}}$.

The column generation method and the branch-and-price method are

efficient techniques for solving large LP and ILP that have (exponentially) many variables. They have been applied to a wide variety of problems [59]. However, there are two fundamental difficulties when applying the column generation and the branch-and-price methods to solve (P1) and $(P1)_{INT}$:

1. In the column generation method, the pricing problem contains both binary variables and continuous variables. In particular, the pricing problem is a Mixed-Integer Programming (MIP) which is difficult to solve.

2. In the branch-and-price method, applying the conventional branching rule that branches on a single variable causes a new constraint to be added at each branch. As a result, a dual variable is added to the corresponding pricing problem. The pricing problem becomes progressively more complex as we go down the branching tree.

The following sections go into the details of the column generation and branch-and-price methods. In particular, we will present details on how the above difficulties arise and how we can overcome them.

3.3 Column Generation Method

In this section, we propose a Column Generation (CG) method to solve (P1). The column generation method decomposes (P1) into two sub-problems – a Restricted Master Problem (RMP) and a Pricing Problem (PP) – and solves them iteratively. The flowchart of the column generation method is shown in Fig. 3.1.

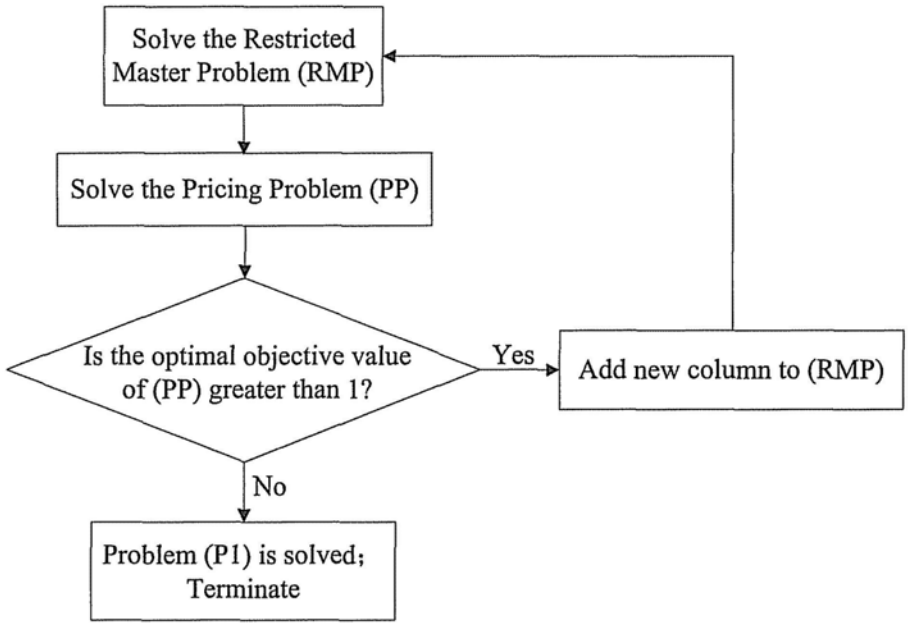

Figure 3.1: Flowchart of the column generation method

3.3.1 Restricted Master Problem

The Restricted Master Problem (RMP) is similar to the original problem (P1) except that only a subset of feasible matchings $\mathcal{E}' \subseteq \mathcal{E}$ is considered. Let $\mathbf{Q}'$ denote the incidence matrix of $\mathcal{E}'$. The restricted master problem is formulated as follows:

$$\begin{aligned} \text{minimize} \quad & V = \mathbf{e}^T\mathbf{u} \\ \text{subject to} \quad & \mathbf{Q}'\mathbf{u} \succeq \mathbf{f}, \\ \text{variables} \quad & \mathbf{u} \succeq 0. \end{aligned} \tag{RMP}$$

An initial subset of feasible matchings $\mathcal{E}'$ can be easily formed by letting the ith matching consist of link l_i only ($1 \leq i \leq |\mathcal{L}|$) and none of the other links. Since there is only one link in each matching, all these $|\mathcal{L}|$ matchings are feasible matchings. The corresponding initial incidence matrix $\mathbf{Q}'$ is an identity matrix.

First we solve (RMP) to optimality. We can achieve this with the simplex method [60] and obtain a primal optimal solution $\mathbf{u}^*$ and a dual optimal solution $\boldsymbol{\omega}^*$. Since we only consider a subset of feasible matchings $\mathcal{E}'$, $\mathbf{u}^*$ may not be the optimal solution to the original problem (P1).

Consider the columns that are in the matrix $\mathbf{Q}$ but not in the matrix $\mathbf{Q}'$. Notice that in (P1), the cost coefficient of every variable in the objective function is 1. The reduced cost of a column Q_k in the matrix $\mathbf{Q}$ but not in $\mathbf{Q}'$ is defined as [60]:

$$\sigma_k = 1 - (\boldsymbol{\omega}^*)^T Q_k. \tag{3.2}$$

The reduced cost σ_k of column Q_k is the amount by which the objective function will improve if the corresponding variable u_k is assumed to be a positive value and is increased by one unit. If the reduced cost σ_k is less than 0, the objective function of (P1) can be further reduced. On the other hand,

if the reduced costs of all the columns that are in the matrix $\mathbf{Q}$ but not in $\mathbf{Q}'$ are all non-negative, this means the current solution $\mathbf{u}^*$ is the optimal solution to (P1).

In the column generation method, instead of computing the reduced costs for all the columns that are in the matrix $\mathbf{Q}$ but not in $\mathbf{Q}'$, we consider the sub-problem of minimizing the reduced cost $\sigma = 1 - (\boldsymbol{\omega}^*)^T Q$, which is equivalent to maximizing $(\boldsymbol{\omega}^*)^T Q$, subject to the constraints that ensure Q is a feasible matching. In linear programming, the dual solution $\boldsymbol{\omega}^*$ is usually called the "shadow price". The connection between the restricted master problem and the sub-problem is through the shadow price $\boldsymbol{\omega}^*$. Therefore this sub-problem in the column generation method is usually called the "pricing problem", which is discussed in the next subsection.

3.3.2 Pricing Problem

The Pricing Problem (PP) is to find a feasible matching Q that maximizes $(\boldsymbol{\omega}^*)^T Q$, which is equivalent to minimizing the reduced cost $1 - (\boldsymbol{\omega}^*)^T Q$. It can be formulated as follows:

$$
\begin{aligned}
\text{maximize} \quad & \sum_{\iota=1}^{|\mathcal{L}|} \omega_{\eta}^* q_{\iota} \\
\text{subject to} \quad & c_{\iota\jmath} + q_{\iota} + q_{\jmath} \leq 2, \\
& \frac{p_{\eta} \cdot G\left(T_{\iota}, R_{\eta}\right)}{\eta_{\iota} + \sum\limits_{l_{\jmath} \in \mathcal{L} \setminus l_{\iota}} p_{\jmath} \cdot G\left(T_{\jmath}, R_{\eta}\right)} \geq q_{\eta} \cdot \gamma_{\iota}, \\
& p_{\eta} \leq q_{\eta} \cdot p_{\max}^{\iota}, \\
\text{variables} \quad & p_{\iota} \geq 0, \\
& q_{\iota} \in \{0, 1\}.
\end{aligned}
\tag{PP}
$$

The coefficient $\boldsymbol{\omega}^* = \{\omega_i^* : 1 \leq i \leq |\mathcal{L}|\}^T$ in the objective function of (PP) is the optimal dual solution to the (RMP) problem in the current iteration. The variables in (PP) are the binary variables $Q = \{q_i : 1 \leq i \leq |\mathcal{L}|\}$ and the continuous variables $\{p_i : 1 \leq i \leq |\mathcal{L}|\}$. Binary variable q_i is 1 if link l_i is active, and 0 otherwise. Continuous variable p_i is the transmission power of link l_i. The first constraint in (PP) is the primary constraint (Definition 1)that ensures the active links form a matching. Specifically, it contains the half-duplex constraint as well as the constraint that a node cannot transmit to or receive from more than one node simultaneously. The second constraint guarantees that the SINR requirement at each active receiver is satisfied. The third constraint states that the transmission powers are limited.[‡]

If the optimal objective value of (PP) is greater than 1, the optimal solution of (PP), $Q^* = \{q_i^* : 1 \leq i \leq |\mathcal{L}|\}$ is said to "price out". Q^* is then passed to (RMP) and the next iteration starts. If the optimal objective value of (PP) is less than or equal to 1, this means the optimal solution $\mathbf{u}^*$ to the (RMP) problem in the current iteration is already the optimal solution to the whole problem (P1), and the column generation terminates.

(RMP) is a small-scale standard linear program that is easy to solve using the simplex method. However, (PP) is a Mixed Integer Program with both binary variables and continuous variables that is quite difficult to solve in general. Therefore, the overall runtime performance of the column generation method depends on how well we can solve the pricing problem (see simulation results in section 3.6).

[‡]The algorithms proposed in this chapter can deal with the constraint that the transmit power p_i is upper-bounded by a maximum transmit power $p_{\max}^i$.

3.3.3 A New Formulation of the Pricing Problem

One of the key contributions of this chapter is that we reformulate the pricing problem (PP) to reduce its complexity. The new formulation enables us to remove the continuous power variables $\{p_i : 1 \leq i \leq |\mathcal{L}|\}$ and merge the primary constraints and the SINR constraints.

Let the vector $\boldsymbol{\gamma}_{\mathcal{M}} = (\gamma_i : \forall i \ s.t. \ l_i \in \mathcal{M})$ be the SINR thresholds at the receivers of the links in $\mathcal{M}$ and the matrix $\mathbf{D}(\boldsymbol{\gamma}_{\mathcal{M}})$ be the diagonal matrix whose diagonal entries are $(\gamma_i : \forall i \ s.t. \ l_i \in \mathcal{M})$, respectively. The SINR requirements (2.2) can be written in matrix form as

$$(\mathbf{I} - \mathbf{D}(\boldsymbol{\gamma}_{\mathcal{M}})\mathbf{B}_{\mathcal{M}})\mathbf{p}_{\mathcal{M}} \succeq \mathbf{v}_{\mathcal{M}}, \tag{3.3}$$

where vector $\mathbf{v}_{\mathcal{M}} = \left(\frac{\gamma_i \eta_i}{G(T_i,R_i)} : \forall i \ s.t. \ l_i \in \mathcal{M}\right)^T$ is the noise power vector normalized by both channel gain $G(T_i, R_i)$ and the SINR requirement γ_i.

When considering the maximum transmit power constraints and the case that different links may have different SINR requirements, the Proposition 1 which gives the necessary and sufficient conditions of deciding whether a matching is feasible needs to be modified as follows:

Proposition 5 *Consider a matching $\mathcal{M}$. Assume that the transmit power vector $\mathbf{p}_{\mathcal{M}}$ is upper bounded by vector $\mathbf{p}_{\max} = (p^i_{\max} : \forall i \ s.t. \ l_i \in \mathcal{M})^T$. The necessary and sufficient conditions for the existence of a positive power vector $\mathbf{p}_{\mathcal{M}} \preceq \mathbf{p}_{\max}$ that satisfies the SINR requirements in (3.3) are*

$$\rho(\mathbf{D}(\boldsymbol{\gamma}_{\mathcal{M}})\mathbf{B}_{\mathcal{M}}) < 1 \qquad and \qquad \mathbf{p}^*_{\mathcal{M}} \preceq \mathbf{p}_{\max}, \tag{3.4}$$

where

$$\mathbf{p}^*_{\mathcal{M}} = (\mathbf{I} - \mathbf{D}(\boldsymbol{\gamma}_{\mathcal{M}})\mathbf{B}_{\mathcal{M}})^{-1}\mathbf{v}_{\mathcal{M}} \tag{3.5}$$

is a componentwise minimum solution to (3.3).

The component-wise minimum power solution in (3.5) is achieved when the inequality in (3.3) is reduced to equality. The physical meaning is that if there is a link in (3.3) satisfied by inequality, say the ith link, we can reduce its transmit power p_i so that the SINR requirement γ_i at the receiver is exactly satisfied. Reducing the power p_i will only reduce the interference power in all the other constraints in (3.3), so the other constraints can still be satisfied. As a result, the component-wise minimum power solution in (3.5) is achieved when the inequality in (3.3) is reduced to equality. Proposition 5 provides easy conditions to check the feasibility of a matching and a minimum solution to the transmit powers of transmitters. In particular, given a matching, if conditions (3.4) are satisfied, the matching is guaranteed to be feasible, and the minimum transmit power vector can be set according to (3.5); otherwise, no matter how we tune the transmit powers, the links in the matching can not be active simultaneously. Incorporating (3.4) and (3.5) into the formulation of the pricing problem enables us to remove the power variables in the pricing problem. Notice that conditions (3.4) can only be applied to a set of links which already forms a matching. On the other hand, we can define a proper version of the channel gain matrix such that conditions (3.4) take care of both the primary and the SINR constraints in the pricing problem.

Consider a general wireless network with link set $\mathcal{L} = \{l_i, 1 \leq i \leq |\mathcal{L}|\}$. For any two different links $l_i, l_j \in \mathcal{L}$ with $c_{ij} = 1$, we re-define the channel gains $G(T_i, R_j)$ and $G(T_j, R_i)$ as:

$$G(T_i, R_j) = \infty \quad \text{and} \quad G(T_j, R_i) = \infty. \tag{3.6}$$

The other channel gains remain the same. The definitions in (3.6) allow us to extend the definition of the relative-channel-gain matrix $\mathbf{B}_{\mathcal{M}}$ defined on a matching $\mathcal{M}$ in (2.3) to $\mathbf{B}_{\mathcal{S}}$, which is defined on an arbitrary subset of links

$\mathcal{S} \subseteq \mathcal{L}$. The matrix $\mathbf{B}_{\mathcal{S}}$ is called virtual relative-channel-gain matrix with elements

$$b_{ij} = \begin{cases} 0, & \text{if } i = j, \\ \frac{G(T_j,R_i)}{G(T_i,R_i)}, & \text{if } i \neq j \text{ and } c_{ij} = 0, \\ \infty, & \text{if } i \neq j \text{ and } c_{ij} = 1. \end{cases} \tag{3.7}$$

Based on the definition of the virtual relative-channel-gain matrix $\mathbf{B}_{\mathcal{S}}$, condition $\rho\left(\mathbf{D}\left(\boldsymbol{\gamma}_{\mathcal{S}}\right)\mathbf{B}_{\mathcal{S}}\right) < 1$ will never hold if $\mathcal{S}$ is not a matching. This means that the necessary and sufficient conditions for a subset of links $\mathcal{S} \subseteq \mathcal{L}$ to be a feasible matching are

$$\rho\left(\mathbf{D}\left(\boldsymbol{\gamma}_{\mathcal{S}}\right)\mathbf{B}_{\mathcal{S}}\right) < 1 \qquad \text{and} \qquad \mathbf{p}_{\mathcal{S}}^{*} \preceq \mathbf{p}_{\max}, \tag{3.8}$$

where

$$\mathbf{p}_{\mathcal{S}}^{*} = \left(\mathbf{I} - \mathbf{D}\left(\boldsymbol{\gamma}_{\mathcal{S}}\right)\mathbf{B}_{\mathcal{S}}\right)^{-1}\mathbf{v}_{\mathcal{S}}. \tag{3.9}$$

One thing to notice is that the channel gain in the matrix $\mathbf{B}_{\mathcal{S}}$ is valid for any wireless channel model, not only the distance-based path loss model described in Chapter 2. Therefore, the centralized optimal algorithms proposed in this Chapter, i.e., the column generation method and the branch-and-price method, can be applied to a more general scenario in which fading and time-varying wireless channels are considered.

We can now simplify the pricing problem as follows:

$$\begin{aligned} \text{maximize} \quad & \sum_{i=1}^{|\mathcal{L}|} \omega_i^{*} q_i \\ \text{subject to} \quad & \rho\left(\mathbf{D}(\boldsymbol{\gamma}_Q)\mathbf{B}_Q\right) < 1, \\ & \left(\mathbf{I} - \mathbf{D}\left(\boldsymbol{\gamma}_Q\right)\mathbf{B}_Q\right)^{-1}\mathbf{v}_Q \preceq \mathbf{p}_{\max}, \\ \text{variables} \quad & q_i \in \{0,1\}, \quad 1 \leq i \leq |\mathcal{L}|. \end{aligned} \tag{SPP}$$

In the Simplified Pricing Problem (SPP), the only variables are the binary variables $Q = \{q_i : 1 \leq i \leq |\mathcal{L}|\}$. The continuous power variables $\{p_i : 1 \leq i \leq$

$|\mathcal{L}|\}$ have been removed. Formulation (SPP) is a binary integer programming problem which is easier to solve than the original pricing problem (PP).

3.3.4 Finding the optimal solution to the pricing problem

We propose a Smart Enumerating (SE) algorithm that finds an optimal solution to (SPP). With the help of conditions (3.8), the SE algorithm can reduce the search space by eliminating the infeasible solutions and the non-optimal solutions in an efficient way The SE algorithm takes much less time than the naive exhaustive search among all the subsets of link set $\mathcal{L}$.

In SE, we first solve (SPP) without considering the constraint set and obtain the corresponding optimal solution $Q_{wc} = \{q_i : 1 \leq i \leq |\mathcal{L}|\}$. Solution Q_{wc} is a set of links that maximizes $\sum_{i=1}^{|\mathcal{L}|} \omega_i^* q_i$ only and can be easily found: we set $q_i = 1$ if the corresponding coefficient $\omega_i^* > 0$ and set $q_i = 0$ if $\omega_i^* \leq 0$.

Next we check if conditions in (3.8) are satisfied by Q_{wc}. If yes, then the active links in Q_{wc} form a feasible matching and the pricing problem is solved. Otherwise, the optimal solution Q^* to (SPP) must be a subset of Q_{wc}. The SE algorithm performs a search among a small number of the subsets of Q_{wc} using the following two criteria:

Criterion 1: If a subset Q_s of Q_{wc} is infeasible, all the supersets of Q_s need not be considered.

Criterion 2: If a subset Q_s of Q_{wc} is feasible, all the subsets of Q_s need not be considered.

Criterion 1 is based on Proposition 2. In Criterion 2, any subset of Q_s will only have an objective value less than Q_s's objective value. With these two criteria, a large number of subsets of Q_{wc} can be eliminated.

SE finds an optimal solution to the binary integer programming (SPP). In general, it still has exponential runtime. However, because of the reduction

in the search space, the SE algorithm is reasonably efficient for modest size networks.

3.4 Branch-and-Price Method

In general, the optimal solution to (P1) may be fractional (i.e., non-integer) and hence not feasible to $(P1)_{INT}$. In this section, we propose a branch-and-price method to address $(P1)_{INT}$.

3.4.1 Branch-and-Price

The branch-and-price method [61] combines the column generation method with the branch-and-bound method to provide optimal integer solutions to $(P1)_{INT}$. Column generation is applied to solve the linear relaxation of the ILP problem at each node in the branch-and-bound tree. The flowchart of the branch-and-price method is shown in Fig. 3.2. The branch-and-price method starts with the original ILP problem $(P1)_{INT}$ as the root node. We first apply the column generation method to solve the linear relaxation (P1) to optimality and obtain an optimal solution $\mathbf{u}^*$. As discussed before, the optimal solution $\mathbf{u}^*$ may not be integral, so we need to perform branching by adding constraints. A typical branching rule is to add constraints that cut off the fractional value in the current optimal solution $\mathbf{u}^*$. Assume a variable u_k^* in $\mathbf{u}^*$ takes on a fractional value β. The physical meaning of the fractional value β is non-integer, fractional number of time slots. This is not a feasible solution to the original problem $(P1)_{INT}$ with integer constraints for time slots. Let $\lfloor\beta\rfloor$ and $\lceil\beta\rceil$ denote the largest integer not greater than β and the smallest integer not less than β, respectively. The original problem $(P1)_{INT}$ (parent node) then branches to two sub-problems (child nodes) by

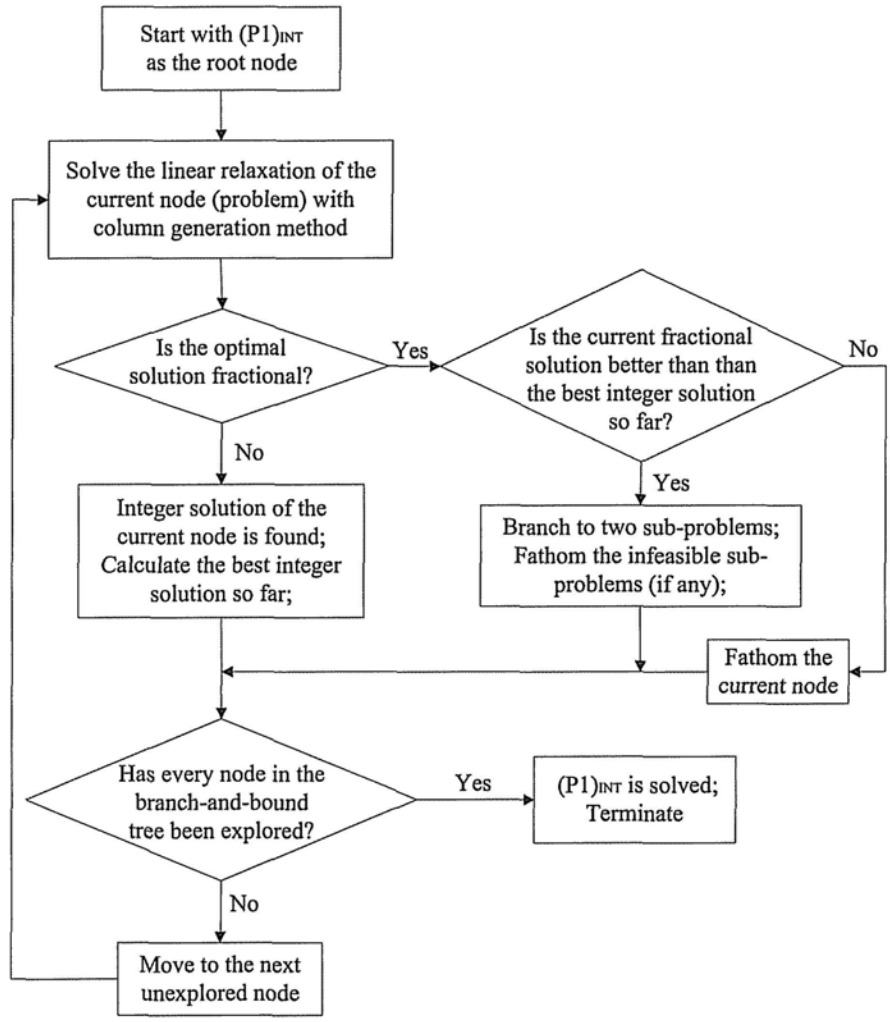

Figure 3.2: Flowchart of the branch-and-price method

adding the constraint

$$u_k \leq \lfloor \beta \rfloor , \tag{3.10}$$

and the constraint

$$u_k \geq \lceil \beta \rceil , \tag{3.11}$$

respectively. After branching, each child node is a new ILP problem. We then apply column generation to solve the LP relaxation to each child node. When the optimal solution to the new LP relaxation at a child node is again fractional, branching continues from that node.

In the branch-and-price method, the lower and upper bounds on the objective value at each node are obtained. The lower bound of a node is obtained by solving the relaxation of that node with column generation. An integer feasible solution of a node can be obtained by rounding up the optimal linear relaxation solution to the nearest integer. This rounding establishes an upper bound on the objective value. We maintain the value C, which is the objective value of the best integer solution across all nodes so far. If the lower bound for some node is greater than or equal to C, this node need not be considered further (i.e., this node is pruned from the branch-and-bound tree). Nodes can also be pruned when the problem in a node is infeasible. The branch-and-price terminates when all the nodes in the branch-and-bound tree have been evaluated and the optimal integer solution to $(\text{P1})_{\text{INT}}$ is found.

3.4.2 Improving the Pricing Rule

A component that is critical to the performance of the branch-and-price method is the branching rule. The conventional branching rule (i.e., (3.10) and (3.11)) adds a new constraint to each of the sub-problems. This causes a new dual variable to be added to the pricing problem. At depth H in the

branch-and-bound tree, there will be H additional dual variables. The size of the pricing problem will increase progressively as we go down the branch-and-bound tree. Another key contribution of this chapter is that we develop a more efficient new branching rule to overcome this problem.

We first modify the formulation $(\text{P1})_{\text{INT}}$ to incorporate an upper bound, g_i, on the number of time slots allocated to each link l_i in set $\mathcal{L}$. The upper bounds for all links are represented by the vector $\mathbf{g} = (g_i : 1 \leq i \leq |\mathcal{L}|)^T$. Initially, g_i simply takes on the value of the total frame length U. The modified formulation is

$$\begin{aligned} \text{minimize} \quad & V = \mathbf{e}^T\mathbf{u} \\ \text{subject to} \quad & \mathbf{f} \preceq \mathbf{Q}\mathbf{u} \preceq \mathbf{g}, \\ \text{variables} \quad & \mathbf{u} \succeq 0 \text{ and integer.} \end{aligned} \tag{3.12}$$

Instead of adding a constraint, the new branching rule changes the upper bound or the lower bound. If the optimal solution $\mathbf{u}^*$ has fractional elements, we calculate the vector $\mathbf{h} = \mathbf{Q}\mathbf{u}^*$. Suppose that an element h_i of $\mathbf{h}$ is fractional. We create two branches, one with

$$\sum_k q_{ik}u_k \leq \lfloor h_i \rfloor , \tag{3.13}$$

and the other with

$$\sum_k q_{ik}u_k \geq \lceil h_i \rceil . \tag{3.14}$$

These two branching inequalities can be carried out by changing the corresponding upper bound g_i to $\lfloor h_i \rfloor$ on one branch and changing the corresponding lower bound f_i to $\lceil h_i \rceil$ on the other branch, respectively. The new branching rule, (3.13) and (3.14), successfully avoids adding an additional constraint into the sub-problem, and thus avoids adding a new dual variable to the corresponding pricing problem.

Branching rule, (3.13) and (3.14), is not applicable to the particular situation in which the optimal solution $\mathbf{u}^*$ is fractional, but all the elements in the vector $\mathbf{h} = \mathbf{Q}\mathbf{u}^*$ are integers. In this case, we revert to the conventional branching rule (3.10) and (3.11).

3.4.3 Convergence speed

The column generation and the branch-and-price methods are guaranteed to find optimal solutions to (P1) and $(\text{P1})_{\text{INT}}$, respectively. But both the column generation and the branch-and-price methods are known to have poor convergence [59]. That is, the improvement in the objective function in the first several iterations are significant, but only little progress per iteration is made when the solution is close to the optimum. This phenomenon is called the "tailing off effect".

3.5 Column Generation and Branch-and-Price Based Heuristic

The column generation method and the branch-and-price method can find optimal solutions to the joint power control and link scheduling problem (P1) and $(\text{P1})_{\text{INT}}$, respectively. However, for large networks, both methods require a long computation time. This is due to the high complexity of the pricing problem In this section, we focus on efficient heuristic algorithms that yield near-optimal solutions with much faster speeds. Our heuristics are built on the foundations of the column generation and the branch-and-price methods.

3.5.1 Heuristic Pricing Problem Solution

Designing an efficient heuristic algorithm for the pricing problem can significantly reduce the complexities of the column generation and the branch-and-price methods. Even if we aim for an optimal solution, such a heuristic algorithm will still help, as explained in the following. Specifically, to obtain an optimal solution for the overall problem, it is not necessary to solve the pricing problem optimally in each iteration – it is sufficient to obtain any feasible matching with an objective value over 1. That is, as long as the new column generated can reduce the cost, it will do, and there is no need to find the best new column to be included. Thus, we can use a heuristic to find a cost-reducing column. Only when the heuristic fails to identify a cost-reducing column is it necessary for us to resort to the SE algorithm to see if a cost-reducing column exists.

If short runtime is more of a concern than solution optimality, the heuristic is also useful for finding a near-optimal solution. In this case, we do not revert to the SE algorithm even if the heuristic fails to find a cost-reducing column. If we adopt this strategy, the column generation method and the branch-and-price method become fast heuristic algorithms for identifying near-optimal solutions for (P1) and $(\text{P1})_{\text{INT}}$, respectively. We set a limit of 256 on the maximum number of iterations in the column generation based heuristic. The column generation heuristic will terminate if the heuristic algorithm for the pricing problem cannot find a better column or the maximum number of iterations is reached. In the branch-and-price based heuristic, we also set a limit of 256 on the maximum number of branchings. Setting the maximum numbers on both the iterations and the branchings will protect the column generation and branch-and-price based heuristic algorithms against exponen-

tial runtime in the worst-case. The simulation results (Fig. 3.7) show that the column generation based heuristic algorithm achieves close to optimal performance (the average percentage cost penalty is below 9%) within 20 iterations in the column generation method, and in that 256 iterations are not needed in general.

We next propose a Combined Sum Criterion Removal (CSCR) heuristic algorithm for the pricing problem. The key idea behind CSCR is to remove one link at a time until the remaining active links form a feasible matching. The flowchart of CSCR is shown in Fig. 3.3.

We first solve (SPP) without considering the constraint set. This step has been discussed in section 3.3.4. If the resulting Q is feasible as per the conditions in (3.8), then the pricing problem is solved. On the other hand, if Q is infeasible, we deactivate one link at a time until the remaining links form a feasible matching. There are two possible causes of the infeasibility: (i) $\rho\left(\mathbf{D}\left(\boldsymbol{\gamma}_Q\right)\mathbf{B}_Q\right) \geq 1$; or (ii) $\rho\left(\mathbf{D}\left(\boldsymbol{\gamma}_Q\right)\mathbf{B}_Q\right) < 1$, but some elements in the component-wise minimum power vector $\mathbf{p}_Q^*$ are greater than the maximum transmit powers allowed. For (i), we use the combined sum criterion to remove one link at a time. Specifically, we set $q_{\tilde{i}} = 0$ for a link $l_{\tilde{i}}$ that achieves the maximum of the row sums and the column sums of matrix $\mathbf{D}\left(\boldsymbol{\gamma}_Q\right)\mathbf{B}_Q$:

$$\tilde{i} = \arg\max_i \left\{ \sum_j \left(\mathbf{D}\left(\boldsymbol{\gamma}_Q\right)\mathbf{B}_Q\right)_{ij}, \sum_k \left(\mathbf{D}\left(\boldsymbol{\gamma}_Q\right)\mathbf{B}_Q\right)_{ki} \right\}. \tag{3.15}$$

The combined sum criterion comes from [57] which investigated the power control problem in cellular systems. The combined sum criterion seeks to minimize the upper bound of the Perron-Frobenius eigenvalue $\rho\left(\mathbf{D}\left(\boldsymbol{\gamma}_Q\right)\mathbf{B}_Q\right)$ assuming that only one link can be removed, so that the condition $\rho\left(\mathbf{D}\left(\boldsymbol{\gamma}_Q\right)\mathbf{B}_Q\right) < 1$ can be satisfied with a high probability. The physical meaning of the combined sum criterion is that, we remove the link that gen-

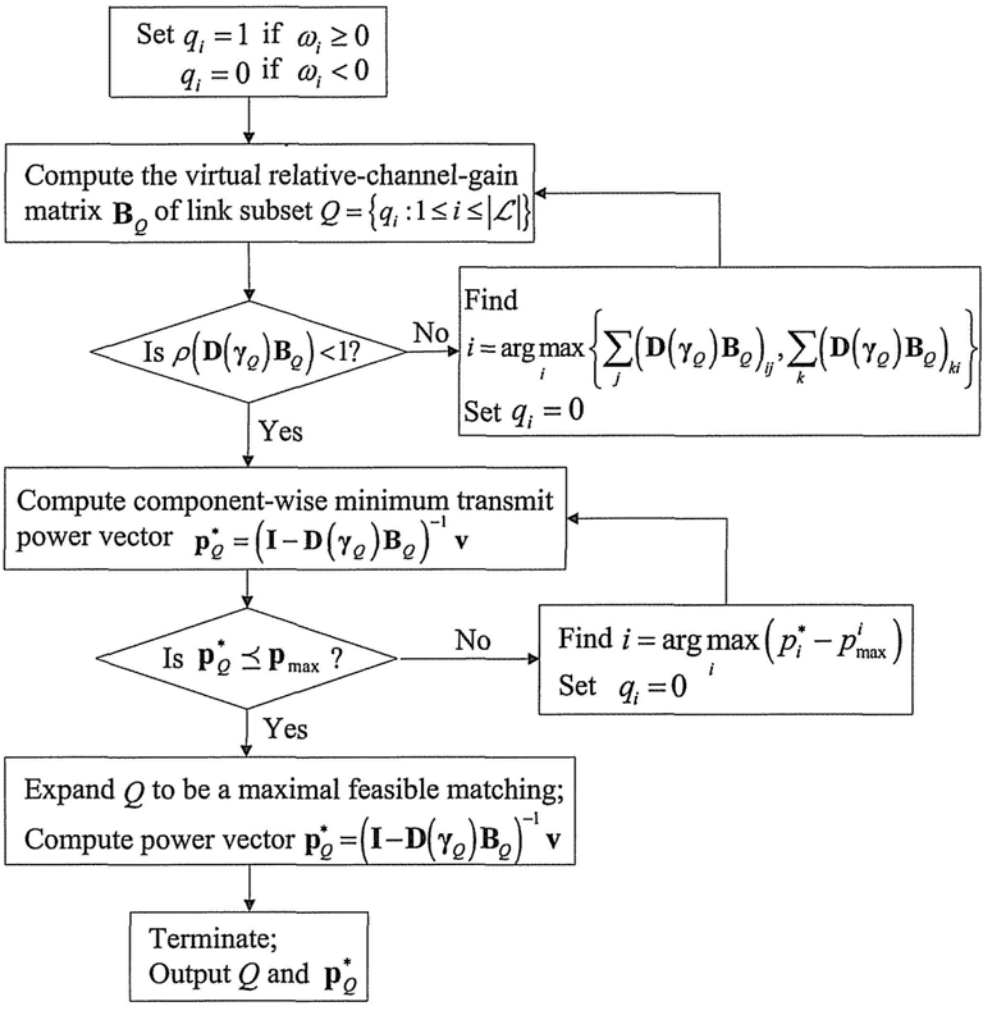

Figure 3.3: Flowchart of the CSCR algorithm

erates or experiences the maximum interference in the network. For (ii), we also remove one link at a time, but each time we remove the link whose transmit power p_i^* exceeds $p_{\max}^i$ by the maximum amount. After the removal process, the resulting Q is guaranteed to be a feasible matching. In the last step of the CSCR heuristic algorithm, we expand Q to a *maximal* feasible matching. This step can be simply performed by considering the remaining links one by one. A link is added if both the conditions in (3.8) are satisfied.

The CSCR heuristic algorithm is simple and computationally efficient. The simulation results in section 3.6 show that it also works well in practice.

3.5.2 Initial Feasible Matchings

For initializing our algorithms, we need a subset of feasible matchings. Section 3.3.1 shows one possibility where the initial feasible matchings for (RMP) are those that contain only one active link. The corresponding initial incidence matrix $\mathbf{Q}'$ is an identity matrix. This choice, although simple, is not necessarily the best choice. A better choice could reduce the number of iterations required in column generation. We propose a heuristic algorithm, referred to as Increasing Demand Greedy Scheduling (IDGS), that solves $(\text{P1})_{\text{INT}}$ heuristically to obtain a good initial subset of feasible matchings. In particular, the IDGS produces a subset of *maximal* feasible matchings which will be used by the optimal solution with high probability.

The IDGS heuristic algorithm is described in Algorithm 1. The inputs are the virtual relative-channel-gain matrix $\mathbf{B}_{\mathcal{L}}$ (as defined in Section 3.3.3), the traffic demand vector $\mathbf{f}$, the SINR requirement vector $\boldsymbol{\gamma}$, and the normalized noise vector $\mathbf{v}$. The outputs of the IDGS algorithm are the set of maximal feasible matchings $\{\mathcal{E}_1, \mathcal{E}_2, \cdots, \mathcal{E}_K\}$, the corresponding transmit power vectors $\{\mathbf{p}_1, \mathbf{p}_2, \cdots, \mathbf{p}_K\}$, and the corresponding airtime allocation vectors

$\{u_1, u_2, \cdots, u_K\}$.

Algorithm 1: Increasing Demand Greedy Scheduling

Input: the virtual relative-channel-gain matrix $\mathbf{B}_{\mathcal{L}}$, the traffic demand vector $\mathbf{f}$, the SINR requirement vector $\boldsymbol{\gamma}$, the normalized noise vector $\mathbf{v}$

Output: a subset of maximal feasible matchings $\{\mathcal{E}_1, \mathcal{E}_2, \cdots, \mathcal{E}_K\}$, the transmit power vectors $\{\mathbf{p}_1, \mathbf{p}_2, \cdots, \mathbf{p}_K\}$, the set of integers $\{u_1, u_2, \cdots, u_K\}$

```
1  Sort the links in increasing order of their traffic demands
   f_1 ≤ f_2 ≤ ··· ≤ f_|L|;
2  k ← 1;
3  while L ≠ ∅ do
4      E_k ← {l_k1}; u_k ← f_k1; i ← |L|;
5      while i ≥ 1 do
6          if E_k ∪ {l_ki} forms a feasible matching then
7              E_k ← E_k ∪ {l_ki}; f_ki := f_k1 − u_k;
8              if f_k,i ≤ 0 then
9                  L ← L \ {l_ki};
10         i ← i − 1;
11     p_k ← (I − D(γ_{E_k}) B_{E_k})^{-1} v_{E_k};
```

In the first step of IDGS, the links are sorted according to their traffic demands in an increasing order. In each iteration of the main scheduling while-loop (lines 3 to 11), we determine one feasible matching $\mathcal{E}_k$, the corresponding transmission power vector $\mathbf{p}_k$, and an integeral airtime allocation u_k. The main idea of IDGS is that we want to eliminate one link from the link set $\mathcal{L}$ in each iteration so that it does not have to be considered in future

iterations. In IDGS, we choose to eliminate the link with the lightest traffic demand. At the same time, we want to allow as many other links to transmit together with the link to be removed as possible. For these other links, we would like to address those links with heavy traffic demands. The purpose of the inner while-loop (lines 5 to 10) is to compose $\mathcal{E}_k$. In the kth iteration, let $l_{k\imath}$ and $f_{k\imath}$ denote the ith link in the remaining link set $\mathcal{L}$ and the remaining traffic demand of link $l_{k\imath}$, respectively. The feasible matching $\mathcal{E}_k$ is formed in a greedy way. We first put link l_{k1} that has the minimum traffic demand among the remaining link set $\mathcal{L}$ into $\mathcal{E}_k$. Then we start from the last link which has the largest traffic demand within the remaining link set $\mathcal{L}$ and add one link to the set $\mathcal{E}_k$ at a time. The link added to the set $\mathcal{E}_k$ must satisfy the condition that the link and all the links already in the $\mathcal{E}_k$ form a feasible matching. This can be done by checking the conditions in (3.8). If adding a link will cause $\mathcal{E}_k$ to be infeasible, we move on to the next link without adding it.

After the feasible matching $\mathcal{E}_k$ is formed, we allocate $u_k = f_{k1}$ time slots to $\mathcal{E}_k$. The transmission power vector of the links in set $\mathcal{E}_k$ is computed by $\left(\mathbf{I} - \mathbf{D}\left(\gamma_{\mathcal{E}_k}\right)\mathbf{B}_{\mathcal{E}_k}\right)^{-1}\mathbf{v}_{\mathcal{E}_k}$. If link $l_{k\imath}$ is selected in the feasible matching $\mathcal{E}_k$, the remaining traffic demand of link $l_{k\imath}$ is updated by subtracting u_k from it. And if all the traffic demand of link $l_{k\imath}$ has been satisfied, link $l_{k\imath}$ can be removed from the link set $\mathcal{L}$.

The IDGS algorithm continues until all the links are removed from the link list. The maximum number of iterations required in IDGS is no larger than the number of links in the network and is typically much smaller.

3.6 Simulation Results

We carry out extensive simulations to evaluate the performances of the proposed column generation method and the branch-and-price method. We conduct our simulations on a computer with a 1.86 GHz CPU and 1 GB of RAM. We use YALMIP [62] to solve the optimization problems. YALMIP is a modeling language for solving both convex and non-convex optimization problems. It relies on external solvers for the actual computations. Specifically, we use CPLEX 9.0 as the solver for both LP and ILP problems, and use the bmibnb as the solver for the general non-linear optimization problems.

In our simulations, random network topologies are generated. The locations of the transmitters are uniformly distributed in a square area of $1000m \times 1000m$. The length of each link ranges from 100 to 200 meters. More specifically, the location of each receiver is randomly chosen within a radius of 200 meters and outside a radius of 100 meters from the corresponding transmitter. A random network with 32 links is shown in Fig. 5.3. The triangular nodes represent the transmitters and the circular nodes represent the receivers. The large-scale path loss model with a typical path loss exponent of 4 is assumed. The maximum transmit power is $100mW$. The required SINR threshold is uniformly distributed over $[10dB, 20dB]$. The traffic demand of each link is a discrete random variable with 10 equally likely values chosen from the set of integers $\{1, 3, 5, \cdots, 19\}$. The expected traffic demand is 10 time slots. For each given number of links, we investigate 1000 random networks and present the averaged results.

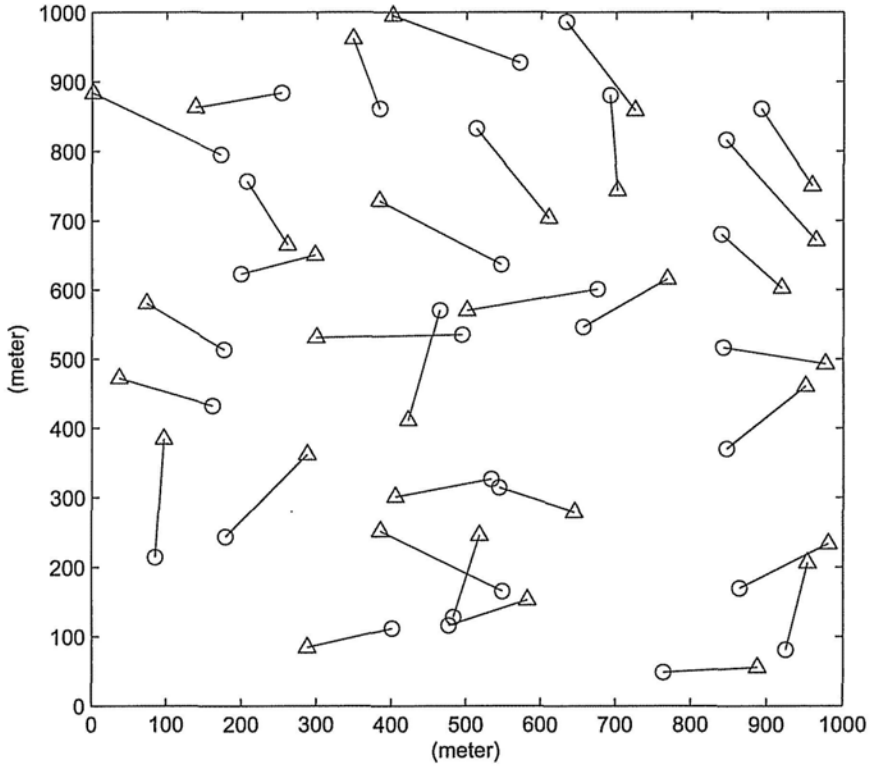

Figure 3.4: Random network topology with 32 links

3.6.1 Finding Optimal Solutions

Our first investigation focuses on finding optimal solutions to problems (P1) and $(P1)_{INT}$. We compare the performances of the following four algorithms:

1. CG-SE (our algorithm): the column generation method in which the pricing problem is simplified as (SPP). The (SPP) is solved with CSCR heuristic first. If the CSCR fails then we turn to the Smart Enumerating (SE) algorithm to solve (SPP) to optimality. The initial feasible matchings are found by the IDGS algorithm.

2. B&P-SE (our algorithm): the branch-and-price method in which the enhanced branching rule (i.e., (3.13) and (3.14)) is used and the linear relaxation at each node is solved with CG-SE.

3. CG-traditional: the column generation method proposed in [54–56].

4. B&P-traditional: the branch-and-price method in which the conventional branching rule (i.e., (3.10) and (3.11)) is used and the linear relaxation at each node is solved with CG-traditional.

The simulation results of random networks with 18 links are shown in Table 3.1. The CG-traditional and CG-SE algorithms find optimal solutions to (P1); the B&P-traditional and B&P-SE algorithms find optimal solutions to $(P1)_{INT}$. Figure 3.5 shows the average runtimes of these four algorithms for networks of different sizes. It is clear that CG-SE outperforms CG-traditional, and B&P-SE outperforms B&P-traditional in terms of the runtime performance. The improvement becomes more significant as the number of links increases. When the networks have 18 links, the average runtimes of CG-traditional and B&P-traditional are 1461.3 seconds and 1576.7 seconds, respectively. However, the average runtimes of CG-SE and B&P-SE

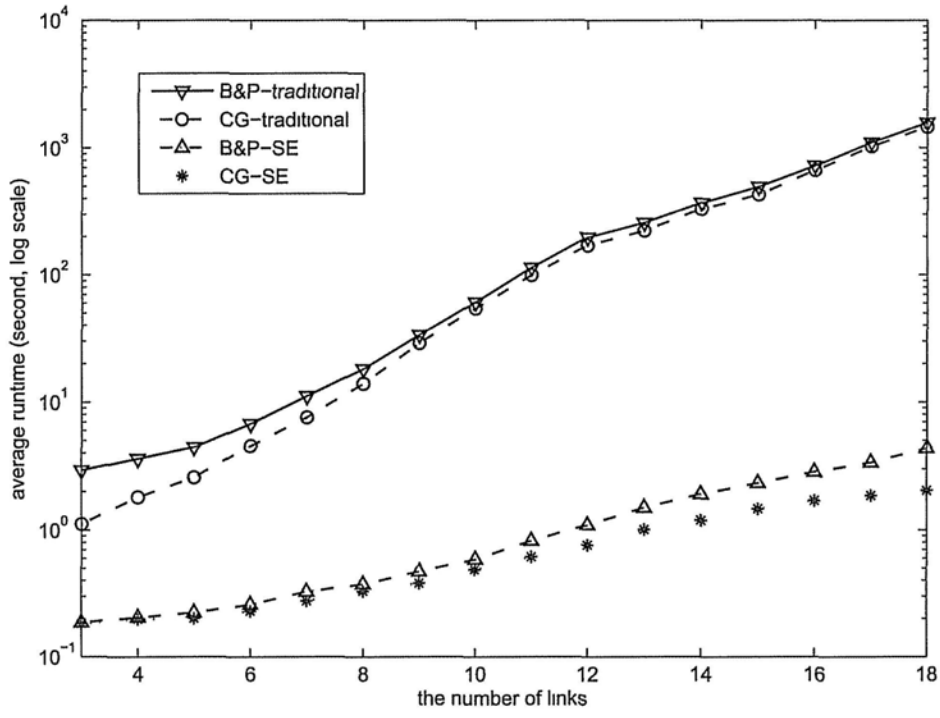

Figure 3 5 Average runtime performance of our column generation method (CG-SE) and branch-and-price method (B&P-SE), compared with traditional column generation method (CG-traditional) and branch-and-price method (B&P-traditional)

Table 3.1: Simulation Results (random networks with 18 links)

Algorithms	Average number of time slots	Average runtime (sec)	Minimum runtime (sec)	Maximum runtime (sec)
CG-traditional	70.7	1461.3	601.52	2170.3
B&P-traditional	70.9	1576.7	630.33	2486.8
CG-SE	70.7	2.031	0.33	6.129
B&P-SE	70.9	4.336	0.33	30.99

are only 2.031 seconds and 4.336 seconds, respectively. CG-SE and B&P-SE reduce the average runtimes by 99.86% and 99.72%, respectively. In column generation and branch-and-price, the computational effort is mainly spent in solving the pricing problem to optimality. The column generation and the branch-and-price become efficient only when the pricing problem can be solved efficiently. In the column generation method proposed in [54–56], the pricing problem (PP) is solved directly with the general optimization solver. However, in CG-SE and B&P-SE, we solve the simplified pricing problem (SPP) with the Smart Enumerating (SE) algorithm instead. Thanks to the Perron-Frobenius eigenvalue condition, the complexity in the pricing problem can be reduced significantly. Furthermore, the Perron-Frobenius eigenvalue condition also serves as an important criterion that is used in the SE algorithm to reduce the search space by eliminating the infeasible solutions and

Table 3.2: Average Runtime Performance of CG-SE and B&P-SE

	29 links	30 links	31 links	32 links
CG-SE	31.50	48.53	92.08	172.90
B&P-SE	57.50	89.24	151.85	269.97

the non-optimal solutions in an efficient way. We can conclude that if we want to guarantee optimality, CG-SE and B&P-SE are much more efficient than CG-traditional and B&P-traditional.

Table 3.2 shows the average runtime performance of CG-SE and B&P-SE when we further increase the number of links in the network. Notice that when the number of links is greater than 18, the computation times of both CG-traditional and B&P-traditional are too large and can not be afforded any more. We find that CG-SE and B&P-SE work efficiently for networks less than 30 links. The average runtimes of CG-SE and B&P-SE are 31.5 seconds and 57.5 seconds for 29-link networks. However, when the number of links further increases, the runtimes of CG-SE and B&P-SE increase dramatically. The average runtimes of CG-SE and B&P-SE increase to 172.90 seconds and 269.97 seconds for 32-link networks, respectively. The reason is that although we are able to reduce the complexity of the pricing problem by incorporating the Perron-Frobenius eigenvalue condition, the pricing problem still has an exponential complexity by nature. Therefore, CG-SE and B&P-SE also have an exponential complexity in the number of links. We can conclude that for modest-size network (i.e., less than 30 links), CG-SE and B&P-SE are computationally efficient optimal algorithms. For large-size network, finding optimal solutions is really difficult. In this situation, we need turn to heuristic

algorithms that find close to optimal solutions with short runtime.

3.6.2 Performance of Column Generation and Branch-and-Price Based Heuristics

Next, we investigate the performances of the column generation and the branch-and-price based heuristics. The column generation and the branch-and-price methods become heuristic algorithms for (P1) and $(\text{P1})_{\text{INT}}$ when the pricing problem is solved sub-optimally with the CSCR heuristic. We study the performances of the following three heuristic algorithms:

1. ISPA: Integrated Scheduling and Power control Algorithm, a heuristic proposed in [58].

2. CG-Heu: the column generation based heuristic for (P1) in which the pricing problem is solved with CSCR only. The initial feasible matchings are found by the IDGS algorithm. The maximum number of iterations is set as 256.

3. B&P-Heu: the branch-and-price based heuristic for $(\text{P1})_{\text{INT}}$ in which the enhanced branching rule (i.e.,(3.13) and (3.14)) is used and the linear relaxation is solved with CG-Heu. The maximum number of branchings is set as 256.

For comparison purpose, we also obtain optimal solutions to (P1) and $(\text{P1})_{\text{INT}}$ with CG-SE and B&P-SE, respectively. We introduce the percentage cost penalty to describe the penalty of the above three heuristic algorithms compared to the optimal solution. Let $V_{algorithm}$ and V_{opt} denote the number of time slots the algorithm needs and the optimal value, respectively. The

percentage cost penalty of each algorithm is defined by

$$P_{algorithm} = \frac{V_{algorithm} - V_{opt}}{V_{opt}} \times 100\%. \tag{3.16}$$

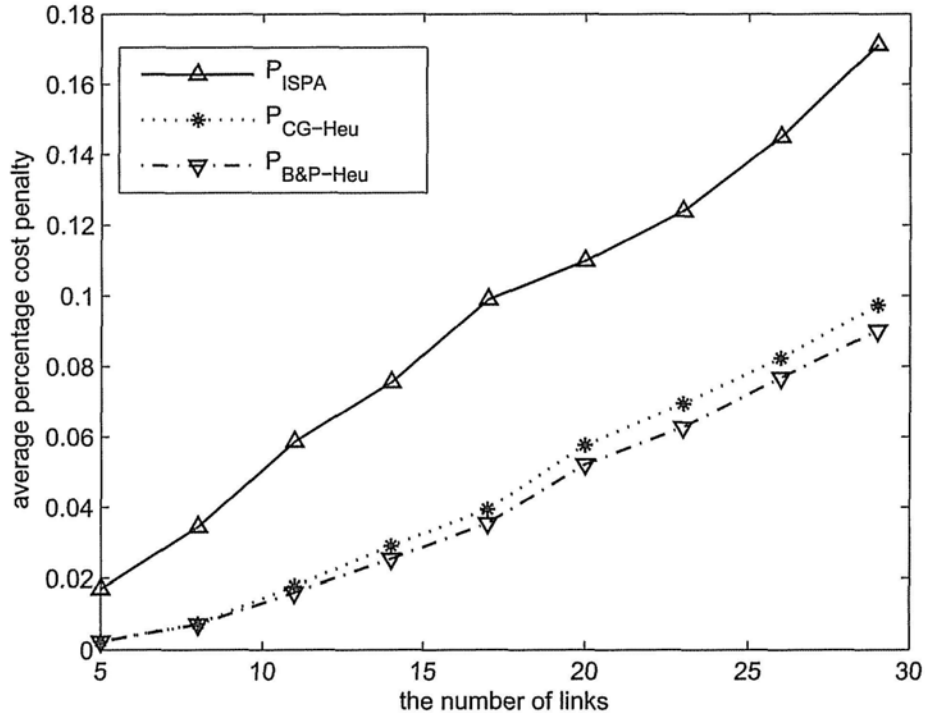

Figure 3.6: Average percentage cost penalty of the column generation and branch-and-price based heuristic algorithms (CG-Heu and B&P-Heu), compared with the ISPA heuristic algorithm

Figure 3.6 shows the performance of the average percentage cost penalty of the three heuristic algorithms as a function of the number of links. We see that the performance of ISPA is the worst among the three algorithms. Compared with P_{ISPA}, $P_{CG\text{-}Heu}$ and $P_{B\&P\text{-}Heu}$ increase much more slowly

with the number of links (i.e., network density). For 29-link networks, the averaged value of P_{ISPA} is 17.12%. However, the averaged values of $P_{CG\text{-}Heu}$ and $P_{B\&P\text{-}Heu}$ are reduced to 9.73% and 9.01%, respectively. For the different sizes of networks we simulated, the averaged values of $P_{CG\text{-}Heu}$ and $P_{B\&P\text{-}Heu}$ are all below 10%. The column generation and the branch-and-price based heuristic algorithms perform much better than the ISPA which is designed in a greedy way. In Fig. 3.6, it is surprising to find that B&P-Heu has better performance than CG-Heu in terms of the average percentage cost penalty. This can be explained as follows. The solution of CG-Heu is the same as the solution of the linear relaxation at the root node in B&P-Heu. In the branch-and-bound tree of B&P-Heu, each node is solved sub-optimally. Therefore, it may happen that in addition to the feasible matchings found at the root node, some more desirable feasible matchings can be found when using CG-Heu to solve the linear relaxation at the child nodes. So it happens that the integer solutions in B&P-Heu can be better than the non-integer solutions in CG-Heu.

Furthermore, the column generation and the branch-and-price based heuristic algorithms can achieve the tradeoff between the performance and the runtime. Figure 3.7 shows the average percentage cost penalty of ISPA and CG-Heu as a function of the number of iterations for random networks with 26 links. The ISPA, which is a greedy heuristic algorithm, can only achieve a fixed average percentage cost penalty of 14.50% with an average runtime of 0.15 seconds. The average runtime of each iteration in CG-Heu is 0.15 seconds, which is equal to the average runtime of ISPA. At the initial point of CG-Heu, the averaged value of $P_{CG\text{-}Heu}$ is 21.83%. The averaged value of $P_{CG\text{-}Heu}$ decreases with the number of iterations. The improvement is significant at the first 10 iterations in CG-Heu but is less significant when

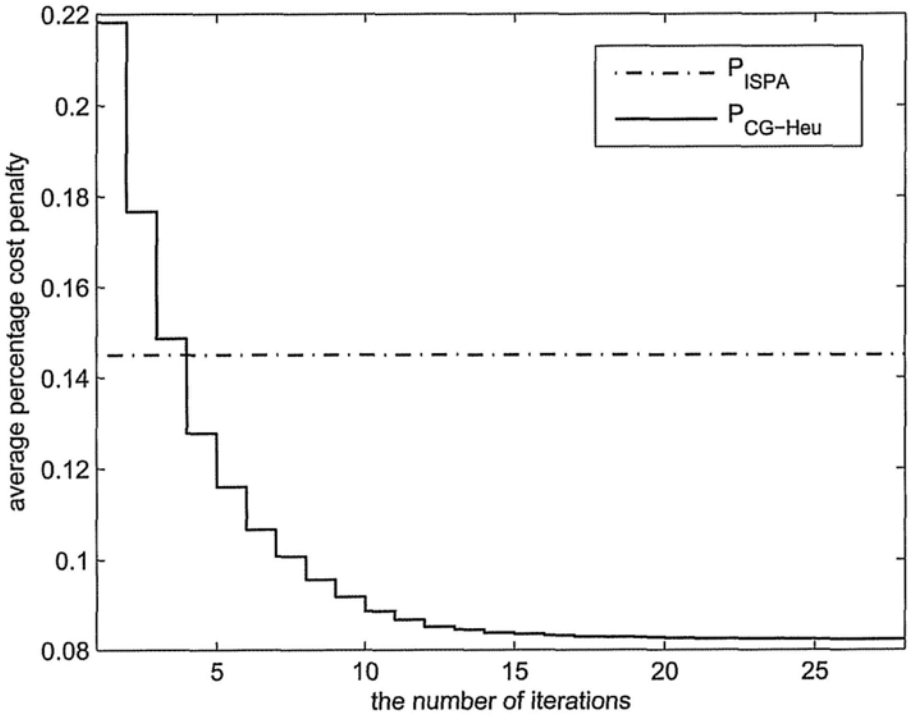

Figure 3.7: Average percentage cost penalty of ISPA and the column generation based heuristic algorithm CG-Heu as a function of the number of iterations

the number of iterations further increases. The averaged value of $P_{CG\text{-}Heu}$ converges to 8.23% after 28 iterations. Therefore, the column generation based heuristic algorithm can achieve the tradeoff between the performance and the runtime by tuning the parameter of the iteration number. Because CG-Heu is applied to solve the linear relaxation of each node in B&P-Heu, similarly, the branch-and-price based heuristic can also achieve the tradeoff between the performance and the runtime by tuning the parameter of the iteration number.

3.7 Summary

In this chapter, we have considered the minimum-length scheduling problem in STDMA wireless networks with power control, subject to traffic demands and SINR constraints. When power control is considered, the feasibility of a set of links under the SINR constraints can be checked by the Perron-Frobenius eigenvalue condition. This turns out to be a rather useful condition for expediting the optimization. We propose the column generation method that finds optimal time schedule and power solutions. The way to solve the pricing problem is the key to the efficiency of the column generation method. We integrate the Perron-Frobenius eigenvalue condition into both the formulation of the pricing problem and the Smart Enumerating (SE) algorithm. Such integration improves the efficiency of the column generation method. We show that our new formulation, together with the SE algorithm, reduces the average runtime of the column generation method by 99.86% for wireless networks with 18 links compared with the traditional column generation method. We further propose the branch-and-price method that combines the column generation with the branch-and-bound to provide optimal integer time

schedule solutions. We develop a new branching rule in the branch-and-price method that maintains the size of the pricing problem after each branching, and thus improves the overall efficiency of the branch-and-price method. For example, our branch-and-price method reduces the average runtime by 99.72% for wireless networks with 18 links compared with the traditional branch-and-price method.

Both the column generation and the branch-and-price methods can be used as heuristic algorithms if we solve the pricing problem sub-optimally. We propose a simple heuristic algorithm, Combined Sum Criterion Removal (CSCR), for the pricing problem. Simulation results show that the column generation and the branch-and-price based heuristics can obtain near-optimal solutions. In particular, the average cost penalties are below 10% for networks with less than 30 links.

Chapter 4

Centralized Approximation Algorithm

4.1 Introduction

4.1.1 Overview

As discussed in Chapter 2, there is a requirement of consecutive transmissions in some practical wireless systems. In this chapter, we propose a polynomial time algorithm, called the Guaranteed and Greedy Scheduling (GGS) algorithm, to solve the power-controlled scheduling problem with consecutive transmission constraint. The GGS algorithm has the following key features:

1. *Guaranteed performance*: GGS has a provable upper bound for the approximation ratio relative to the optimal solution.

2. *Wide applicability of the algorithm*: GGS and its bounded approximation ratio are general. They are applicable for any network topology.

3. *Easy extension*: GGS can easily be modified to solve the power-controlled scheduling problem without consecutive transmission con-

straint. Interestingly, the proved upperbound for the approximation ratio remains valid.

4.1.2 Related Work

STDMA scheduling with the objective of minimizing the total frame length has been extensively studied since 1980s. The centralized scheduling algorithms but without power control have been studied in [42, 63, 64]. Ref. [63] presented a greedy scheduling method with a proven bounded approximation ratio under the assumption that nodes are uniformly distributed in a square. Ref. [42] proposed an approximate algorithm based on square coloring. The approximation ratio depends on the link length diversity in the network.

Implementing power control can increase the system performance but complicates the analysis. Only in recent years, there have been much research effort on cross-layer study of joint scheduling and power control (e.g., [41,47,48,54–56,58,65–68]). In [65], the authors proposed a simple heuristic of two alternating phases solution: a central controller first selects a set of valid links in a greedy way that eliminates strong interference in phase one, and then applies the power control algorithm based on [57] to find the minimal power solutions in phase two. Reference [67] formulated the joint scheduling and power control problem with fairness considerations and solved it using a serial linear programming rounding heuristic algorithm. Ref. [47, 48, 58] proposed heuristic algorithms for the power controlled scheduling problem. The authors in [47, 48] gave an upper bound on the number of time slots required by their heuristic scheduling algorithms. However, they did not provide a lower bound for optimal scheduling. Without benchmarking with optimal scheduling, it is difficult to evaluate their algorithms. To the best of our knowledge, the GGS algorithm proposed in this thesis is the first polynomial

time algorithm with a provable approximation ratio for the power-controlled scheduling *with and without* consecutive transmission constraints.

In section 4.2, we introduce the polynomial-time algorithm, the Guaranteed and Greedy Scheduling (GGS) to solve the joint power control and scheduling algorithm with consecutive transmission constraint. The analysis of GGS is given in section 4.3. Section 4.4 presents the simulation results. A summary of this chapter is given in section 4.5.

4.2 Scheduling Algorithm

As discussed in Chapter 2, we find that the JPS-CC (Joint Power control and Scheduling problem with Consecutive transmission Constraints) is NP-complete. It is unlikely to find a polynomial-time algorithm to solve JPS-CC optimally. In this section, we propose a polynomial-time approximate algorithm, called the Guaranteed and Greedy Scheduling (GGS) algorithm, to solve JPS-CC. The scheduling in GGS consists of two parts: the guaranteed scheduling and the greedy scheduling. In the guaranteed scheduling part, it is guaranteed that the selected links form a feasible matching without the need of checking the feasibility. In the greedy scheduling part, additional links are added to those already in the feasible matching one by one in a greedy way in a decreasing order of the traffic demand, provided the physical interference constraint can still be met with proper power control.

Consider a wireless network with link set $\mathcal{L} = \{l_i, 1 \leq i \leq |\mathcal{L}|\}$. The inputs of the algorithm are the network topology and the traffic demand vector $\mathbf{f} = \{f_i, 1 \leq i \leq |\mathcal{L}|\}$. The output of the algorithm is the schedule $\mathcal{SCH} = \{\mathbf{p}(t), 1 \leq t \leq V\}$. Each element $\mathbf{p}(t)$ denotes the transmit power vector at a particular time slot t. The Guaranteed and Greedy Scheduling

(GGS) algorithm is described in Algorithm 2.

Algorithm 2: Guaranteed and Greedy Scheduling (GGS)

Input: a set of links $\mathcal{L}$, the traffic demand vector $\mathbf{f}$

Output: a successful schedule $\mathcal{SCH}$

1 **for** *each link* $l_i \in \mathcal{L}$ **do**

2 $\quad \lambda_i \leftarrow \left\lfloor \log_2 \frac{d_{\max}}{d_{ii}} \right\rfloor + 1$; $\tau_i \leftarrow$ ordering of link i (decreasing traffic demand);

3 $t \leftarrow 1$;

4 *Main Scheduling Loop*

4.2.1 Initialization Phase

During the initialization phase (lines 1 to 3 in Algorithm 2), each link l_i in $\mathcal{L}$ is assigned two values: λ_i and τ_i.

Let $d_{\max}$ and $d_{\min}$ denote the longest and the shortest link length, respectively. The first assigned value λ_i is related to the link length d_{ii},and is given by $\lambda_i = \left\lfloor \log_2 \frac{d_{\max}}{d_{ii}} \right\rfloor + 1$. Then d_{ii} satisfies $\frac{d_{\max}}{2^{\lambda_i}} < d_{ii} \leq \frac{d_{\max}}{2^{\lambda_i - 1}}$. Let $K = \left\lfloor \log_2 \frac{d_{\max}}{d_{\min}} \right\rfloor + 1$, thus λ_i is an integer between 1 and K. According to $\boldsymbol{\lambda}$, the links in $\mathcal{L}$ are partitioned into K subsets $\{\mathcal{L}^k, 1 \leq k \leq K\}$. The links belong to the same subset $\mathcal{L}^k$ have the same λ value which is equal to k, and the lengths of the links in the subset $\mathcal{L}^k$ differ by at most a factor of two. Links with larger λ values have shorter link lengths. We will perform scheduling of the links one group at a time in the guaranteed scheduling part.

The second assigned value τ_i is related to the traffic demand f_i. In particular, τ_i is the ordering of link l_i (an integer between 1 and $|\mathcal{L}|$) when the links in set $\mathcal{L}$ are sorted according to the traffic demands in a decreasing order.

Algorithm 3: Main Scheduling Loop

for $k = 1$ **to** $\left\lfloor \log_2 \frac{d_{\max}}{d_{\min}} \right\rfloor + 1$ **do**
  Divide the Euclidean plane into hexagons with side length $A = \frac{W \cdot d_{\max}}{2^{k-1}}$;
  Color these hexagons with 3 colors;
  for $q = 1$ **to** 3 **do** `/* Select color q */`
    $t_{start} \leftarrow t$;
    while $\mathcal{L}^{k,q} \neq \emptyset$ **do**
      for $m = 1$ **to** $\left|\mathcal{H}^{k,q}\right|$ **do**
        if *previous link in* $H^{k,q}(m)$ *has finished transmission* **then**
          pick a new link $l_i \in \mathcal{L}^{k,q}$ with $R_i \in H^{k,q}(m)$;
          $\mathcal{S}_t \leftarrow \mathcal{S}_t \cup \{l_i\}$; $f_i \leftarrow f_i - 1$;
          if $f_i == 0$ **then**
            $\mathcal{L}^{k,q} \leftarrow \mathcal{L}^{k,q} \setminus \{l_i\}$; $\mathcal{L} \leftarrow \mathcal{L} \setminus \{l_i\}$
          else $\mathcal{S}_{t+1} \leftarrow \mathcal{S}_{t+1} \cup \{l_i\}$
      $t \leftarrow t + 1$;
    $t_{end} \leftarrow t$;
    for $j = 1$ **to** $|\mathcal{L}|$ **do**
      find link l_i such that $\tau_i == j$; $f_{temp}(i) \leftarrow f_i$;
      for $t = t_{start}$ **to** t_{end} **do**
        if $T_i, R_i \notin \mathcal{T}_{\mathcal{S}_t} \cup \mathcal{R}_{\mathcal{S}_t}$ **and** $\rho\left(\mathbf{B}_{\mathcal{S}_t \cup \{l_i\}}\right) < \frac{1}{\gamma_0}$ **then**
          $f_{temp}(i) = f_{temp}(i) - 1$;
          if $f_{temp}(i) == 0$ **then**
            add l_i to sets $\{\mathcal{S}_t, \cdots, \mathcal{S}_{t-f_i+1}\}$; $\mathcal{L} \leftarrow \mathcal{L} \setminus \{l_i\}$;
            $\mathcal{L}^{k,q} \leftarrow \mathcal{L}^{k,q} \setminus \{l_i\}$
        else $f_{temp}(i) \leftarrow f_i$;
    for $t = t_{start}$ **to** t_{end} **do**
      allocate power $\boldsymbol{p}(t) = \left(\mathbf{I} - \gamma_0 \mathbf{B}_{\mathcal{S}_t}\right)^{-1} \cdot \mathbf{v}_{\mathcal{S}_t}$

4.2.2 Main Scheduling Loop

The main scheduling "for" loop is shown in Algorithm 3. It consists of two parts: guaranteed scheduling (lines 2 to 15 in Algorithm 3) and greedy scheduling (lines 16 to 23 in Algorithm 3). In the guaranteed scheduling, links with a shorter link length (i.e., a larger λ value) are considered first. In particular, in the kth iteration of the main scheduling "for" loop, the traffic demands of the links in subset $\mathcal{L}^k$ are satisfied completely in guaranteed scheduling. In addition, if there is slackness remaining in the SINR constraints after subset $\mathcal{L}^k$ is scheduled, the traffic demands of some of links with a longer link length (i.e., a smaller λ value) than the links in subset $\mathcal{L}^k$ are also satisfied in the greedy scheduling of the kth iteration by using power control. In this way, there will be less links in later rounds.

At the start of the kth iteration of the main scheduling "for" loop, we divide the Euclidean plane into hexagons with side length $A = W \cdot \frac{d_{\max}}{2^{k-1}}$, where

$$W = \left[6\gamma_0 \left(1 + \frac{2^\alpha}{(3\sqrt{3}-2)^\alpha(\alpha-2)}\right)\right]^{\frac{1}{\alpha}} + 1. \tag{4.1}$$

Color these hexagonal cells with three colors such that no two adjacent cells share the same color, as shown in Fig. 4.1. For $q = 1, 2, 3$, let $\mathcal{H}^{k,q} = \{H^{k,q}(m), 1 \leq m \leq \left|\mathcal{H}^{k,q}\right|\}$ denote the set of hexagons with color q in the kth iteration. Based on the locations of the receivers, the links in subset $\mathcal{L}^k$ are further divided into 3 subsets $\{\mathcal{L}^{k,q}, q = 1, 2, 3\}$. Subset $\mathcal{L}^{k,q}$ denotes the subset of links in $\mathcal{L}^k$ with receivers located in hexagons of color q (i.e., set $\mathcal{H}^{k,q}$). For m from 1 to $\left|\mathcal{H}^{k,q}\right|$, we can pick any link from $\mathcal{L}^{k,q}$ whose receiver is located within hexagon $H^{k,q}(m)$. If such a link does not exist, then no link is picked. The selected links in $\mathcal{H}^{k,q}$ (at most $\left|\mathcal{H}^{k,q}\right|$ of them) are guaranteed to form a feasible matching (see Theorem 2).

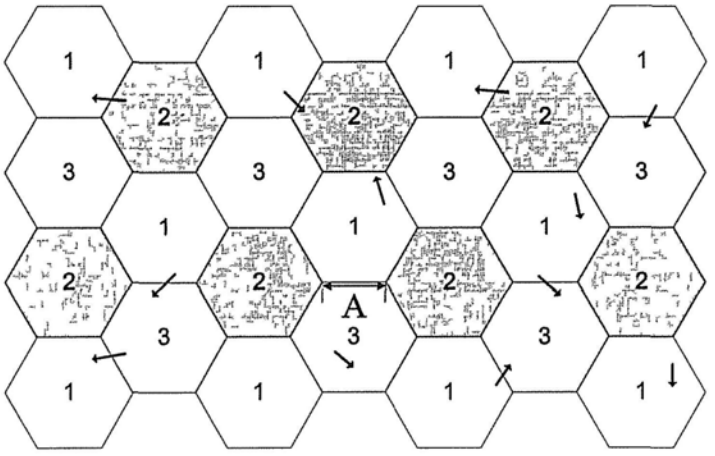

Figure 4.1: Hexagon coloring

In the qth iteration of the guaranteed scheduling part (lines 6 to 14 in Algorithm 3), the demands of links in subset $\mathcal{L}^{k,q}$ are completely satisfied as follows. The links whose receivers are in the same hexagon are activated one by one; each link finishes transmitting its own traffic for the current frame in consecutive time slots. On the other hand, those links whose receivers belong to different hexagons in $\{H^{k,q}(m), 1 \leq m \leq |\mathcal{H}^{k,q}|\}$ can transmit simultaneously. Let $F^{k,q}(m), 1 \leq m \leq |\mathcal{H}^{k,q}|$, denote the sum of the traffic of the links in subset $\mathcal{L}^{k,q}$ whose receivers are located in hexagon $H^{k,q}(m)$. Let $F^{k,q} = \max_m F^{k,q}(m)$. It is clear that the traffic of the links in subset $\mathcal{L}^{k,q}$ can be satisfied within $F^{k,q}$ time slots, say from time slot t_{start} to t_{end}. The links whose traffic are already satisfied are removed from sets $\mathcal{L}$ and $\mathcal{L}^{k,q}$.

In the guaranteed scheduling part of the GGS algorithm, each subset $\mathcal{L}^k$ is considered separately. The links which belong to the same subset $\mathcal{L}^k$ have almost equal length (differ by at most a factor of two). Consider the links

in subset $\mathcal{L}^k$, it is guaranteed that for every three hexagons, one link can be scheduled. The spatial reuse area is 3 times the hexagon area. The side length of the hexagon is proportional to the length of the links in subset $\mathcal{L}^k$. For the link subset with shorter length, the spatial reuse area is also reduced and the number of concurrent transmissions is increased. The hexagon coloring in the guaranteed scheduling is motivated by the square coloring proposed in [42]. By improving the square coloring to hexagon coloring, spatial ruse can be significantly improved. See section 4.4.2 for detailed comparison.

The links scheduled in the guaranteed scheduling part can use a sufficiently large common power for their transmissions (see the Proof of Theorem 2). Power control is not fully utilized in this part. The purpose of the greedy scheduling (lines 16 to 23 in Algorithm 3) is to "squeeze" more links in the time slots t_{start} to t_{end} using power control. Links in the updated set $\mathcal{L}$ are considered according to the τ_i value, i.e., a link with a larger traffic demand is considered first. A link l_i is selected to be active in f_i consecutive time slots if there exists f_i consecutive time slots from time slot t_{start} to t_{end} such that l_i and previously scheduled links form a feasible matching (both the Perron-Frobenius eigenvalue condition and the matching definition need to be satisfied for the new link set $\mathcal{S}_t \cup \{l_i\}$, as shown in line 19). After the greedy scheduling part, the links scheduled to transmit from t_{start} to t_{end} are finally determined. At last (lines 24 and 25), the transmission powers in each time slot are allocated according to equation (2.5).

The key idea of the GGS algorithm is to group links according to their link lengths. The links that have similar link lengths are scheduled together, and links that have different link lengths are scheduled separately. The purpose of doing so is to scale spatial reuse systematically. The spatial reuse area is proportional to the link length. Therefore, given the same area, more

links with shorter link length can be active simultaneously. In the greedy scheduling part of the GGS, by adopting power control, more links may be scheduled into the feasible matchings created in the guaranteed scheduling. Thus the number of concurrent transmissions can be further increased.

If we remove the consecutive transmission constraints in both the guaranteed scheduling part and the greedy scheduling part, the GGS algorithm still provides an efficient way to solve the power-controlled scheduling problem in which no consecutive transmission constraint is imposed.

4.2.3 Validity Analysis

In this subsection, we will show the validity of the GGS algorithm. Specifically, we will prove that the wireless links scheduled in each time slot in the guaranteed scheduling part (lines 6 to 14 in Algorithm 3) form a feasible matching. In each time slot, among the hexagons in $\mathcal{H}^{k,q}$, at most one link is selected in each hexagon. The receivers of the links selected in each time slot are located in different hexagons in $\mathcal{H}^{k,q} = \{H^{k,q}(m), 1 \leq m \leq |\mathcal{H}^{k,q}|\}$. We consider the case that in each hexagon $H^{k,q}(m)$ one link l_{i_m} is selected. The selected links are denoted by $\{l_{i_m}, 1 \leq m \leq |\mathcal{H}^{k,q}|\}$.

Theorem 2 *In the guaranteed scheduling, the links in* $\{l_{i_m}, 1 \leq m \leq |\mathcal{H}^{k,q}|\}$ *form a feasible matching.*

Proof: We first show that the selected links in $\{l_{i_m}, 1 \leq m \leq |\mathcal{H}^{k,q}|\}$ form a matching based on its definition (Definition 2). Then we show that the relative channel gain matrix corresponding to the matching $\{l_{i_m}, 1 \leq m \leq |\mathcal{H}^{k,q}|\}$ satisfies condition (2.4).

The receivers of the links selected in each time slot are located in different hexagons in $\mathcal{H}^{k,q} = \{H^{k,q}(m), 1 \leq m \leq |\mathcal{H}^{k,q}|\}$. We consider the case that in

each hexagon $H^{k,q}(m)$ one link l_{i_m} is selected. The selected links are denoted by $\{l_{i_m}, 1 \leq m \leq |\mathcal{H}^{k,q}|\}$. We first show that the links in $\{l_{i_m}, 1 \leq m \leq |\mathcal{H}^{k,q}|\}$ form a matching by its definition. The lengths of all the links in $\{l_{i_m}, 1 \leq m \leq |\mathcal{H}^{k,q}|\}$ range from $\frac{d_{\max}}{2^k}$ to $\frac{d_{\max}}{2^{k-1}}$. Consider link l_{i_m}. Its receiver R_{i_m} is in the hexagon $H^{k,q}(m)$. So the transmitter T_{i_m} must be located in the shadow area shown in Fig. 4.2 (a).

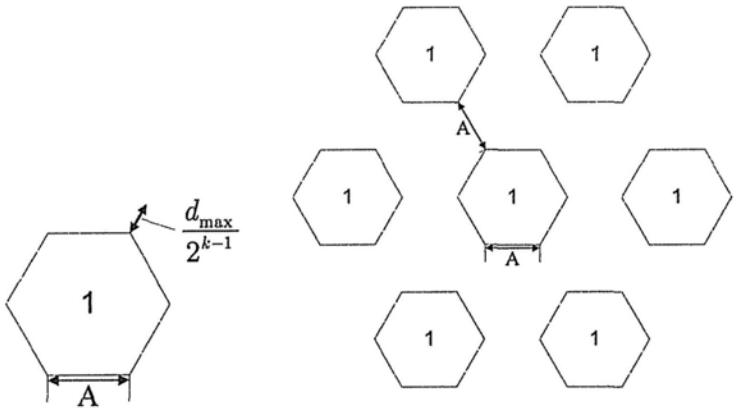

(a) The location of transmitter T_{i_m}

(b) The locations of transmitters of link l_{i_m} and the links whose receivers are located within $H^{k,q}(m)$'s first layer neighbor hexagons in $\mathcal{H}^{k,q}$.

Figure 4.2: The locations of the transmitters

The side length of the hexagon in set $\mathcal{H}^{k,q}$ is equal to $A = W \cdot \frac{d_{\max}}{2^{k-1}}$, where $W = \left\lceil 6\gamma_0 \left(1 + \frac{2^\alpha}{(3\sqrt{3}-2)^\alpha(\alpha-2)}\right)\right\rceil^{\frac{1}{\alpha}} + 1$. Given $\alpha > 2$ and $\gamma_0 \geq 1$, we know that $W > 2$. So the side length $A = W \cdot \frac{d_{\max}}{2^{k-1}} > 2 \cdot \frac{d_{\max}}{2^{k-1}}$. This means that the side length of each hexagon is greater than twice the longest link length. Consider hexagon $H^{k,q}(m)$ and all the other hexagons in $\mathcal{H}^{k,q}$, which are the hexagons with the same color as $H^{k,q}(m)$. These hexagons are located at different layers

of hexagon $H^{k,q}(m)$. If we represent hexagons in $\mathcal{H}^{k,q}$ by vertices in a graph and use an edge to connect two adjacent hexagons that have the same color, then the uth layer hexagons of $H^{k,q}(m)$ means the hexagons that are u hops away from hexagon $H^{k,q}(m)$ in the graph. Consider $H^{k,q}(m)$ and all its first layer neighbor hexagons in $\mathcal{H}^{k,q}$. The transmitters are located in different areas in the Euclidean plane as shown in the shadow areas in Fig. 4.2 (b). So, it is not possible for any link and its neighbor links to share a common node. Consider all the links in $\{l_{i_m}, 1 \leq m \leq |\mathcal{H}^{k,q}|\}$. It is easy to find that all the transmitters are located in different region of the Euclidean plane. So all the links in $\{l_{i_m}, 1 \leq m \leq |\mathcal{H}^{k,q}|\}$ are located in different region of the Euclidean plane. So the links $\{l_{i_m}, 1 \leq m \leq |\mathcal{H}^{k,q}|\}$ form a matching.

We then prove that the matching $\{l_{i_m}, 1 \leq m \leq |\mathcal{H}^{k,q}|\}$ is feasible by showing that its relative channel gain matrix satisfies condition (2.4). Consider any row of the channel gain matrix $\mathbf{B}$ corresponding to matching $\{l_{i_m}, 1 \leq m \leq |\mathcal{H}^{k,q}|\}$, for example the mth row. The sum of the mth row S_{row} is

$$S_{row}(m) = \sum_{n=1, n\neq m}^{|\mathcal{H}^{k,q}|} \frac{d^{-\alpha}(T_{i_n}, R_{i_m})}{d^{-\alpha}(T_{i_m}, R_{i_m})}.$$

$d(T_{i_m}, R_{i_m})$ is the link length of link l_{i_m} which satisfies $\frac{d_{\max}}{2^k} < d(T_{i_m}, R_{i_m}) \leq \frac{d_{\max}}{2^{k-1}}$. The receiver of link l_{i_m} is located in hexagon $H^{k,q}(m)$. $d(T_{i_n}, R_{i_m})$ is the distance between the transmitter of link l_{i_n} and the receiver of link l_{i_m} when $n \neq m$. Let $H^{k,q}(n) \in \mathcal{H}^{k,q}$ denote the hexagon in which the receiver of link l_{i_n} is located.

Let OO_1 denote the distance between the centers of hexagon $H^{k,q}(m)$ and its first layer neighbor hexagon. We can find that $\mathrm{OO}_1 = 3A$, where A is the side length of the hexagon. And there are a total of 6 hexagons in the first layer. Let OO_u, $(u \geq 2)$ denote the distance between the centers of the uth

layer hexagon and hexagon $H^{k,q}(m)$. We can find that $\mathrm{OO}_u \geq \frac{3\sqrt{3}}{2}uA$. And there are totally $6u$ hexagons in the uth layer.

If $H^{k,q}(n)$ is the first layer neighbor hexagon of $H^{k,q}(m)$, $d(T_{i_n}, R_{i_m})$ satisfies the following inequality:

$$\begin{aligned} d(T_{i_n}, R_{i_m}) &\geq \mathrm{OO}_1 - 2A - d(T_{i_n}, R_{i_n}) && (4.2)\\ &\geq 3A - 2A - d(T_{i_n}, R_{i_n}) && (4.3)\\ &\geq A - d(T_{i_n}, R_{i_n}) \geq W \cdot \frac{d_{\max}}{2^{k-1}} - \frac{d_{\max}}{2^{k-1}} && (4.4)\\ &\geq (W-1)\frac{d_{\max}}{2^{k-1}}. && (4.5) \end{aligned}$$

Because $d(T_{i_m}, R_{i_m}) \leq \frac{d_{\max}}{2^{k-1}}$, we have

$$\frac{d^{-\alpha}(T_{i_n}, R_{i_m})}{d^{-\alpha}(T_{i_m}, R_{i_m})} \leq \frac{\left((W-1)\frac{d_{\max}}{2^{k-1}}\right)^{-\alpha}}{\left(\frac{d_{\max}}{2^{k-1}}\right)^{-\alpha}} = \frac{1}{(W-1)^{\alpha}}.$$

If $H^{k,q}(n)$ is the uth layer neighbor hexagon of $H^{k,q}(m)$ $(u \geq 2)$, $d(T_{i_n}, R_{i_m})$ satisfies the following inequality:

$$\begin{aligned} d(T_{i_n}, R_{i_m}) &\geq \mathrm{OO}_u - 2A - d(T_{i_n}, R_{i_n}) && (4.6)\\ &\geq \left(\frac{3\sqrt{3}}{2}u - 2\right)A - d(T_{i_n}, R_{i_n}) && (4.7)\\ &\geq \left(\left(\frac{3\sqrt{3}}{2}u - 2\right)W - 1\right)\frac{d_{\max}}{2^{k-1}} \qquad (u \geq 2). && (4.8) \end{aligned}$$

Because $d(T_{i_m}, R_{i_m}) \leq \frac{d_{\max}}{2^{k-1}}$, we have

$$\begin{aligned} \frac{d^{-\alpha}(T_{i_n}, R_{i_m})}{d^{-\alpha}(T_{i_m}, R_{i_m})} &\leq \frac{\left(\left(\left(\frac{3\sqrt{3}}{2}u - 2\right)W - 1\right)\frac{d_{\max}}{2^{k-1}}\right)^{-\alpha}}{\left(\frac{d_{\max}}{2^{k-1}}\right)^{-\alpha}} && (4.9)\\ &= \frac{1}{\left(\left(\frac{3\sqrt{3}}{2}u - 2\right)W - 1\right)^{\alpha}} \qquad (u \geq 2). && (4.10) \end{aligned}$$

So the sum of the mth row satisfies the following inequality:

$$
\begin{aligned}
S_{row}(m) &= \sum_{n=1,n\neq m}^{|\mathcal{H}^{k,q}|} \frac{d^{-\alpha}(T_{i_n}, R_{i_m})}{d^{-\alpha}(T_{i_m}, R_{i_m})} \\
&\leq \frac{6}{(W-1)^{\alpha}} + \sum_{u=2}^{\infty} \frac{6u}{\left(\left(\frac{3\sqrt{3}}{2}u - 2\right)W - 1\right)^{\alpha}} \\
&\leq \frac{6}{(W-1)^{\alpha}} + \sum_{u=2}^{\infty} \frac{6u}{\left(\left(\frac{(3\sqrt{3}-2)W-1}{2}\right)u\right)^{\alpha}} \qquad (4.11) \\
&\leq \frac{6}{(W-1)^{\alpha}} + \frac{6}{\left(\frac{(3\sqrt{3}-2)W-1}{2}\right)^{\alpha}} \sum_{u=2}^{\infty} \frac{u}{u^{\alpha}} \\
&\leq \frac{6}{(W-1)^{\alpha}} + \frac{6}{\left(\frac{(3\sqrt{3}-2)W-1}{2}\right)^{\alpha}} \left(\sum_{u=2}^{\infty} \frac{1}{u^{\alpha-1}}\right) \\
&\leq \frac{6}{(W-1)^{\alpha}} + \frac{6}{\left(\frac{(3\sqrt{3}-2)W-1}{2}\right)^{\alpha}} \left(\frac{1}{\alpha-2}\right) \qquad (4.12) \\
&< \frac{6}{(W-1)^{\alpha}} + \frac{6}{\left(\left(\frac{3\sqrt{3}-2}{2}\right)(W-1)\right)^{\alpha}} \left(\frac{1}{\alpha-2}\right) \qquad (4.13) \\
&= \frac{6}{(W-1)^{\alpha}} \left(1 + \frac{2^{\alpha}}{\left(3\sqrt{3}-2\right)^{\alpha}} \left(\frac{1}{\alpha-2}\right)\right) \\
&= \frac{6\left(1 + \frac{2^{\alpha}}{\left(3\sqrt{3}-2\right)^{\alpha}} \left(\frac{1}{\alpha-2}\right)\right)}{\left(\left(6\gamma_0\left(1 + \frac{2^{\alpha}}{(3\sqrt{3}-2)^{\alpha}(\alpha-2)}\right)\right)^{\frac{1}{\alpha}} + 1 - 1\right)^{\alpha}} \qquad (4.14) \\
&= \frac{1}{\gamma_0},
\end{aligned}
$$

where (4.11) follows because $\left(\frac{3\sqrt{3}}{2}u - 2\right)W - 1 \geq \left(\frac{(3\sqrt{3}-2)W-1}{2}\right)u$, $\forall u \geq 2$ and $W > 2$; (4.12) follows from a bound on Riemann's zeta function; (4.13) follows because $\frac{(3\sqrt{3}-2)W-1}{2} > \left(\frac{3\sqrt{3}-2}{2}\right)(W-1)$ for all W; and (4.14) follows from the definition of W in (4.1). This means the sum of any row of matrix

$\mathbf{B}$ is less than $\frac{1}{\gamma_0}$. According to Proposition 3, we can find that

$$\rho(\mathbf{B}) \leq \max(S_{row}) < \frac{1}{\gamma_0}.$$

So condition (2.4) is satisfied. Therefore, $\{l_{i_m}, 1 \leq m \leq \left|\mathcal{H}^{k,q}\right|\}$ is a feasible matching.

One thing to notice is that $\{l_{i_m}, 1 \leq m \leq \left|\mathcal{H}^{k,q}\right|\}$ can be feasible if every transmitter in $\{T_{i_m}, 1 \leq m \leq \left|\mathcal{H}^{k,q}\right|\}$ uses a common, but sufficiently large transmit power P_t. If every transmitter uses the same transmit power, then actually $S_{row}(m)$ is the ratio of interference power to signal power $\frac{P_S}{P_I}$ at receiver R_{i_m}. To simplify notations, let Y denote $\frac{6}{(W-1)^\alpha} + \frac{6}{\left(\frac{(3\sqrt{3}-2)W-1}{2}\right)^\alpha}\left(\frac{1}{\alpha-2}\right)$, which is a function of W and γ_0 as given in (4.12). Because $S_{row}(m) \leq Y$, so the total interference at R_{i_m} satisfies $P_I \leq Y \cdot P_S$. Because the signal power $P_S = P_t G_0 d^{-\alpha}(T_{i_m}, R_{i_m})$, so the SINR at receiver R_{i_m} satisfies

$$\frac{P_S}{P_I + \eta_{i_m}} \geq \frac{P_t G_0 d^{-\alpha}(T_{i_m}, R_{i_m})}{Y \cdot P_t G_0 d^{-\alpha}(T_{i_m}, R_{i_m}) + \eta_{i_m}}. \tag{4.15}$$

The requirement for the right hand side of (4.15) to be no less than γ_0 is

$$P_t \geq \frac{\gamma_0 \eta_{i_m}}{G_0\left(1 - Y\gamma_0\right)} d^\alpha(T_{i_m}, R_{i_m}).$$

Therefore if we use a common transmit power P_t which satisfies

$$P_t \geq \left(\frac{\gamma_0}{G_0\left(1 - Y\gamma_0\right)}\right) \max_{1 \leq m \leq \left|\mathcal{H}^{k,q}\right|} \left(\eta_{i_m} \cdot d^\alpha(T_{i_m}, R_{i_m})\right)$$

then $\{l_{i_m}, 1 \leq m \leq \left|\mathcal{H}^{k,q}\right|\}$ can be feasible. □

In Theorem 2, we prove that if in each hexagon $H^{k,q}(m)$ at most one link is selected, the selected links $\{l_{i_m}, 1 \leq m \leq \left|\mathcal{H}^{k,q}\right|\}$ form a feasible matching. In the guaranteed scheduling part, it could be the case that in some hexagons we do not pick any link. In this case, it is clear that the selected set of links still form a feasible matching according to Proposition 2. So the links which are scheduled in each time slot in the guaranteed scheduling part form a feasible matching.

4.3 Analysis of GGS Algorithm

In this section, we present two key features of the GGS algorithm. First, it has a bounded approximation ratio [69,70] relative to the optimal scheduling algorithm. Second, it has a polynomial time complexity.

Given any instance of the JPS-CC problem, let V_{GGS} and V_{opt} denote the frame lengths obtained by the GGS algorithm and the optimal scheduling algorithm, respectively. The approximation ratio of the GGS algorithm is defined by $\frac{V_{GGS}}{V_{opt}}$, which is no smaller than 1. An algorithm with a smaller approximation ratio reaches a solution closer to the optimal. Notice that the precise values of V_{GGS} and V_{opt} are difficult to obtain. In particular, we can not compute V_{opt} in polynomial time. Next we will find an upper bound of V_{GGS} and an lower bound of V_{opt}, which lead to an upper bound on the approximation ratio.

In GGS, $\mathcal{L}$ is partitioned into K subsets, $\{\mathcal{L}^k, 1 \leq k \leq K\}$, according to link lengths. Each subset $\mathcal{L}^k$ is further divided into 3 subsets, $\{\mathcal{L}^{k,q}, q = 1,2,3\}$, based on the locations of the receivers. Each hexagon $H^{k,q}(m)$ contains a number of links belonging to subset $\mathcal{L}^{k,q}$. $F^{k,q}(m)$ is the total traffic of the links in $H^{k,q}(m)$ and $F^{k,q}$ is the maximum traffic among all hexagons in $\mathcal{H}^{k,q}$. Let $F^k = \max_{q=1,2,3}\{F^{k,q}\}$ and $F_{\max} = \max_{k=1,\cdots,K}\{F^k\}$.

Lemma 2 *The GGS algorithm achieves a frame length no larger than* $3KF_{\max}$.

Proof: We consider the worst case in which no link is selected in the greedy scheduling part at all. Since $F^{k,q}$ is the maximum traffic among all hexagons in $\mathcal{H}^{k,q}$, the total traffic demands of the links in subset $\mathcal{L}^{k,q}$ can be satisfied within $F^{k,q}$ time slots in the kth iteration of the guaranteed

scheduling part (lines 5 to 15 in Algorithm 3). So the frame length of the GGS algorithm satisfies the following inequality:

$$V_{GGS} \leq \sum_{k=1}^{K} \sum_{q=1}^{3} F^{k,q} \leq \sum_{k=1}^{K} 3F^{k} \leq 3KF_{\max}. \tag{4.16}$$

□

Let $\hat{H}$ denote the hexagon with the maximum traffic sum $F_{\max}$ over all hexagons generated. Suppose the hexagon $\hat{H}$ is in the kth iteration of the main scheduling "for" loop and it is colored with color q. The links whose receivers are located in the hexagon $\hat{H}$ are denoted by $\mathcal{L}^{k,q}(\hat{H})$. Let $N_{\max}$ denote the maximum number of links in subset $\mathcal{L}^{k,q}(\hat{H})$ which can be active simultaneously. In the worst case of GGS, no link is selected in the greedy scheduling, and links within the same hexagon do not scheduled to transmit together in the guaranteed scheduling part. However, in reality, it is possible for some of the links within the same hexagon to transmit together in an optimal schedule. We need to consider what is the best that an optimal scheduling could achieve. Therefore, finding an upper bound on $N_{\max}$ is crucial to achieve a bounded approximation ratio of GGS. $N_{\max}$ is the maximum number of concurrent links when *power control* is considered. When power control is allowed, each transmitter can use a different transmit power. It is not possible to calculate the total interference power as in the wireless network that uses fixed transmit power [42]. Fortunately we successfully use two novel methods to upper bound $N_{\max}$.

To simplify notations, we define

$$N_1 = \left\lfloor \frac{1}{\gamma_0} \left(2\left(2W+1\right)\right)^{\alpha} + 1 \right\rfloor, \tag{4.17}$$

$$N_2 = \begin{cases} \left\lfloor 3\left(\frac{2W}{\sqrt[\alpha]{\gamma_0}-1}\right)^2 + 3\left(\frac{2W}{\sqrt[\alpha]{\gamma_0}-1}\right) + 1 \right\rfloor, & \text{if } \gamma_0 > 1 \\ \infty, & \text{otherwise} \end{cases} \tag{4.18}$$

and

$$N = \min\{N_1, N_2\} \tag{4.19}$$

N_1 and N_2 denote the upper bounds of $N_{\max}$ obtained by two different methods

Lemma 3 *The maximum number of concurrent transmissions $N_{\max}$ in the hexagon $\hat{H}$ is upper bounded by N*

Proof: First we show that $N_{\max}$ is upper bounded by N_1 We prove this by contradiction Consider any two links l_i and l_j in subset $\mathcal{L}^{k,q}(\hat{H})$ Since both the receivers R_i and R_j are located in hexagon $\hat{H}$, we have the following two inequalities

$$\frac{d_{\max}}{2^k} < d(T_i, R_i) \leq \frac{d_{\max}}{2^{k-1}},$$

$$d(T_j, R_i) \leq 2A + \frac{d_{\max}}{2^{k-1}} = (2W+1)\ \frac{d_{\max}}{2^{k-1}}$$

So any non-zero element in the relative channel gain matrix $\mathbf{B}$ satisfies the following inequality

$$\frac{d^{-\alpha}(T_j, R_i)}{d^{-\alpha}(T_i, R_i)} > \frac{\left((2W+1)\ \frac{d_{\max}}{2^{k-1}}\right)^{-\alpha}}{\left(\frac{d_{\max}}{2^k}\right)^{-\alpha}} = \frac{1}{(2(2W+1))^{\alpha}}$$

Suppose $N_1 + 1$ links can be active simultaneously There are N_1 non-zero elements in each row of the relative channel gain matrix $\mathbf{B}$ We can find that

for any row, the row sum S_{row} satisfies the following inequality:

$$S_{row} > N_1 \cdot \frac{1}{(2\,(2W+1))^{\alpha}} \tag{4.20}$$

$$> \left(\frac{1}{\gamma_0}\,(2\,(2W+1))^{\alpha}\right) \cdot \frac{1}{(2\,(2W+1))^{\alpha}} \tag{4.21}$$

$$= \frac{1}{\gamma_0}. \tag{4.22}$$

According to Proposition 3 we find that

$$\rho(\mathbf{B}) \geq \min(S_{row}) > \frac{1}{\gamma_0}.$$

So condition (2.4) can not be satisfied, which means $N_1 + 1$ number of links can not be active simultaneously. This is contradictory to our assumption. So we have

$$N_{\max} \leq N_1. \tag{4.23}$$

Next we show that $N_{\max}$ is also upper bounded by N_2. Consider any two links l_i and l_j in subset $\mathcal{L}^{k,q}(\hat{H})$. We have the following four inequalities:

$$\frac{d_{\max}}{2^k} < d(T_i, R_i) \leq \frac{d_{\max}}{2^{k-1}}, \tag{4.24}$$

$$\frac{d_{\max}}{2^k} < d(T_j, R_j) \leq \frac{d_{\max}}{2^{k-1}}, \tag{4.25}$$

$$d(T_i, R_j) \leq d(R_i, R_j) + d(T_i, R_i), \tag{4.26}$$

$$d(T_j, R_i) \leq d(R_i, R_j) + d(T_j, R_j). \tag{4.27}$$

Inequalities (4.26) and (4.27) are the triangle inequalities.

The Perron-Frobenius eigenvalue corresponding to the two-link channel-gain matrix (i.e., the channel-gain matrix of l_i and l_j) satisfies the following

inequality:

$$\rho(\mathbf{B}_2) = \sqrt{\frac{d(T_i,R_j)^{-\alpha}\cdot d(T_j,R_i)^{-\alpha}}{d(T_j,R_j)^{-\alpha}\cdot d(T_i,R_i)^{-\alpha}}} \tag{4.28}$$

$$\geq \sqrt{\left(1+\frac{d(R_i,R_j)}{d(T_i,R_i)}\right)^{-\alpha}\left(1+\frac{d(R_i,R_j)}{d(T_j,R_j)}\right)^{-\alpha}} \tag{4.29}$$

$$> \left(1+\frac{d(R_i,R_j)}{\frac{d_{\max}}{2^k}}\right)^{-\alpha}. \tag{4.30}$$

If l_i and l_j can be active simultaneously, condition $\rho(\mathbf{B_2}) < \frac{1}{\gamma_0}$ needs to be satisfied, which means the following inequality must be satisfied

$$\left(1+\frac{d(R_i,R_j)}{\frac{d_{\max}}{2^k}}\right)^{-\alpha} < \frac{1}{\gamma_0}.$$

When $\gamma_0 \leq 1$, the above equation is always satisfied, in which case we define $N_2 = \infty$. When $\gamma_0 > 1$, there is a minimum distance requirement on the distance between R_i and R_j:

$$d(R_i,R_j) > (\gamma_0{}^{\frac{1}{\alpha}} - 1)\frac{d_{\max}}{2^k}, \quad (\gamma_0 > 1).$$

If $N_{\max}$ number of links can be active simultaneously, according to Proposition 2, we know that any two links of these $N_{\max}$ links can be active simultaneously. This means the distance of any two receivers should be greater than $(\gamma_0{}^{\frac{1}{\alpha}} - 1)\frac{d_{\max}}{2^k}$. We know that all the receivers are located in the hexagon $\hat{H}$ with side length A. Reference [71] gives a tight upper bound on the number of nodes packed in a Jordan polygon with minimum distance requirement. The bound is related to both the area and the perimeter of the Jordan polygon. When applying the result in [71] to our problem, we have

$$N_{\max} \leq \left\lfloor 3\left(\frac{2W}{\gamma_0^{\frac{1}{\alpha}}-1}\right)^2 + 3\left(\frac{2W}{\gamma_0^{\frac{1}{\alpha}}-1}\right) + 1 \right\rfloor, (\gamma_0 > 1). \tag{4.31}$$

So $N_{\max}$ is also upper bounded by N_2.

According to (4.23) and (4.31), we know $N_{\max}$ is upper bounded by the minimum of N_1 and N_2:

$$N_{\max} \leq \min\{N_1, N_2\} = N.$$

□

Theorem 3 *The approximation ratio of the GGS algorithm is at most* $3KN$.

Proof: Consider the links in subset $\mathcal{L}^{k,q}(\hat{H})$. The number of time slots that an optimal scheduling algorithm needs to satisfy the traffic demands of the links in subset $\mathcal{L}^{k,q}(\hat{H})$ can not be less than $\frac{F_{\max}}{N_{\max}}$. Because $\mathcal{L}^{k,q}(\hat{H})$ is only a subset of the total wireless link set $\mathcal{L}$, the number of time slots that an optimal scheduling algorithm needs to schedule all the links in $\mathcal{L}$ satisfies the following inequality:

$$V_{opt} \geq \frac{F_{\max}}{N_{\max}} \geq \frac{F_{\max}}{N}. \tag{4.32}$$

The physical meaning of N is the upper bound of the maximum number of concurrent transmissions in one particular hexagon. According to equations (4.17), (4.18), and (4.19), N is a constant dependent on the SINR requirement γ_0 and the path loss exponent α.

In Lemma 2, we show that the upper bound on the total number of time slots of the GGS algorithm is $3KF_{\max}$. Here $K = \left\lfloor \log_2 \frac{d_{\max}}{d_{\min}} \right\rfloor + 1$, which defines the length diversity of the links in the network. So the bound of the approximation ratio can be derived as follows:

$$\frac{V_{GGS}}{V_{opt}} \leq \frac{3KF_{\max}}{\frac{F_{\max}}{N}} \leq 3KN. \tag{4.33}$$

□

Several remarks are in order for Theorem 3:

1. The approximation ratio bound of the GGS algorithm has a good scalability property: it is only related to the maximum number of concurrent transmissions in one hexagon, thus independent of either the total area of the network or the total number of links in the network.

2. Since we do not make any assumption on the distribution of the links when we derive the approximation ratio of $3KN$, Theorem 3 works for any network topology.*

3. Even if we do not impose the consecutive transmission constraints, (4.16) is still a valid upper bound on V_{GGS} and (4.32) is still a valid lower bound on V_{opt}. So Theorem 3 is valid with or without consecutive transmission constraints.

We are aware that the approximation ratio bound for GGS is loose. This is mainly limited by the bounding techniques on $N_{\max}$. For example, if $\gamma_0 = 10$ and $\alpha = 4$, which are typical for wireless communications, then we have $N_1 = 9041$, $N_2 = 321$, and $N = \min\{N_1, N_2\} = N_2 = 321$. Although N_2 is a tighter bound compared with N_1 given the parameters, it is still a loose bound on $N_{\max}$. And this leads to the a loose approximation ratio bound for GGS. For example, if the link length diversity $K = 1$, the approximation ratio is $3KN = 963$. When power control is considered, bounding $N_{\max}$ is difficult, and we are the first to succeed in bounding $N_{\max}$. Finding a tight bound on $N_{\max}$ would be an interesting but challenging problem for further study in the future. Another thing to notice is that although the approximation ratio bound for GGS is loose, the actual performance of GGS is relatively good (see simulation results in section 4.4).

*Given the network topology, it is possible to further reduce N by examining the specific hexagon with the maximum number of links.

Finally, we study the time complexity of the GGS algorithm. Define $F_{total} = \sum_{i=1}^{|\mathcal{L}|} f_i$, which is the total traffic demands of the links in the network.

Theorem 4 (Time Complexity) *The GGS algorithm is a polynomial-time algorithm with complexity* $O(K \cdot F_{total} \cdot |\mathcal{L}|^4)$.

Proof: We examine the time complexity of each part in the GGS algorithm. The GGS contains the initial step (lines 1 to 3 in Algorithm 2) and the main scheduling "for" loop.

The initial step contains ordering the links and assigning two values to each link in set $\mathcal{L}$, and has a complexity of $O(|\mathcal{L}| \log_2 |\mathcal{L}|)$.

Each iteration of the main scheduling "for" loop consists of the guaranteed scheduling (lines 5-15 in Algorithm 3), the greedy scheduling (lines 16-23 in Algorithm 3), and the power allocation (lines 24-25 in Algorithm 3).

The guaranteed scheduling (lines 5-15 in Algorithm 3) can be solved by finding the color of the hexagon that each link belongs to. For each link, this can be done in a constant time. The number of links to be considered in the guaranteed scheduling is no larger than $|\mathcal{L}|$, so the guaranteed scheduling requires a complexity of $O(|\mathcal{L}|)$.

The number of time slots generated in the guaranteed scheduling is at most F_{total} In the greedy scheduling (lines 16-23 in Algorithm 3), we need to check each link in the remaining set whether it can be "squeezed" into the feasible matchings obtained in the guaranteed scheduling part For each considered link, we need at most F_{total} checking of the feasibility of a set of links. Checking whether a set of links form a feasibility matching requires the computation of the Perron-Frobenius eigenvalue, and thus has a complexity of $O(|\mathcal{L}|^3)$ So a complexity of $O(F_{total} \cdot |\mathcal{L}|^3)$ is needed for each considered link. There are at most $|\mathcal{L}|$ links to be considered. So the greedy scheduling

totally requires a complexity of $O(F_{total} \cdot |\mathcal{L}|^4)$.

The power allocation (lines 24-25 in Algorithm 3) requires a complexity of $O(F_{total} \cdot |\mathcal{L}|^3)$ (because the computation of the inverse matrix requires a complexity of $O(|\mathcal{L}|^3)$).

So each iteration of the main scheduling "for" loop requires a complexity of $O(|\mathcal{L}| + F_{total} \cdot |\mathcal{L}|^4 + F_{total} \cdot |\mathcal{L}|^3)$, which is equivalent to $O(F_{total} \cdot |\mathcal{L}|^4)$. Since there all total $3K$ iterations of the main scheduling "for" loop, the main scheduling "for" loop can be accomplished with a complexity of $O(K \cdot F_{total} \cdot |\mathcal{L}|^4)$.

Therefore, the overall complexity of the GGS algorithm is $O(|\mathcal{L}| \log_2 |\mathcal{L}| + K \cdot F_{total} \cdot |\mathcal{L}|^4)$, which is equivalent to $O(K \cdot F_{total} \cdot |\mathcal{L}|^4)$. So the GGS algorithm is a polynomial-time algorithm. □

4.4 Numerical Results

In this section, we present numerical results of the GGS algorithm to gain further insights on how consecutive transmission and power control influence the network performance. In our simulations, random network topologies are generated. The transmitters are uniformly distributed in a square area of $2000m \times 2000m$. The length of each link ranges from 10 to 50 meters. Each receiver is randomly located between $2m$ and $60m$ from its corresponding transmitter. Link traffic demands are uniformly distributed in the set $[1, 3, 5, \cdots, 19]$ with an average value of 10 time slots.

4.4.1 The Influence of Consecutive Scheduling

Consecutive scheduling specified in some standard such as 802.16. In this case, we have no choice but to impose the requirement. However, even if

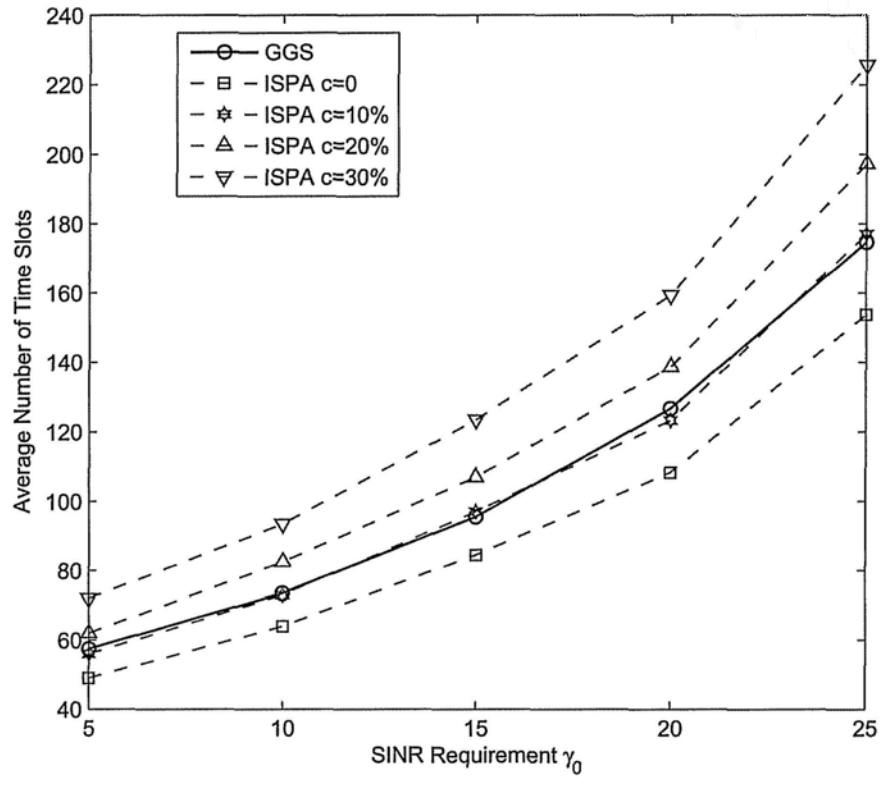

Figure 4.3: The average frame lengths of the GGS algorithm compared to the ISPA algorithm with different choices of the reduction ratio c (the number of links= 500, $\alpha = 4$)

consecutive scheduling is not required a priori, it may still be desirable if the overhead due to fragmented, non-consecutive, scheduling is large. An interesting question is at what point consecutive scheduling becomes more desirable than non-consecutive scheduling. We conduct simulation studies to gain a better understanding of this question. Note that finding the optimal solutions to the joint power control and scheduling problem (with or without consecutive transmission constraint) for large-size networks needs a very long runtime, because the problem is NP-hard. Therefore, for large-size networks, we do not benchmark our heuristic algorithm against the optimal algorithm. Instead, we compare the performance of our GGS, which impose consecutive transmission to that of the Integrated Scheduling and Power control Algorithm (ISPA) proposed in [58]. As far as we know, ISPA has the best performance among existing power-controlled non-consecutive algorithms.

On one hand, given the same traffic demands, consecutive transmission constraint may result in an increase of frame length. On the other hand, the overhead at the MAC layer can be reduced. This is mainly due to two reasons as discussed in section 4.1. First, the guard time of the time slots allocated to the same links can be used for data transmission in consecutive scheduling. Second, the header information can be compressed when consecutive transmissions consist of traffic belonging to the same flow. Let c denote the reduction ratio of the overhead at the MAC layer. Let f_i and e_i denote the number of time slots required on link l_i with consecutive scheduling and without consecutive scheduling, respectively. The reduction ratio c is defined by

$$c = \frac{e_i - f_i}{e_i} \times 100\%. \tag{4.34}$$

Given f_i, the traffic demand without consecutive constraint can be calculated by $e_i = \frac{f_i}{1-c}$.

We simulate random wireless networks with 500 links and the path loss exponent $\alpha = 4$. Figure 4.3 shows the average frame lengths of the GGS algorithm compared to the ISPA algorithm with different choices of the reduction ratio c. We find that the comparison between consecutive scheduling and non-consecutive scheduling is influenced by the overhead reduction ratio c. We see that GGS needs longer frame length than ISPA if the reduction ratio $c = 0$. This is the case, however, only if we do not consider the benefit of overhead reduction at the MAC layer due to consecutive transmission constraints. When the reduction ratio $c = 10\%$, the GGS algorithm and the ISPA algorithm have similar performance. The GGS algorithm outperforms the ISPA algorithm when the reduction ratio c is further increased. At $\gamma_0 = 25dB$, the GGS algorithm achieves a frame length reduction of more than 11.5% and 22.6% when $c = 20\%$ and $c = 30\%$, respectively. Under the particular choice of network parameters here, if using consecutive transmission can reduce the MAC overhead by more than 10%, then consecutive scheduling achieves better network performance than the traditional joint power control and scheduling problem without consecutive constraint. This physical meaning is that if the MAC overhead reduction ratio c is large, the consecutive transmission scheduling needs shorter frame length than the non-consecutive scheduling. For example, for the packet that has short payload, the MAC overhead reduction is significant if using consecutive transmission scheduling, and the total time slots needed can be reduced.

4.4.2 Performance with and without Power Control

GGS consists of two scheduling parts: the guaranteed scheduling part and the greedy scheduling part. In the guaranteed scheduling part, the scheduled links can be active with the same transmitter power. In the greedy scheduling,

power control allows more links to be added. We investigate the performances of the following three algorithms:

1. AAS (an existing algorithm without power control): the Approximate Algorithm for the Scheduling problem proposed in [42].

2. GS (our algorithm without power control): the Guaranteed Scheduling part (lines 2-15 in Algorithm 3) of Algorithm 2.

3. GGS (our algorithm with power control): the complete Algorithm 2.

We first study the network performance of GS which does not use power control. Then, we study the performance of the GGS to gain further insights into how power control can improve the network performance.

In Fig. 4.4, we compare the *spatial reuse ratio* of the hexagon coloring in the GS algorithm with the square coloring in the AAS algorithm computed based on theoretical analysis. This is motivated by the fact that both the two algorithms do not use power control, and the main difference is in their coloring mechanisms. Here the spatial reuse ratio is defined as the ratio of the smallest spatial reuse area in AAS (four squares) to the one in GS (three hexagons). Because the effects of the cumulative interference are treated differently in the two coloring schemes, the sides of the square and the hexagon are different even given the same α and γ_0. A large value of spatial reuse ratio means that our GS algorithm offers better performance (since it can accommodate more links within a given area). Figure 4.4 shows the spatial reuse ratio as a function of the SINR requirements γ_0. Different curves represent different choices of path loss exponent α. We can see that the spatial reuse ratios are greater than 1 (i.e., our proposed algorithm is better) for $\gamma_0 \geq 5dB$ and $\alpha \geq 2.5$. These parameter settings are typical for wireless communications. When $\gamma_0 = 10dB$ and $\alpha = 4$, the spatial reuse ratio is more than 1.5.

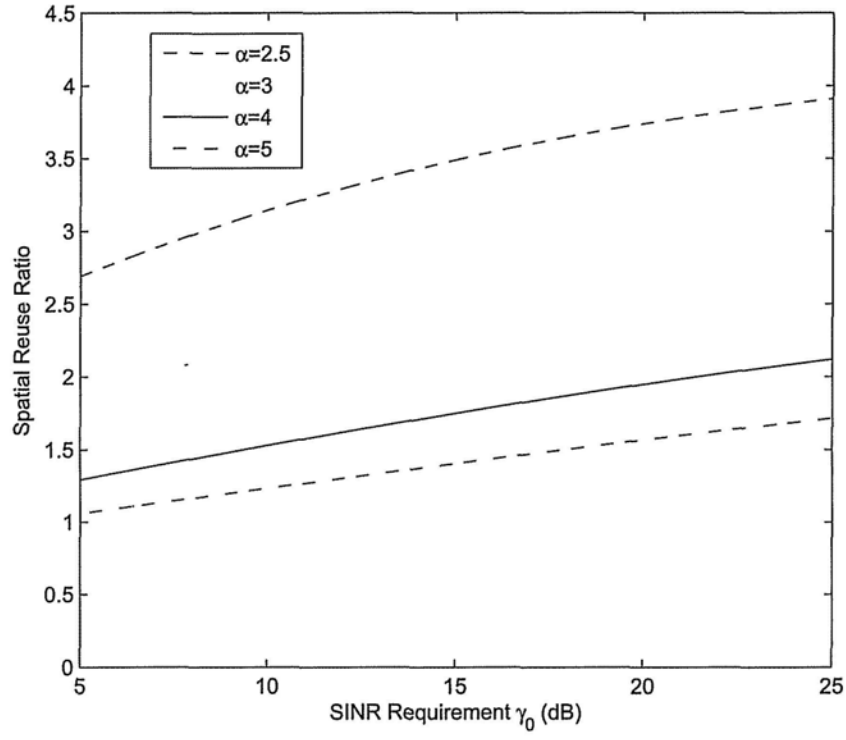

Figure 4.4: Analytical results of spatial reuse ratio

Also, the spatial reuse ratio increases when γ_0 increases or α decreases. This is the case where the separation among links must be larger to meet the SINR targets. For a fixed range of link length, although the areas of both squares and hexagons increase, the hexagons expand much slower which leads to a larger spatial reuse ratio.

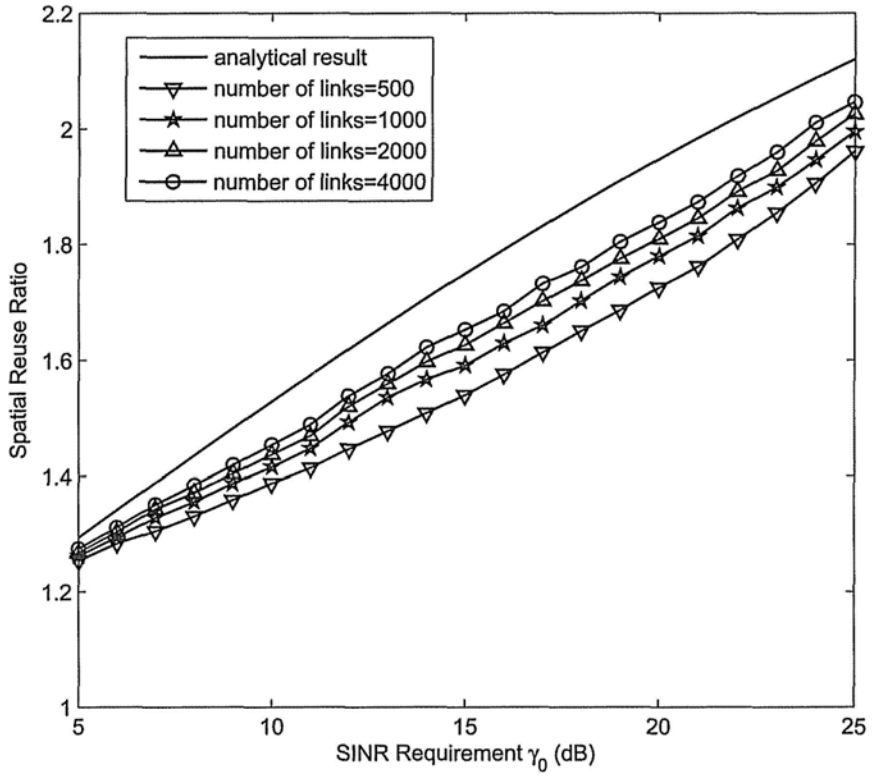

Figure 4.5: Spatial reuse ratio (simulations v.s. analysis) with $\alpha = 4$

In Fig. 4.5, we compare the simulated performance ratio between GS and AAS with the theoretical results in Fig. 4.4. Under the assumption that

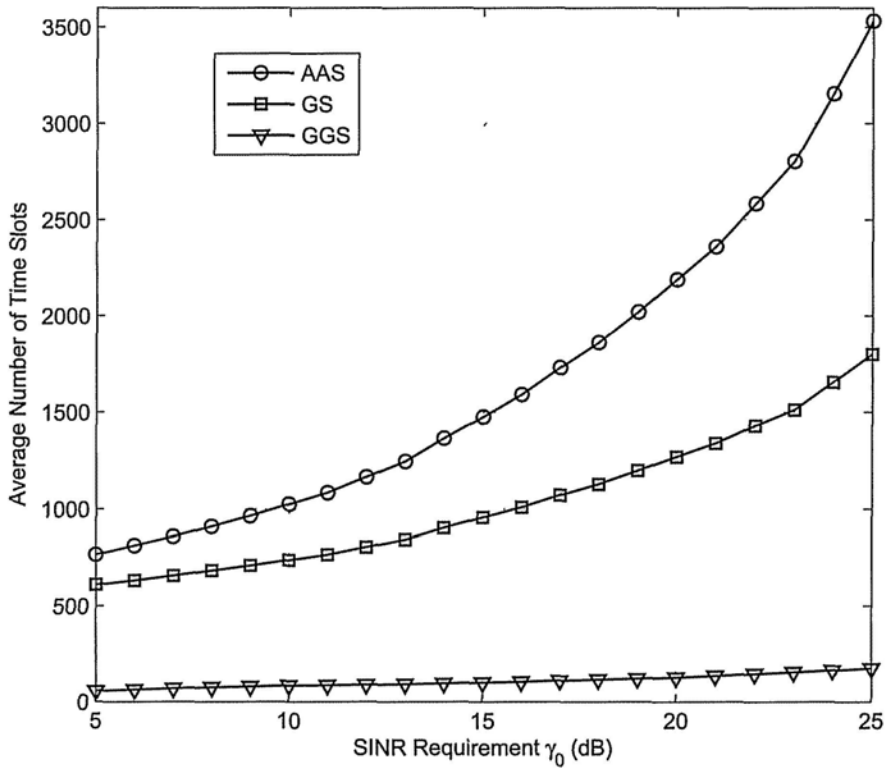

Figure 4.6: Average frame lengths (the number of links= 500, $\alpha = 4$)

$\alpha = 4$, Fig. 4.5 shows that the trends of the simulated results closely follow the theoretical results. It also shows that the gap between the simulation and theoretical results becomes smaller when the network becomes denser. The gap is likely due to fact that a link which could be scheduled in theory does not exist in practice. The probability of this happening decreases as the network becomes more dense.

Figure 4.6 shows the average frame lengths of these three algorithms as a function of SINR requirements γ_0. We simulate random wireless networks with 500 links and the path loss exponent $\alpha = 4$. It is clear from Fig. 4.6 that GGS outperforms GS, which in turn outperforms AAS. The better spatial reuse demonstrated in Fig. 4.4 explains why GS is better than AAS. By adding a greedy power control component, GGS achieves further improvement over GS. The improvement becomes more significant when the SINR requirement increases. The average frame length of GGS grows much slower than GS and AAS with SINR target increase. At $\gamma_0 = 25dB$, using AAS algorithm as the base line, GS achieves a frame length reduction of more than 50% and GGS achieves more than 90%.

4.5 Summary

In this chapter, we have considered the problem of joint power control and minimum-frame-length scheduling in wireless networks, under the physical interference model and subject to consecutive transmission constraints. As far as we know, this problem has not been studied before. We proposed a polynomial-time algorithm, called the Guaranteed and Greedy Scheduling (GGS), for this problem. GGS has a provable upper bound for its approximation ratio. GGS and its approximation ratio are applicable to any network

topology. Furthermore, GGS can be easily modified to solve the power-controlled scheduling without consecutive transmission constraint, and the provable upper bound for the approximation ratio remains valid. Through extensive simulations, we observe that consecutive scheduling can achieve shorter frame length than non-consecutive scheduling if consecutive transmission can reduce MAC overhead by more than 10%. Furthermore, power control can significantly improve the network performance. Compared to the AAS algorithm that uses a common fixed transmit power, GGS achieves a frame length reduction of more than 90%.

Chapter 5

Distributed Scheduling Algorithm

5.1 Introduction

5.1.1 Overview

In this chapter, we move to distributed scheduling under the physical interference model. As discussed in the previous chapters, in order to optimizing spatial reuse and network throughput, it is desirable to allow as many links as possible to transmit together in an interference-safe (or collision-free) manner. In the literature, most studies on interference-safe transmissions are under the coordination of a centralized STDMA (Spatial-reuse Time Division Multiple Access) (e.g., see [54–56, 63–68, 72–84]). Less well understood is the issue of interference-safe transmissions under the coordination of a distributed scheduling protocol.

The CSMA (Carrier-Sense Multiple-Access) protocol, such as IEEE 802.11, is the most widely adopted distributed scheduling protocol in practice. As the growth of 802.11 network deployments continues unabated, we

are witnessing an increasing level of mutual interference among transmissions in such networks. It is critical to establish a rigorous conceptual framework upon which effective solutions to interference-safe transmissions can be constructed.

Within this context, this chapter has three major contributions listed as follows (more detailed overview is given in the succeeding paragraphs):

1. We propose the concept of a *safe carrier-sensing range* that guarantees interference-safe transmissions in CSMA networks under the *physical interference model.*

2. We show that the concept is implementable using a very simple Incremental-Power Carrier-Sensing (IPCS) mechanism.

3. We demonstrate that implementation of the safe carrier-sensing range under IPCS can significantly improve spatial reuse and network throughput as compared to the conventional absolute-power carrier sensing mechanism.

Regarding 1), this work considers the physical interference model [40], in which the interference at a receiver node i consists of the cumulative power received from all the other nodes that are currently transmitting (except its own transmitter). This model is known to be more practical, but is much more difficult to analyze than the widely studied protocol interference model (also termed the pairwise interference model in [32]) in the literature. Under the physical interference model, a set of simultaneously transmitting links are said to be interference-safe if the SINRs (Signal-to-Interference-plus-Noise Ratios) at the receivers of all these links are above a threshold. Given a set of links $\mathcal{L}$ in the network, there are many subsets of links, $\mathcal{S} \subset \mathcal{L}$, that are interference-safe. The set of all such subsets

$\mathcal{F} = \{\mathcal{S} \mid$ the SINR requirements of all links are satisfied$\}$ constitutes the feasible interference-safe state space. For centralized STDMA, all subsets are available for scheduling, and a STDMA schedule is basically a sequence $(\mathcal{S}_t)_{t=1}^{n}$ where each $\mathcal{S}_t \in \mathcal{F}$. For CSMA, because of the random and distributed nature of the carrier-sensing operations by individual nodes, the simultaneously transmitting links $\mathcal{S}^{CS}$ may or may not belong to $\mathcal{F}$. Let $\mathcal{F}^{CS} = \{\mathcal{S}^{CS} \mid$ simultaneous transmissions of links in $\mathcal{S}^{CS}$ are allowed by the carrier-sensing operation$\}$. The CSMA network is said to be interference-safe if $\mathcal{F}^{CS} \subseteq \mathcal{F}$. This is also the condition for the so-called hidden-node free operation [32]. However, this issue was studied under the context of an idealized protocol interference model in [32] rather than the practical physical interference model of interest here. In this chapter, we show that if the carrier-sensing mechanism can guarantee that the distance between every pair of transmitters is separated by a *safe carrier-sensing range*, then $\mathcal{F}^{CS} \subseteq \mathcal{F}$ can be guaranteed and the CSMA network is interference-safe even under the physical interference model. We believe that the safe carrier-sensing range established in this chapter is a tight upperbound and achieves good spatial reuse. Another issue is how to implement the concept of safe carrier-sensing range in practice.

This brings us to 2) above. In traditional carrier sensing based on power threshold (e.g., that of the *basic mode* in IEEE 802.11), the absolute power received is being monitored. This power consists of the sum total of powers received from all the other transmitters. It is impossible to infer from this absolute power the exact separation of the node from each of the other transmitters. This leads to subpar spatial reuse. Fortunately, we show that a simple mechanism that monitors the incremental power changes over time, IPCS, will enable us to map the power profile to the required distance in-

formation. We believe that this contribution, although simple, is significant in that it shows that the theoretical concept of *safe carrier-sensing range* can be implemented rather easily in practice. It also ties up a loose end in many other prior theoretical works that implicitly assume the use of a carrier-sensing range (safe or otherwise) without an explicit design to realize it. That is, IPCS can be used to implement the required carrier-sensing range in these works, not just our *safe carrier-sensing range* here. Without IPCS, and using only the conventional carrier-sensing mechanism, the results in these prior works would have been overly optimistic. Given the implementability of safe carrier-sensing range, the next issue is how tight the simultaneously transmitting nodes can be packed.

This brings us to 3) above. In the conventional carrier sensing mechanism, in order that the detected absolute power is below the carrier-sensing power threshold, the separation between a newly active transmitter and other existing active transmitters must increase progressively as the number of concurrent transmissions increases. That is, the cost of ensuring interference-safe transmissions becomes progressively higher and higher in the "packing process". This reduces spatial reuse and the overall network throughput. Fortunately, with IPCS, the required separation between any pair of active transmitters remains constant as the *safe carrier-sensing range*, and is independent of the number of concurrent transmissions. Indeed, our simulation results indicate that compared to the conventional carrier-sensing mechanism, IPCS mechanism improves the spatial reuse and the network throughput by more than 60%.

5.1.2 Related Work

In the literature, most studies on carrier sensing (e.g., [32–34, 85–87]) are based on the protocol interference model. For a link under the protocol interference model, the interferences from the other links are considered one by one. If the interference from each of the other links on the link concerned does not cause a collision, then it is assumed that there is no collision overall. Ref. [32] established the carrier-sensing range required to prevent hidden-node collisions in CSMA networks under the protocol interference model. The resulting carrier-sensing range is too optimistic and can not eliminate hidden-node collisions if the more accurate physical interference model is adopted instead.

A number of recent papers studied the CSMA networks under the physical interference model (e.g., [88–90]). However, none of them addressed the implementation of a carrier-sensing range based on power detection. Ref. [88] studied the asymptotic capacity of large-scale CSMA networks with hidden-node-free designs. The focus of [88] is on "order" result rather than "tight" result. For example, for the noiseless case, if $\gamma_0 = 10dB$ and $\alpha = 4$, the safe carrier-sensing range derived in [88] is $8.75d_{\max}$. In this chapter, we show that setting the safe carrier-sensing range to $5.27d_{\max}$ is enough to prevent hidden-node collisions.

The authors in [89, 90] attempted to improve spatial reuse and capacity by tuning the transmit power and the carrier-sensing range. Although the physical interference model is considered in [89,90], spatial reuse and capacity are analyzed based on carrier-sensing range. In particular, they assumed that the transmitters of concurrent transmission links can be uniformly packed in the network. As discussed in this chapter, such uniform packing can not be

Table 5.1: Summary of the Related Work

Interference Models	Protocol Interference Model	Physical Interference Model
Absolute power carrier sensing	many (e.g., [32,85])	[89,90]
Incremental power carrier sensing	**This work**	**This work**

realized using the current 802.11 carrier-sensing mechanism. Therefore, the results in [89,90] are overly optimistic without an appropriate carrier-sensing mechanism. IPCS fills this gap so that the theoretical results of [89,90] remain valid. We summarize the key related models and results in the literature in Table 5.1*.

Section 5.2 presents the physical interference model in CSMA network and the carrier sensing mechanism that is currently used in the 802.11 protocol. Section 5.3 derives the safe carrier-sensing range that successfully prevents the hidden-node collisions under the physical interference model. Section 5.4 presents the IPCS mechanism. Section 5.5 evaluates the performance of IPCS in terms of spatial reuse and network throughput. A summary of this chapter is given in section 5.6.

*This chapter focuses on the incremental-power carrier-sensing (IPCS) mechanism under the physical interference model. But IPCS proposed in this chapter can also deal with the protocol interference model.

5.2 System Model

5.2.1 Physical Interference Model in CSMA

Under the physical interference model, a receiver decodes its signal successfully if and only if the received Signal-to-Interference-plus-Noise Ratio (SINR) is above a certain threshold. In 802.11, each packet transmission on a link l_i consists of a DATA frame in the forward direction (from T_i to R_i) followed by an ACK frame in the reverse direction (from R_i to T_i). The packet transmission is said to be successful if and only if both the DATA frame and the ACK frame are received correctly. Let $\mathcal{L}'$ ($\mathcal{L}''$) denote the set of links that transmit concurrently with the DATA (ACK) frame on link l_i. The set of links that have concurrent transmissions with link l_i is $\mathcal{L}' \cup \mathcal{L}''$. Under the physical interference model, a successful transmission on link l_i needs to satisfy the following conditions:

$$\frac{P_t \cdot G(T_i, R_i)}{\sum_{l_j \in \mathcal{L}'} P_t \cdot G(S_j, R_i) + \eta} \geq \gamma_0, \quad \text{(DATA frame)} \tag{5.1}$$

and

$$\frac{P_t \cdot G(R_i, T_i)}{\sum_{l_j \in \mathcal{L}''} P_t \cdot G(S_j, T_i) + \eta} \geq \gamma_0, \quad \text{(ACK frame)} \tag{5.2}$$

where P_t is the transmit power, η is the average noise power, and γ_0 is the SINR threshold for successful reception. We assume that all nodes in the network use the same transmit power P_t and adopt the same SINR threshold γ_0. For a link l_j in $\mathcal{L}'$ or $\mathcal{L}''$, S_j represents the sender of link l_j, which can be either T_j or R_j. This is because both DATA and ACK transmissions on link l_j may cause interference to link l_i.

5.2.2 Existing Carrier Sensing Mechanism in 802.11

If there exists a link $l_i \in \mathcal{L}$ such that not both (5.1) and (5.2) are satisfied, then there is collision in the network. In 802.11, carrier sensing is designed to prevent collision due to simultaneous transmissions that cause the violation of either (5.1) or (5.2). In this work, we assume carrier sensing by energy detection. Consider a link l_i. If transmitter T_i senses a power $P^{CS}(T_i)$ that exceeds a power threshold P_{th}, i.e.,

$$P^{CS}(T_i) > P_{th}, \tag{5.3}$$

then T_i will not transmit and its backoff countdown process will be frozen. This will prevent the DATA frame transmission on l_i. In CSMA networks, carrier sensing is done by transmitters (because the transmitters have to decide whether to go ahead to transmit a packet). The receivers do not take part in detecting the channel. A transmitter, by doing carrier sensing, is actually trying to estimate whether its transmission (if it goes ahead to transmit) will cause SINR violation at the receivers of other concurrent transmission or at its own receiver.

In most studies of 802.11 networks, the concept of a carrier-sensing range CSR is introduced. The carrier-sensing range CSR is mapped from the carrier-sensing power threshold P_{th}:

$$CSR = \left(\frac{P_t G_0}{P_{th}}\right)^{\frac{1}{\alpha}},$$

where G_0 is the reference channel at the reference distance $d_0 = 1m$. Consider two links, l_i and l_j. If the distance between transmitters T_i and T_j is no less than the carrier-sensing range, i.e.,

$$d(T_i, T_j) \geq CSR, \tag{5.4}$$

then T_i and T_j can not carrier sense each other, and thus can initiate concurrent transmissions between them. The pairwise relationship can be generalized to a set of links $\mathcal{S}^{CS} \subseteq \mathcal{L}$. If the condition in (5.4) is satisfied by all pairs of transmitters in set $\mathcal{S}^{CS}$, then all links in $\mathcal{S}^{CS}$ can transmit concurrently.

Setting an appropriate carrier-sensing range is crucial to the performance of 802.11 networks. If CSR is too large, spatial reuse will be unnecessarily limited. If CSR is not large enough, then hidden-node collisions may occur. The underlying cause of hidden-node collisions are as follows. A number of transmitters transmit simultaneously because condition (5.4) is satisfied by all pairs of the transmitters. However, there is at least one of the links not satisfying either (5.1) or (5.2). As a result, collisions happen and the carrier sensing mechanism is said to have failed in preventing such collisions.

We now define a *safe carrier-sensing range* that always prevents the hidden-node collisions in 802.11 networks under the physical interference model.

Definition 7 (***Safe-***$CSR_{physical}$) *Let $\mathcal{S}^{CS} \subseteq \mathcal{L}$ denote a subset of links that are allowed to transmit concurrently under a carrier-sensing range CSR. Let $\mathcal{F}^{CS} = \{\mathcal{S}^{CS}\}$ denote all such subsets of links in the network. A CSR is said to be a Safe-$CSR_{physical}$ if for any $\mathcal{S}^{CS} \in \mathcal{F}^{CS}$ and for any link $l_i \in \mathcal{S}^{CS}$, both conditions* (5.1) *and* (5.2) *are satisfied, with $\mathcal{L}' = \mathcal{L}'' = \mathcal{S}^{CS} \setminus \{l_i\}$.*

5.3 Safe Carrier-sensing Range under Physical Interference Model

In this section, we derive a sufficient condition for *Safe-*$CSR_{physical}$.

5.3.1 The Need for RS(Re-Start) Mode

When discussing the hidden-node free design, it is required that the receivers are operated with the "RS (Re-Start) mode" [32]. The reason is that although the carrier-sensing range is sufficiently large for the SINR requirements of all nodes, transmission failures can still occur due to the "Receiver-Capture effect".

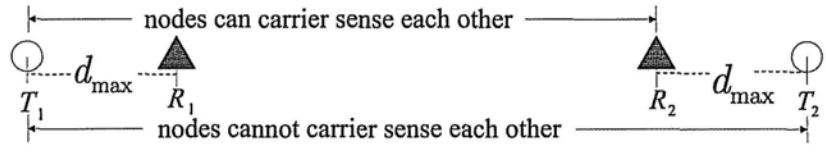

Figure 5.1: Collision due to "Receiver-Capture effect"

Take a two-link case shown in Fig. 5.1 as an example. In Fig. 5.1, $d(T_1, T_2) > CSR$ and $d(T_1, R_2) < CSR$. So the transmitters T_1 and T_2 can not carrier-sense each other, but R_2 can sense the signal transmitted from T_1. Suppose that CSR is set large enough to guarantee the SINR requirements on l_1 and l_2 (both the DATA frames and the ACK frames). If T_1 transmits first, then R_2 will have sensed the signal of T_1 and the default operation in most 802.11 products is that R_2 will not attempt to receive the later signal from T_2, even if the signal from T_2 is stronger. This will cause the transmission on link l_2 to fail. It is further shown in [32] that no matter how large the carrier-sensing range is, we can always come up with an example that gives rise to transmission failures, if the "Receiver-Capture effect" is not dealt with properly. This kind of collisions can be solved with a receiver "RS (Re-Start) mode". With RS mode, a receiver will switch to receive the stronger packet

as long as the SINR threshold γ_0 for the later link can be satisfied. In the following discussion, we also make the same assumption.

5.3.2 Insufficiency of Safe Carrier Sensing Range under the Protocol Interference Model

Ref. [32] studied the safe carrier-sensing range under the *protocol interference model*. The threshold is given as follows:

$$Safe\text{-}CSR_{protocol} = \left(\gamma_0^{\frac{1}{\alpha}} + 2\right) d_{\max}, \tag{5.5}$$

where $d_{\max} = \max_{l_i \in \mathcal{L}} d(T_i, R_i)$ is the maximum link length in the network. However, the protocol interference model does not take into account the cumulative nature of interferences from other links. The threshold given in (5.5) is overly optimistic and is not large enough to prevent hidden-node collisions under the *physical interference model*, as illustrated by the three-link example in Fig. 5.2.

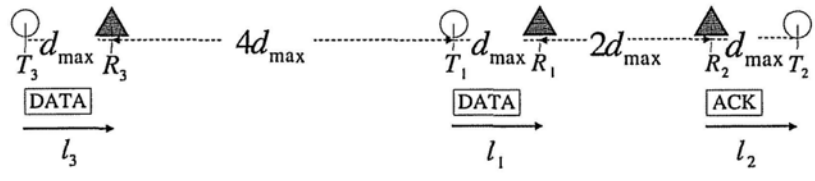

Figure 5.2: Setting the carrier-sensing range as $Safe\text{-}CSR_{protocol}$ is insufficient to prevent hidden-node collisions under the physical interference model

In Fig. 5.2, suppose that the SIR requirement $\gamma_0 = 8$ and the path-loss exponent $\alpha = 3$. According to (5.5), it is enough to set the carrier-sensing range as $\left(\gamma_0^{\frac{1}{\alpha}} + 2\right) d_{\max} = 4d_{\max}$ and the carrier sensing power threshold $P_{th} = P_t G_0 \left(4d_{\max}\right)^{-3} = 0.0156 P_t G_0 d_{\max}^{-3}$. In Fig. 5.2, there are three

links: l_1, l_2, and l_3 with the same link length $d_{\max}$. The distance $d(R_1, R_2)$ equals $2d_{\max}$ and the distance $d(T_1, R_3)$ equals $4d_{\max}$. Since the distance $d(T_1, T_2) = 4d_{\max} = \left(\gamma_0^{\frac{1}{\alpha}} + 2\right) d_{\max}$, from (5.4), we find that T_1 and T_2 can simultaneously initiate transmissions since they can not carrier sense each other. We can verify that the SIR requirements of both DATA and ACK transmissions on l_1 and l_2 are satisfied. This means l_1 and l_2 can indeed successfully transmit simultaneously.

Suppose that l_3 wants to initiate a transmission when T_1 is sending a DATA frame to R_1 and R_2 is sending an ACK frame to T_2. Transmitter T_3 senses a power $P^{CS}(T_3)$ given by

$$\begin{aligned} P^{CS}(T_3) &= P_t G_0 \cdot (5d_{\max})^{-3} + P_t G_0 \cdot (8d_{\max})^{-3} \\ &= 0.00995 \cdot P_t G_0 d_{\max}^{-3} < P_{th}. \end{aligned}$$

This means that T_3 can not sense the transmissions on l_1 and l_2, and can initiate a DATA transmission. However, when all these three links are active simultaneously, the SIR at R_1 is

$$\frac{P_t G_0 (d_{\max})^{-3}}{P_t G_0 (6d_{\max})^{-3} + P_t G_0 (2d_{\max})^{-3}} = 7.714 < \gamma_0.$$

This means the cumulative interference powers from l_2 and l_3 will corrupt the DATA transmission on l_1 due to the insufficient SIR at R_1. This example shows that setting the carrier-sensing range as in (5.5) is not sufficient to prevent collisions under the physical interference model. Choosing the parameters $\alpha = 3$ and $\gamma_0 = 8$ is just for easy illustration. In fact, we can always construct a three-link example like Fig. 5.2 with the same conclusion for any choice of α and γ_0.

5.3.3 Safe Carrier-sensing Range under Physical Interference Model

We next establish a threshold for $Safe\text{-}CSR_{physical}$ so that the system will remain safe under the physical interference model.

Theorem 5 *Setting*

$$Safe\text{-}CSR_{physical} = (K_1 K_2 + 2) d_{\max}, \tag{5.6}$$

where

$$K_1 = \left(6\gamma_0 \left(1 + \left(\frac{2}{\sqrt{3}} \right)^{\alpha} \frac{1}{\alpha - 2} \right) \right)^{\frac{1}{\alpha}}, \tag{5.7}$$

and

$$K_2 = \left(\frac{P_t G_0}{P_t G_0 - \gamma_0 (d_{\max})^{\alpha} \eta} \right)^{\frac{1}{\alpha}}, \tag{5.8}$$

is sufficient to ensure interference-safe transmissions under the physical interference model.

Proof: With the receiver's RS mode, in order to prevent hidden-node collisions in 802.11 networks, we only need to show that condition (5.6) is sufficient to guarantee the satisfaction of both the SIR requirements (5.1) and (5.2) of all the concurrent transmission links.

Let $\mathcal{S}^{CS}$ denote a subset of links that are allowed to transmit concurrently under the $Safe\text{-}CSR_{physical}$ setting in (5.6). Consider any two links l_i and l_j in $\mathcal{S}^{CS}$, we have

$$d(T_j, T_i) \geq Safe\text{-}CSR_{physical} = (K_1 K_2 + 2) d_{\max}.$$

Because both the lengths of links l_i and l_j satisfy

$$d(T_i, R_i) \leq d_{\max}, \quad d(T_j, R_j) \leq d_{\max},$$

we have the following based on the triangular inequality

$$d(T_j, R_i) \geq d(T_j, T_i) - d(T_i, R_i) \geq (K_1K_2 + 1)d_{\max},$$
$$d(R_j, T_i) \geq d(T_i, T_j) - d(T_j, R_j) \geq (K_1K_2 + 1)d_{\max},$$
$$d(R_j, R_i) \geq d(R_i, T_j) - d(T_j, R_j) \geq K_1K_2 d_{\max}.$$

We take the most conservative distance $K_1K_2d_{\max}$ in our interference analysis (i.e., we will pack the links that transmit concurrently in a tightest manner given the $Safe\text{-}CSR_{physical}$ in (5.6)). Consider any two links l_i and l_j in $\mathcal{S}^{CS}$. The following four inequalities are satisfied:

$$d(T_i, T_j) \geq K_1K_2d_{\max}, \quad d(T_i, R_j) \geq K_1K_2d_{\max},$$
$$d(T_j, R_i) \geq K_1K_2d_{\max}, \quad d(R_i, R_j) \geq K_1K_2d_{\max}.$$

Consider any link l_i in $\mathcal{S}^{CS}$. We will show that the SINR requirements for both the DATA frame and the ACK frame can be satisfied. We first consider the SINR requirement of the DATA frame. The SINR at R_i is:

$$SINR = \frac{P_tG_0d^{-\alpha}(T_i, R_i)}{\sum_{l_j \in \mathcal{S}^{CS}, j \neq i} P_tG_0d^{-\alpha}(S_j, R_i) + \eta}.$$

For the received signal power, we consider the worst case that $d(T_i, R_i) = d_{\max}$. So we have

$$P_tG_0d^{-\alpha}(T_i, R_i) \geq P_tG_0d_{\max}^{-\alpha}. \tag{5.9}$$

To calculate the cumulative interference power, we consider the worst case that all the other concurrent transmission links have the densest packing†, in

†The scenario for the worst case interference calculation is used to derive the safe-carrier sensing range that can prevent hidden-node collisions in any network topology. We want to guarantee absolute safety here. In practical wireless system, this worst case scenario may have low probability. A probabilistic approach that bounds the probability of hidden-node collisions, together with the consideration of fading, will be for future work.

which the link lengths of all the other concurrent transmission links are equal to zero. In this case, the links degenerate to nodes. The minimum distance between any two links in $\mathcal{S}^{CS}$ is $K_1K_2d_{\max}$. The densest packing of nodes with the minimum distance requirement is the hexagon packing (as shown in Fig. 5.3).

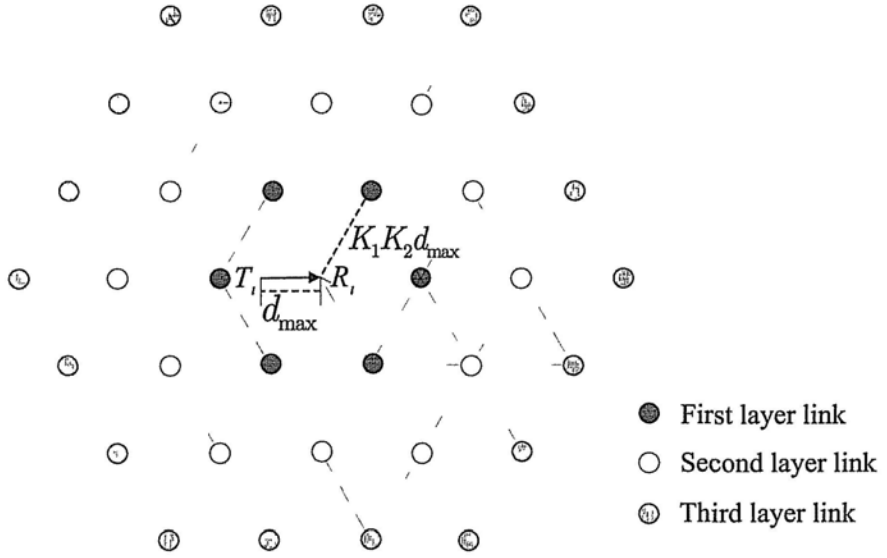

Figure 5.3: The packing of the interfering links in the worst case

If link l_j is the first layer neighbor link of link l_i, we have $d(S_j, R_i) \geq K_1K_2d_{\max}$. Thus we have

$$\begin{aligned} P_tG_0d^{-\alpha}(S_j, R_i) &\leq P_tG_0(K_1K_2d_{\max})^{-\alpha} \\ &= \frac{1}{(K_1K_2)^{\alpha}} \cdot P_tG_0d_{\max}^{-\alpha}, \end{aligned}$$

and there are at most 6 neighbor links in the first layer.

If link l_j is the nth layer neighbor link of link l_i with $n \geq 2$, we have $d(S_j, R_i) \geq \frac{\sqrt{3}}{2} n \cdot K_1 K_2 d_{\max}$. Thus we have

$$\begin{aligned} P_t G_0 d^{-\alpha}(S_j, R_i) &\leq P_t G_0 \left(\frac{\sqrt{3}}{2} n K_1 K_2 d_{\max} \right)^{-\alpha} \\ &= \frac{1}{\left(\frac{\sqrt{3}}{2} n K_1 K_2 \right)^{\alpha}} P_t G_0 d_{\max}^{-\alpha}, \end{aligned}$$

and there are at most $6n$ neighbor links in the nth layer.

So the cumulative interference power satisfies:

$$\begin{aligned} &\sum_{l_j \in S^{CS}, j \neq i} P_t G_0 d^{-\alpha}(S_j, R_i) \\ \leq &\left(6 \left(\frac{1}{K_1 K_2} \right)^{\alpha} + \sum_{n=2}^{\infty} 6n \left(\frac{2}{\sqrt{3} n K_1 K_2} \right)^{\alpha} \right) P_t G_0 d_{\max}^{-\alpha} \\ = &6 \left(\frac{1}{K_1 K_2} \right)^{\alpha} \left(1 + \sum_{n=2}^{\infty} n \left(\frac{2}{\sqrt{3} n} \right)^{\alpha} \right) P_t G_0 d_{\max}^{-\alpha} \\ = &6 \left(\frac{1}{K_1 K_2} \right)^{\alpha} \left(1 + \left(\frac{2}{\sqrt{3}} \right)^{\alpha} \sum_{n=2}^{\infty} n \left(\frac{1}{n} \right)^{\alpha} \right) P_t G_0 d_{\max}^{-\alpha} \\ = &6 \left(\frac{1}{K_1 K_2} \right)^{\alpha} \left(1 + \left(\frac{2}{\sqrt{3}} \right)^{\alpha} \sum_{n=2}^{\infty} \frac{1}{n^{\alpha-1}} \right) P_t G_0 d_{\max}^{-\alpha} \\ \leq &6 \left(\frac{1}{K_1 K_2} \right)^{\alpha} \left(1 + \left(\frac{2}{\sqrt{3}} \right)^{\alpha} \frac{1}{\alpha - 2} \right) P_t G_0 d_{\max}^{-\alpha}, \end{aligned} \tag{5.10}$$

where (5.10) follows from a bound on Riemann's zeta function.

According to (5.9) and (5.10), we find that the SINR of the DATA frame of link l_i at the receiver R_i satisfies:

$$\begin{aligned} SINR &= \frac{P_t G_0 d^{-\alpha}(T_i, R_i)}{\sum_{l_j \in S^{CS}, j \neq i} P_t G_0 d^{-\alpha}(S_j, R_i) + \eta}. \\ &\geq \frac{P_t G_0 d_{\max}^{-\alpha}}{6 \cdot \left(\frac{1}{K_1 K_2}\right)^{\alpha} \left(1 + \left(\frac{2}{\sqrt{3}}\right)^{\alpha} \frac{1}{\alpha - 2}\right) \cdot P_t G_0 d_{\max}^{-\alpha} + \eta} \\ &= \frac{P_t G_0 d_{\max}^{-\alpha}}{\left(\frac{P_t G_0 d_{\max}^{-\alpha}}{\gamma_0}\right) \cdot \left(\frac{P_t G_0 - \gamma_0 (d_{\max})^{\alpha} \eta}{P_t G_0}\right) + \eta} \qquad (5.11) \\ &= \gamma_0, \end{aligned}$$

where (5.11) follows from the definitions of K_1 and K_2 as shown in (5.7) and (5.8), respectively. So the DATA frame transmission on l_i can be guaranteed to be successful. The proof that the SINR requirement of the ACK frame on link l_i can be satisfied follows a similar procedure as above. So condition (5.6) is sufficient to satisfy the SINR requirements of the successful transmissions of both the DATA and ACK frames. This means that condition (5.6) is sufficient for preventing hidden-node collisions in CSMA networks under the physical interference model. □

Condition (5.6) provides a sufficiently large carrier-sensing range that prevents the hidden-node collisions in CSMA networks. Therefore, there is no need to set a CSR larger than the values given in (5.6). Setting a larger CSR than (5.6) will only decrease the spatial reuse.

The terms K_1 and K_2 in (5.6) reflect the impact of the cumulative interference power from other concurrent transmission links and the background noise power on the safe carrier sensing range setting, respectively. So we refer K_1 and K_2 as interference factor and noise factor, respectively.

The Noise Factor K_2

The noise factor K_2 is a function of the SNR margin (also called the noise margin). Let τ denote the SNR margin, which can be defined as

$$\tau = \frac{P_t G_0}{\gamma_0 (d_{\max})^{\alpha} \eta}.$$

The transmit power P_t should be set to make sure that the SNR margin is no less than 1. The physical meaning is that the transmit power should be large enough to satisfy the SNR requirement γ_0 in the case that there is only one link in the network. The noise factor K_2 is a function of the SNR margin:

$$K_2 = \left(\frac{\tau}{\tau - 1}\right)^{\frac{1}{\alpha}}.$$

The term K_2 is no less than 1. When the SNR margin $\tau = 1$ (i.e., $0dB$), the noise factor $K_2 = \infty$. According to (5.6), we find that $\textit{Safe-CSR}_{\textit{physical}} = \infty$. The physical meaning is that if the transmit power P_t is just enough to let the SNR at the receiver meet the require threshold γ_0, then no other links can have concurrent transmissions in the network. Fig. 5.4 shows the noise factor K_2 as a function of the SNR margin τ. Different curves represent different choices of the path-loss exponent α. From Fig. 5.4, we find that as the SNR margin τ increases, the noise factor K_2 decreases rapidly. As the SNR margin goes to infinity, the noise factor K_2 converges to 1. When $K_2 = 1$, the term K_2 can be removed from (5.6) and condition (5.6) is simplified to $\textit{Safe-CSR}_{\textit{physical}} = (K_1 + 2)d_{\max}$. In this case, the safe carrier sensing range requirement is only affected by the cumulative interference power. The more the noise factor K_2 is close to 1, the smaller the noise power impacts on the safe carrier sensing range requirement. In practice, the 802.11 network operates with an SNR margin ranging from $6dB$ to $10dB$ [91]. From Fig. 5.4,

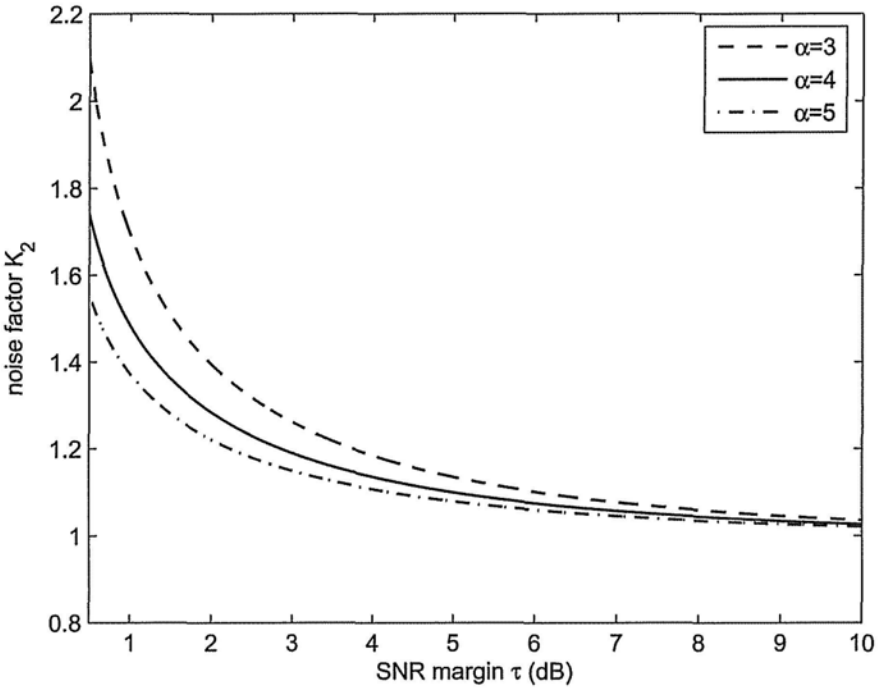

Figure 5.4: The term K_2

we can find that the noise factor K_2 is very close to 1, and the impact of the noise power to the safe carrier sensing range requirement is small.

The Impact of Different Interference Models

Let us consider the impact of different interference models to the safe carrier sensing range requirements. In order to have a clear comparison between different interference models, we set the noise power $\eta = 0$. So we have $Safe\text{-}CSR_{physical} = (K_1 + 2)d_{\max}$. Let us compare $Safe\text{-}CSR_{physical}$ with $Safe\text{-}CSR_{protocol}$ with different values of γ_0 and α. For example, if $\gamma_0 = 10$ and $\alpha = 4$, which are typical for wireless communications,

$$Safe\text{-}CSR_{protocol} = 3.78 \cdot d_{\max},$$
$$Safe\text{-}CSR_{physical} = 5.27 \cdot d_{\max}.$$

Compared with $Safe\text{-}CSR_{protocol}$, $Safe\text{-}CSR_{physical}$ needs to be increased by a factor of 1.4 to ensure successful transmissions under the physical interference model.

Given a fixed path-loss exponent α, both $Safe\text{-}CSR_{protocol}$ and $Safe\text{-}CSR_{physical}$ increase in the SIR requirement γ_0. This is because the separation among links must be enlarged to meet a larger SIR target. For example, if $\alpha = 4$, we have

$$Safe\text{-}CSR_{protocol} = \left(2 + \gamma_0^{\frac{1}{4}}\right) d_{\max},$$
$$Safe\text{-}CSR_{physical} = \left(2 + \left(\frac{34}{3}\gamma_0\right)^{\frac{1}{4}}\right) d_{\max}.$$

The ratio of $Safe\text{-}CSR_{physical}$ to $Safe\text{-}CSR_{protocol}$ is

$$\frac{Safe\text{-}CSR_{physical}}{Safe\text{-}CSR_{protocol}} = \frac{2 + \left(\frac{34}{3}\gamma_0\right)^{\frac{1}{4}}}{2 + \gamma_0^{\frac{1}{4}}},$$

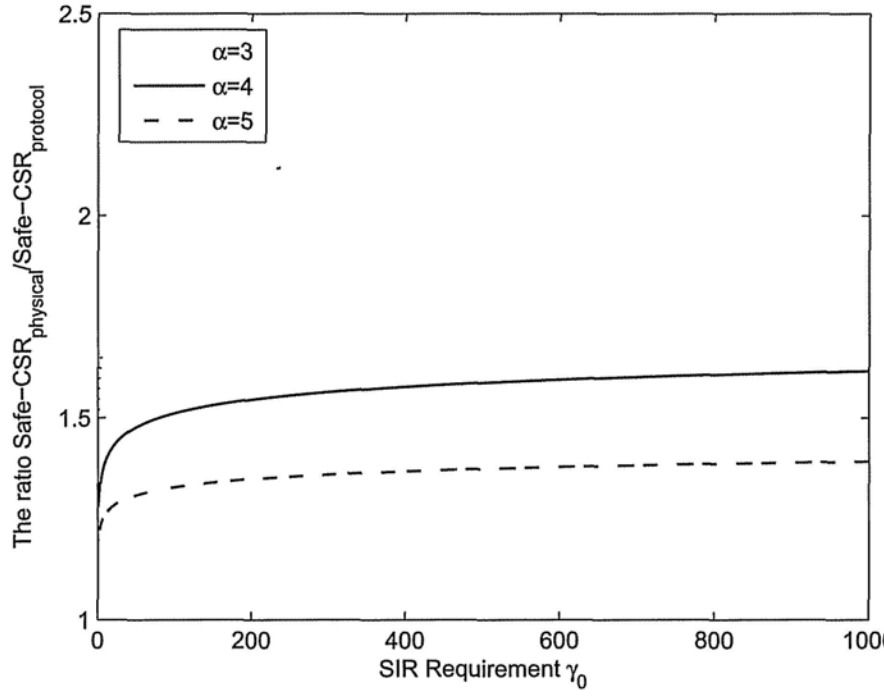

Figure 5 5: The ratio of $Safe\text{-}CSR_{physical}$ to $Safe\text{-}CSR_{protocol}$

which is an increasing function of γ_0, and converges to a constant as γ_0 goes to infinity.

$$\max_{\gamma_0} \frac{Safe\text{-}CSR_{physical}}{Safe\text{-}CSR_{protocol}} = \lim_{\gamma_0 \to \infty} \frac{Safe\text{-}CSR_{physical}}{Safe\text{-}CSR_{protocol}}$$
$$= \lim_{\gamma_0 \to \infty} \frac{2 + \left(\frac{34}{3}\gamma_0\right)^{\frac{1}{4}}}{2 + \gamma_0^{\frac{1}{4}}} = \left(\frac{34}{3}\right)^{\frac{1}{4}} \approx 1\ 8348$$

Figure 5 5 shows the ratio $\frac{Safe\text{-}CSR_{physical}}{Safe\text{-}CSR_{protocol}}$ as a function of the SIR requirements γ_0. Different curves represent different choices of the path-loss exponent α. The ratio $\frac{Safe\text{-}CSR_{physical}}{Safe\text{-}CSR_{protocol}}$ increases when γ_0 increases or α decreases. For each choice of α, the ratio converges to a constant as γ_0 goes to infinity.

This shows that, compared with the protocol interference model, the safe carrier-sensing range under the physical interference model will not increase unbounded.

5.4 A Novel Carrier Sensing Mechanism

We now discuss the implementation of $Safe\text{-}CSR_{physical}$. We first describe the difficulty of implementing the safe carrier-sensing range in (5.6) using the existing physical carrier-sensing mechanism in the current 802.11 protocol. Then, we propose a new Incremental-Power Carrier-Sensing (IPCS) mechanism to resolve this implementation issue.

5.4.1 Limitation of Conventional Carrier-Sensing Mechanism

In the current 802.11 MAC protocol, given the safe carrier-sensing range $Safe\text{-}CSR_{physical}$, the carrier-sensing power threshold P_{th} is set as

$$P_{th} = P_t G_0 \left(Safe\text{-}CSR_{physical}\right)^{-\alpha}. \tag{5.12}$$

Before transmitting, a transmitter T_i compares the power it senses, $P^{CS}(T_i)$, with the power threshold P_{th}. A key disadvantage of this approach is that $P^{CS}(T_i)$ is a cumulative power from all the other nodes that are concurrently transmitting. The cumulative nature makes it impossible to tell whether $P^{CS}(T_i)$ is from one particular nearby transmitter or a group of far-off transmitters [92]. This reduces spatial reuse, as illustrated by the example in Fig. 5.6.

There are four links in Fig. 5.6, with $Safe\text{-}CSR_{physical}$ set as in (5.6). In Fig. 5.6, the distance $d(T_1, T_2)$ is equal to $Safe\text{-}CSR_{physical}$. From (5.4), we find that T_1 and T_2 can not carrier sense each other, thus they can transmit simultaneously.

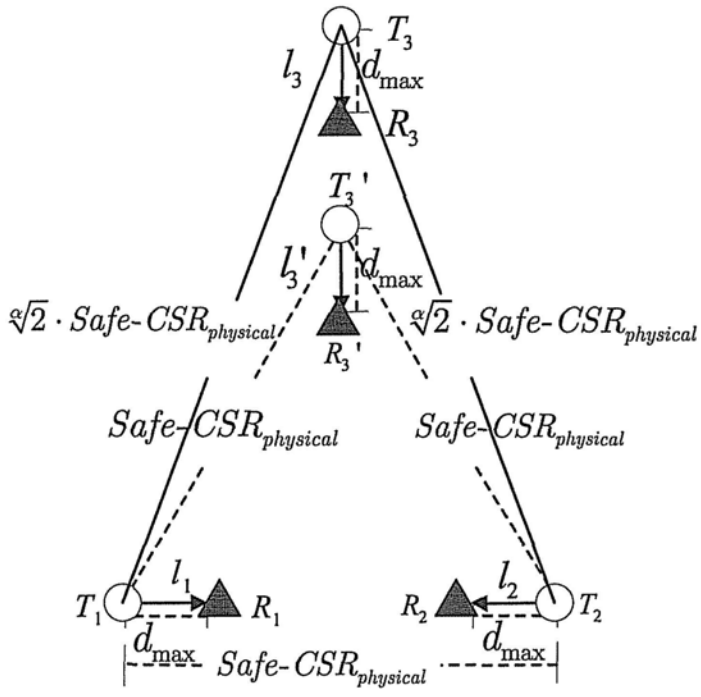

Figure 5.6: Conventional carrier-sensing mechanism will reduce the spatial reuse in 802.11 networks. Link l_3 is placed based on the absolute power sensing mechanism in current 802.11, and link l_3' is placed based on the $Safe\text{-}CSR_{physical}$ as enabled by our IPCS mechanism.

First, consider the location requirement of the third link l_3' that can have a concurrent transmission with both l_1 and l_2, assuming that each transmitter can perfectly differentiate the distances from the other transmitters. Suppose that the third link is located on the middle line between l_1 and l_2. Based on the carrier-sensing range analysis, the requirements are $d(T_3', T_1) \geq \textit{Safe-CSR}_{physical}$ and $d(T_3', T_2) \geq \textit{Safe-CSR}_{physical}$. So the third link can be located in the position of l_3', shown in Fig. 5.6. Furthermore, as the number of links increases, a tight packing of the concurrent transmitters will result in a regular equilateral triangle packing with side length $\textit{Safe-CSR}_{physical}$. The "consumed area" of each transmitter is a constant given by $A = \frac{\sqrt{3}}{2}\textit{Safe-CSR}_{physical}^2$.

Now, let us consider the location requirement of the third link l_3 under the carrier-sensing mechanism of the current 802.11 protocol. In order to have concurrent transmissions with both l_1 and l_2, the cumulative power sensed by T_3 due to transmissions of both links l_1 and l_2 should be no larger than P_{th}, i.e.,

$$\begin{aligned} P^{CS}(T_3) &= P_t G_0 d(T_3, T_1)^{-\alpha} + P_t G_0 d(T_3, T_2)^{-\alpha} \\ &= 2 \cdot P_t G_0 d(T_3, T_1)^{-\alpha} \leq P_{th}, \end{aligned}$$

where P_{th} is given in equation (5.12). So the minimum distance requirement on $d(T_3, T_1)$ and $d(T_3, T_2)$ is

$$d(T_3, T_1) = d(T_3, T_2) \geq \left(2\frac{P_t G_0}{P_{th}}\right)^{\frac{1}{\alpha}} = \sqrt[\alpha]{2} \cdot \textit{Safe-CSR}_{physical},$$

as shown in Fig. 5.6. Since $\sqrt[\alpha]{2}$ is always greater than 1, the requirement of the separation between transmitters is increased from $\textit{Safe-CSR}_{physical}$ (i.e., $d(T_1, T_2)$) to $\sqrt[\alpha]{2}\textit{Safe-CSR}_{physical}$ (i.e., $d(T_1, T_3)$ and $d(T_2, T_3)$). The requirement on the separation between transmitters will increase progressively as the

number of concurrent links increases, and the corresponding packing of transmitters will be more and more sparse. As a result, spatial reuse is reduced as the number of links increases.

Another thing to notice is that the order of the transmissions also affects spatial reuse in the conventional carrier-sensing mechanism. Consider the three links, l_1, l_2 and l_3 in Fig. 5.6 again. If the sequence of transmissions is $\{l_1, l_2, l_3\}$, as discussed above, T_1, T_2 and T_3 sense a power no greater than P_{th}, and thus l_1, l_2 and l_3 can be active simultaneously. If the sequence of transmissions on these links is $\{l_2, l_3, l_1\}$, however, both T_2 and T_3 sense a power no larger than P_{th}. But the cumulative power sensed by T_1 in this case is

$$\begin{aligned} & P^{CS}(T_1) = P_t G_0 d(T_3, T_1)^{-\alpha} + P_t G_0 d(T_2, T_1)^{-\alpha} \\ =& P_t G_0 \left(\sqrt[\alpha]{2} Safe\text{-}CSR_{physical} \right)^{-\alpha} + P_t G_0 \left(Safe\text{-}CSR_{physical} \right)^{-\alpha} \\ =& \frac{3}{2} P_{th} > P_{th}. \end{aligned}$$

Therefore, T_1 will sense the channel busy and will not initiate the transmission on l_1. The spatial reuse is unnecessarily reduced because there would have been no collisions had T_1 decided to transmit[††].

5.4.2 Incremental-Power Carrier-Sensing (IPCS) Mechanism

We propose an enhanced physical carrier-sensing mechanism called Incremental-Power Carrier-Sensing (IPCS) to solve the issues identified in Section 5.4.1. Specifically, the IPCS mechanism can implement the safe carrier-sensing range accurately by separating the detected powers from multiple concurrent transmitters.

[††]This corresponds to the exposed-node phenomenon.

Before explaining the details of IPCS, we want to emphasize that there are two fundamental causes for collisions in a CSMA network. Besides hidden nodes, collisions can also happen when the backoff mechanisms of two transmitters count down to zero simultaneously, causing them to transmit together. Note that for the latter, each of the two transmitters is not aware that the other transmitter will begin transmission at the same time. Based on the power that it detects, it could perfectly be safe for it to transmit together with the existing active transmitters, only if the other transmitter did not decide to join in at the same time. There is no way that the carrier-sensing mechanism can prevent this kind of collisions. This work addresses the hidden-node phenomenon only. To isolate the second kind of collisions, we will assume in the following discussion of IPCS that no two transmitters will transmit simultaneous[‡]. Conceptually, we could imagine the random variable associated with backoff countdown to be continuous rather than discrete, which means that the starting/ending of one link's transmission will coincide with the starting/ending of another link's transmission with zero probability.

The key idea of IPCS is to utilize the whole carrier-sensing power history, not just the carrier-sensing power at one particular time instance. In CSMA networks, each transmitter T_i carrier senses the channel except during its transmission of DATA or reception of ACK. The power being sensed increases if a new link starts to transmit, and decreases if an active link finishes its transmission. As a result, the power sensed by transmitter T_i, denoted by $P_i^{CS}(t)$, is a function of time t.

[‡]Collisions due to simultaneous countdown-to-zero can be tackled by an exponential backoff mechanism in which the transmission probability of each node is adjusted in a dynamic way based on the busyness of the network. In WiFi, for example, the countdown window is doubled after each collision. The probability of this kind of collisions can be made small with a proper design of the backoff mechanism.

In IPCS, instead of checking the absolute power sensed at time t, the transmitter checks increments of power in the past up to time t. If the packet duration t_{packet} (including both DATA and ACK frames and the SIFS in between) is a constant for all links, then it suffices to check the power increments during the time window $[t - t_{packet}, t]$[§]. Let $\{t_1, t_2, \cdots, t_k, \cdots\}$ denote the time instances when the power being sensed changes, and $\{\Delta P_i^{CS}(t_1), \Delta P_i^{CS}(t_2), \cdots, \Delta P_i^{CS}(t_k), \cdots\}$ denote the corresponding increments, respectively. In IPCS, transmitter T_i considers the channel to be *idle* at time t if the following conditions are met:

$$\Delta P_i^{CS}(t_k) \leq P_{th}, \quad \forall t_k \text{ such that } t - t_{packet} \leq t_k \leq t, \tag{5.13}$$

where P_{th} is the carrier-sensing power threshold determined according to CSR; otherwise, the channel is considered to be *busy*. Since $\Delta P_i^{CS}(t_k)$ is negative if a link stops transmission at some time t_k, we only need to check the instances where the power increments are positive.

By checking every increment in the detected power over time, T_i can separate the powers from all concurrent transmitters, and can map the power profile to the required distance information. In this way, IPCS can ensure the separations between any two transmitters of all the transmitters are tight in accordance with Theorem 5.

Theorem 6 *If the carrier-sensing power threshold P_{th} in the IPCS mechanism is set as:*

$$P_{th} = P_t G_0 \left(\textit{Safe-CSR}_{physical}\right)^{-\alpha}, \tag{5.14}$$

where $\textit{Safe-CSR}_{physical}$ is the safe carrier-sensing range in (5.6)*, then it is sufficient to prevent hidden-node collisions under the physical interference*

[§]This assumption is used to simplify explanation only. In general, we could check a time window sufficiently large to cover the maximum packet size among all links.

model.

Proof: Consider any link l_i in the link set $\mathcal{L}$. Transmitter T_i will always do carrier sensing except when it transmits DATA frame or receives ACK frame. We show that condition (5.14) is sufficient to prevent hidden-node collisions in the following two situations, which cover all the possible transmission scenarios:

1. Link l_i has monitored the channel for at least t_{packet} before its backoff counter reaches zero and it transmits.

2. Link l_i finishes a transmission; then monitors the channel for less than t_{packet} when its backoff counter reaches zero; then it transmits its next packet.

Let us first consider case 1):

We show that for the links that are allowed to transmit simultaneously, the separation between any pair of transmitters is no less than the safe carrier-sensing range $Safe\text{-}CSR_{physical}$. We use inductive proof method. Suppose that before l_i starts to transmit, there are already M links transmitting and they are collectively denoted by the link set $\mathcal{S}^{CS}$. Without loss of generality, suppose that these M links begin to transmit one by one, according to the order $l_1, l_2, \cdots, l_M$. For any link $l_j \in \mathcal{S}^{CS}$, let t_j and t'_j denote the times when link l_j starts to transmit the DATA frame and the ACK frame, respectively.

In our inductive proof, by assumption we have

$$d(T_j, T_k) \geq Safe\text{-}CSR_{physical}, \forall j, k \in \{1, \cdots, M\}, j \neq k. \tag{5.15}$$

We now show that condition (5.15) will still hold after link l_i starts its transmission.

Before link l_i starts its transmission, transmitter T_i monitors the channel for a time period of t_{packet}. So T_i at least senses M increments in the carrier-sensing power $P_i^{CS}(t)$ that happen at time $t_1, t_2, \cdots, t_M$ when the links in $\mathcal{S}^{CS}$ start to transmit their DATA frames. There may also be some increments in the $P_i^{CS}(t)$ that happen at $t'_1, t'_2, \cdots, t'_M$ if the links in $\mathcal{S}^{CS}$ start to transmit the ACK frames before link l_i starting it transmission. In the IPCS mechanism, at least the following M inequalities must be satisfied if T_i can start its transmission:

$$\Delta P_i^{CS}(t_j) \leq P_{th}, \quad \text{for} \quad j = 1, \cdots, M.$$

Because

$$\Delta P_i^{CS}(t_j) = P_t G_0 d(T_i, T_j)^{-\alpha},$$
$$P_{th} = P_t G_0 \left(Safe\text{-}CSR_{physical}\right)^{-\alpha},$$

we have

$$d(T_i, T_j) \geq Safe\text{-}CSR_{physical} \quad \text{for} \quad j = 1, \cdots, M.$$

Thus, we have shown that the separation between any pair of transmitters in the link set $\mathcal{S}^{CS} \cup l_i$ is no less than $Safe\text{-}CSR_{physical}$ after link l_i starting transmission.

Now let us consider case 2):

Before starting the transmission of the $(m+1)$th packet, link l_i first finishes the transmission of the mth packet (from time $t_i(m)$ to $t_i(m)+t_{packet}$), and waits for a DIFS plus a backoff time (from time $t_i(m)+t_{packet}$ to $t_i(m+1)$). Let $\mathcal{S}^{CS}$ denote the set of links that are transmitting when l_i starts the $(m+1)$th packet at time $t_i(m+1)$. Consider any link l_j in set $\mathcal{S}^{CS}$. Because the transmission time of every packet in the network is t_{packet}. We

know that the start time t_j of the concurrent transmission on link l_j must range from $t_i(m)$ to $t_i(m+1)$, i.e., $t_i(m) < t_j < t_i(m+1)$.

If $t_i(m)+t_{packet} < t_j < t_i(m+1)$, this means t_j is in the DIFS or the backoff time of link l_i. During this period, transmitter T_i will do carrier sensing. The IPCS mechanism will make sure that the distance between T_i and T_j satisfies $d(T_i, T_j) \geq Safe\text{-}CSR_{physical}$.

If $t_i(m) < t_j < t_i(m)+t_{packet}$, this means t_j falls into the transmission time of the mth packet of link l_i. During the transmission time, T_i is not able to do carrier sensing because it is in the process of transmitting the DATA frame or receiving the ACK frame. However, the transmitter T_j will do carrier sensing before it starts to transmit at time t_j. The carrier sensing done by T_j can make sure that the distance between T_i and T_j satisfies $d(T_i, T_j) \geq Safe\text{-}CSR_{physical}$.

So for any link l_j in $\mathcal{S}^{CS}$, we have $d(T_i, T_j) \geq Safe\text{-}CSR_{physical}$. □

Let us use Fig. 5.6 again to show how IPCS can implement the safe carrier-sensing range successfully. We set the carrier-sensing power threshold P_{th} as in (5.14). We will show that the location requirement of the third link under IPCS is the same as indicated by the safe carrier-sensing range (location l_3' in Fig. 5.6).

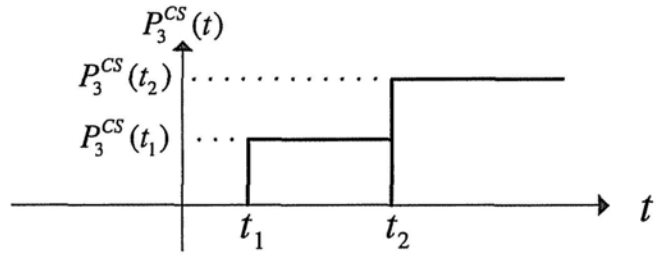

Figure 5.7: The power sensed by transmitter T_3' as a function of time

The transmitter of the third link will only initiate its transmission when it senses the channel to be idle. Its carrier-sensed power is shown in Fig. 5.7. Without loss of generality, suppose that link l_1 starts transmission before l_2. The third transmitter detects two increments in its carrier-sensed power at time instances t_1 and t_2 which are due to the transmissions of T_1 and T_2, respectively. In the IPCS mechanism, the third transmitter will believe that the channel is idle (i.e., it can start a new transmission) if the following is true:

$$\begin{cases} \Delta P_3^{CS}(t_1) = P_t G_0 d(T_3', T_1)^{-\alpha} \leq P_{th}, \\ \Delta P_3^{CS}(t_2) = P_t G_0 d(T_3', T_2)^{-\alpha} \leq P_{th}. \end{cases} \tag{5.16}$$

Substituting P_{th} in (5.14) to (5.16), we find that the requirements in (5.16) are equivalent to the following distance requirements:

$$\begin{cases} d(T_3', T_1) \geq Safe\text{-}CSR_{physical}, \\ d(T_3', T_2) \geq Safe\text{-}CSR_{physical}. \end{cases}$$

So the third link can be located at the position of l_3', as shown in Fig. 5.6, instead of far away at the location of l_3 as in the conventional carrier-sensing mechanism.

Compared with the conventional carrier-sensing mechanism, the advantages of IPCS are

1. IPCS is a pairwise carrier-sensing mechanism. In the IPCS mechanism, the power from each and every concurrent link is checked individually. This is equivalent to checking the separation between every pair of concurrent transmission links With IPCS, all the analyses based on the concept of a carrier-sensing range remain valid

2. IPCS improves spatial reuse and network throughput. In the conventional carrier-sensing mechanism, the link separation requirement in-

creases as the number of concurrent links increases. In IPCS, however, the link separation requirement remains the same. Furthermore, because IPCS is a pairwise mechanism, the order of the transmissions of links will not affect the spatial reuse.

5.5 Simulations Results

We perform simulations to evaluate the relative performance of IPCS and conventional Carrier Sensing (CS). In our simulations, the nodes are located within in a square area of $300m \times 300m$. The locations of the transmitters are generated according to a Poisson point process. The length of a link is uniformly distributed between 10 and 20 meters. More specifically, the receiver associated with a transmitter is randomly located between the two concentric circles of radii $10m$ and $20m$ centered on the transmitter. We study the system performance under different link densities by varying the number of links in the square from 1 to 200 in our simulations.

The simulations are carried out based on the 802.11b protocol. The carrier frequency is $2.4GHz$. The reference channel gain G_0 at the reference distance $d_0 = 1m$ and the carrier frequency of $2.4GHz$ is $-24.9dB$ [93]. The common physical layer link rate is $11Mbps$. The packet size is 1460 Bytes. The minimum and maximum backoff window $CW_{\min}$ and $CW_{\max}$ are 31 and 1023, respectively. The slot time is $20\mu s$. The SIFS and DIFS are $10\mu s$ and $50\mu s$, respectively. The transmit power P_t is set as $100mW$. The noise power N is assumed to be 0. The path-loss exponent α is 4, the SINR requirement γ_0 is 20, and the corresponding $Safe\text{-}CSR_{physical}$ equals $117.6m$ based on (5.6). That is, the carrier-sensing power threshold $P_{th} = P_t G_0 \left(Safe\text{-}CSR_{physical}\right)^{-\alpha} = 1.69 \times 10^{-9} mW$.

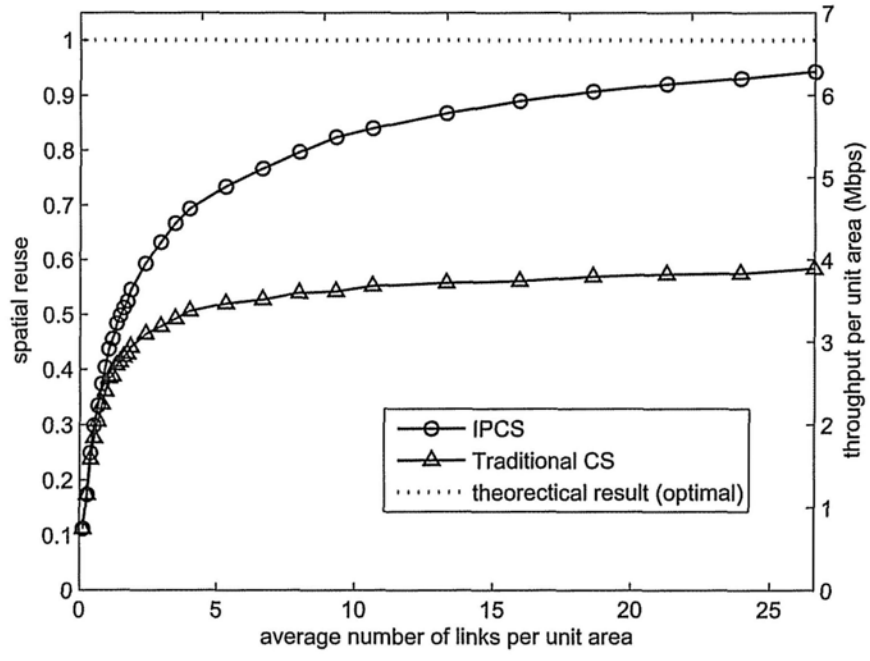

Figure 5.8: Spatial reuse and network throughput under IPCS and the conventional CS mechanisms

In Fig. 5.8, we plot spatial reuse and network throughput under IPCS and the conventional CS mechanisms. Simulation results show that network throughput is proportional to spatial reuse. So we plot these two results in the same figure. We define a "unit area" as the "consumed area" of each "active" transmitter under the tightest packing. Given $Safe\text{-}CSR_{physical} = 117.6m$, according to the carrier-sensing range analysis, the "unit area" is $\frac{\sqrt{3}}{2} Safe\text{-}CSR^2_{physical} = 1.197 \times 10^4 m^2$. The x-axis is the average number of links (i.e., all links, including active and inactive links) per unit area as we vary the total

number of links in the whole square. That is, the x-axis corresponds to the link density of the network. The left y-axis is the spatial reuse, or the average "active" link density in the network. The maximum value of the spatial reuse is 1, which is shown as a dashed line in Fig. 5.8. The right y-axis is the throughput per unit area.

It is clear from Fig. 5.8 that IPCS outperforms the conventional CS. The improvement becomes more significant when the network becomes denser. At the densest point in the figure, spatial reuses under IPCS and conventional CS are 0.9424 and 0.5834, respectively. The network throughputs per unit area are $6.66Mbps$ and $4.08Mbps$, respectively. Using conventional CS as the base line, the IPCS improves spatial reuse and network throughput by more than 60%.

Under the conventional CS, in order to make sure the cumulative detected power is no larger than the power threshold P_{th}, the packing of concurrent transmission links will become more and more sparse as additional number of links attempt to transmit. Under IPCS, this does not occur. As a result, the improvement in spatial reuse is more significant as the network becomes denser.

We also find that when the network becomes denser and denser, spatial reuse under IPCS becomes very close to the theoretical maximum result. The small gap is likely due to the fact that a link which could be active concurrently under IPCS does not exist in the given topology. The probability of this happening decreases as the network becomes denser.

5.6 Summary

In this chapter, we derive a threshold on the safe carrier-sensing range that is sufficient to prevent hidden-node collisions under the physical interference model. We show that the safe carrier-sensing range required under the physical interference model is larger than that required under the protocol interference model by a constant multiplicative factor.

We propose a novel carrier-sensing mechanism called Incremental-Power Carrier-Sensing (IPCS) that can realize the safe carrier-sensing range concept in a simple way. The IPCS checks every increment in the detected power so that it can separate the detected power of every concurrent transmitter, and then maps the power profile to the required distance information. Our simulation results show that IPCS can boost spatial reuse and network throughput by more than 60% relative to the conventional carrier-sensing mechanism in the current 802.11 protocol.

Chapter 6

Conclusions and Future Work

6.1 Conclusions

Scheduling is a key research issue in wireless networks and has attracted research attentions for more than 10 years. Most works in this area adopted the protocol interference model to model interference, i.e., the interferences among wireless links are modeled to be pairwise relationships. The practical cumulative nature of the interference power is thus largely missing. In this thesis, we concentrate on the wireless scheduling problem under the *physical interference model*. Under the physical interference model, a receiver decodes its signal successfully if the received SINR is above a certain threshold. Here, the interference is the sum of the powers received from all the concurrent transmitters at the receiver other than its own transmitter. The most difficult part of the scheduling algorithm design under the physical interference model is how to deal with the cumulative interference power. If power control is further allowed such that each transmitter can choose the most appropriate transmit power, the problem becomes even harder.

This thesis covers complexity analysis and algorithm designs (both central-

ized and distributed) for the wireless scheduling problem under the physical interference model. We start by proving that the power controlled scheduling *with* consecutive transmission constraint under the physical interference model is NP-complete. The key idea of the proof is to construct a network in which any two links can be active simultaneously; but any three links can not be active simultaneously even with power control. Then we show that a known NP-complete problem, the Partition Problem, can be reduced to the power controlled consecutive scheduling problem in polynomial time. To the best of our knowledge, this is the first NP-completeness proof for the power controlled scheduling problem with consecutive transmission constraint.

The centralized scheduling algorithms for the power-controlled scheduling proposed in this thesis cover both optimal algorithm and approximation algorithm. In Chapter 3, we propose a column generation algorithm that finds the optimal schedules and transmit powers for the power controlled scheduling problem under the physical interference model. We further consider the realistic case where the number of time slots allocated to a link should be an integer. Building upon the column generation method, we propose the branch-and-price method which can find the optimal integer solution. By simplifying the pricing problem and with a new branching rule, we significantly improve the efficiency of both the column generation and the branch-and-price methods. We find that for modest-size networks (i.e., less than 30 links), the column generation and the branch-and-price methods are computationally efficient. However, for large-size networks, finding optimal schedules and power allocations consumes extraordinary large amounts of time.

In Chapter 4, we propose a centralized approximation algorithm, called the Guaranteed and Greedy Scheduling (GGS) algorithm, to solve the power-controlled scheduling problem with the consecutive transmission constraint.

GGS is a polynomial time algorithm that has a provable upper bound for the approximation ratio relative to the optimal solution. The key to achieve this approximation ratio is to find the upper bound for the maximum number of links that can be active simultaneously in a given area with power control. GGS can easily be modified to solve the power-controlled scheduling problem without the consecutive transmission constraint. The proved upperbound for the approximation ratio remains valid. To the best of our knowledge, the GGS algorithm proposed in this thesis is the first polynomial time algorithm with a provable approximation ratio for the power-controlled scheduling *with and without* consecutive transmission constraints.

We move to the distributed scheduling algorithm design in Chapter 5. We establish a rigorous conceptual framework in CSMA networks such that the transmissions are interference-safe (or hidden-node free) under the physical interference model. Specifically, we derive a tight safe carrier-sensing range that guarantees the transmissions are interference-safe under the physical interference model. We find that the concept of a safe carrier-sensing range, although amenable to elegant analytical results, is inherently not compatible with the conventional power-threshold carrier-sensing mechanism (e.g., that currently used in IEEE 802.11). We solve this implementation issue by proposing a novel carrier-sensing mechanism, called Incremental-Power Carrier-Sensing (IPCS), which can realize the safe carrier-sensing range concept in a simple way Instead of monitoring the absolute detected power, the IPCS mechanism monitors every increment in the detected power. This means that IPCS can separate the detected power of every concurrent transmitter, and map the power profile to the required distance information. Our extensive simulation results indicate that IPCS can boost spatial reuse and network throughput by more than 60% relative to the conventional carrier-

sensing mechanism. The IPCS mechanism proposed in this thesis also fills the gap between the concept of carrier sensing range, which has been widely used in the theoretical studies of CSMA networks, and the real implementation in practice. Therefore, many prior theoretical works that assume the use of a carrier-sensing range, although are overly optimistic in current carrier sensing mechanism in 802.11, remain valid under the IPCS mechanism.

6.2 Future Work

The wireless scheduling under the physical interference model is becoming a research area of increasing interest recently, and there are many interesting topics for further investigation. Here we briefly discuss some possible directions:

- The rigorous complexity study of the power controlled scheduling without consecutive transmission constraint is still an open problem.
- The GGS algorithm proposed in this thesis serves as the first polynomial-time algorithm with bounded approximation ratio for the power controlled scheduling problem. However, the bound may be loose for some network cenarios. Finding an approximation algorithm with a tighter bound for the approximation ratio would be an interesting problem.
- In this thesis, the safe carrier sensing range which guarantees interference-safe transmissions in CSMA networks is common for all transmitters in the network. Allowing the carrier-sensing range to vary from transmitter to transmitter according to the local network topologies may improve the spatial reuse further.

- For the distributed scheduling design, we focus on the carrier sensing mechanism based on energy detection (i.e., the basic mode in 802.11). We have not considered virtual carrier sensing (i.e., the RTS/CTS mode in 802.11). Ensuring hidden-node free (or interference-safe) operation under virtual carrier sensing is rather complicated even under the protocol interference model (see [34] for details.) We would like to further study the problem of interference-safe transmissions for virtual carrier sensing under the physical interference model.

- Last but not least, the fading and time-varying effects of the wireless channel have not been fully addressed in this thesis. In this thesis, we have mainly focused on the log-distance path model in the physical interference model. If the channel does not change very fast, i.e., for the slow fading channel, the channel gains and the cross gains of the links in the network can be estimated. Therefore, the relative channel gain matrix can be obtained. We find that the centralized optimal algorithms proposed in Chapter 3, i.e., the column generation method and the branch-and-price method, can still be applied.

  However, the centralized approximation algorithm, the GGS, together with its approximation ratio is only valid for the distance based path loss model. When considering the fading and time-varying effects, it is difficult to provide deterministic performance bounds on the proposed heuristic algorithm as well as the optimal algorithm.

  Ref. [94] studied the minimum-frame-length scheduling under fast fading channel where the channel states change substantially within a frame, and cannot be tracked. It is found that although the instantaneous channel gain can not be obtained, the scheduler can still find the Pareto-

efficient sets of links by estimating the path-loss gain only.

For the distributed scheduling design in this thesis, we also assume the log-distance path model in the physical interference model. Although it is more realistic than the widely-used protocol interference model, the fading and time-varying features of wireless channel have not been considered. In the framework of interference-safe transmissions in CSMA networks studied in this thesis, the change in the detected power (increment or decrement) is only due to a start (or end) of another transmission in the network. Therefore, our IPCS can detect the activities of the other links in the network, and can eliminate the hidden-node collisions. When channel fading is considered, it will influence both the detected powers by transmitters and the interference powers at the receivers. No matter how low the power threshold is set in the carrier sensing mechanism, it cannot totally eliminate the hidden-node collisions. A first step to address the impact of the fading channel in the study of interference-safe transmissions in CSMA networks would be to estimate the probability of a hidden-node collision given that the power threshold in the carrier sensing mechanism is set to the safe power threshold under the simple path loss model. A further step would be to investigate the carrier-sensing power threshold in order that the probability of hidden-node collision is below a certain bound. These are all interesting yet challenging topics for further study.

Bibliography

[1] "Nice talking to you ... mobile phone use passes milestone," in *http://www.guardian.co.uk/technology/2009/mar/03/mobile-phones1*, March 2009.

[2] "Wireless LAN networking - white paper," in *http://www.usr.com/download/whitepapers/wireless-wp.pdf.*

[3] W. Kiess and M. Mauve, "A survey on real-world implementations of mobile ad-hoc networks," *Ad Hoc Networks*, vol. 5, pp. 324–339, Apr. 2007.

[4] R. Ramanathan and J. Redi., "A brief overview of ad hoc networks: challenges and directions," *IEEE Comm. Mag.*, vol. 40, no. 5, p. 20C22, May 2002.

[5] A. Ephremedis and T. Truong, "A distributed algorithm for efficient and interference free broadcasting in radio networks," in *Proc. IEEE INFOCOM*, 1988.

[6] S. Even, O. Goldreich, S. Moran, and P. Tong, "On the NP-completeness of certain network testing problems," *Networks*, vol. 14, pp. 1–24, 1984.

[7] B. N. Clark, C. J. Colbourn, and D. S. Johnson, "Unit disk graphs," *Discrete Mathematics*, vol. 86, p. 165C177, 1990.

[8] S. T. McCormick, "Optimal approximation of sparce hessians and its equivalence to a graph coloring problem," *Mathematics Programming*, vol. 26, no. 2, pp. 153–171, 1983.

[9] R. Ramaswami and K. K. Parhi, "Distributed scheduling of broadcasts in a radio network," in *Proc. IEEE INFOCOM*, 1989.

[10] E. Arikan, "Some complexity results about packet radio networks," *IEEE Trans. Infomation Theory*, vol. 30, no. 4, pp. 681–685, Jul. 1984.

[11] G. Sharma, R. R. Mazumdar, and N. B. Shroff, "Maximum weighted matching with interference constraints," in *4th Annual IEEE International Conference on Pervasive Computing and Commmunications Workshop*, Mar. 2006.

[12] G. Sharma, R. Mazumdar, and N. Shroff, "On the complexity of scheduling in wireless networks," in *Proc. ACM MOBICOM*, 2006.

[13] S. Ramanathan, *Scheduling Algorithms for Multi-hop Radio Networks.* PhD Dissertation, University of Delaware, 1992.

[14] M. Alicherry, R. Bathia, and L. Li, "Joint channel assignment and routing for throughput optimization in multi-radio wireless mesh networks," in *Proc. ACM MOBICOM*, 2005.

[15] G. Agnarsson and M. Halldorsson, "Coloring powers of planar graphs," in *Proceedings of the 11the Annual Symposium on Discrete Mathematics (SODA)*, Jan. 2000.

[16] H. Hunt, M. V. Marathe, V. Radhakrishnan, S. S. Ravi, D. J. Rosenkrantz, and R. E. Stearns, "NC-approximation schemes for NP-

and PSPACE -hard problems for geometric graphs," *Journal of Algorithms*, vol. 26, no. 2, pp. 238–274, 1998.

[17] R. Nelson and L. Kleinrock, "Spatial-tdma: a collision-free multihop channel access protocol," *IEEE Trans. Communications*, vol. 33, pp. 934–944, Sep. 1985.

[18] X. Ma, *Broadcast Scheduling Algorithms in Multi-hop Packet Radio Networks.* PhD Dissertation, University of Delaware, 2000.

[19] M. L. Huson and A. Sen, "Broadcast scheduling algorithms for radio networks," in *Proc. IEEE Mil. Comm. Conf.*, 1995.

[20] E. L. Lloyd and X. Ma, "Experimental results on broadcast scheduling in radio networks," in *Proceedings of Advanced Telecommunications/Information Distribution Research Program (ATIRP) Conference*, 1997.

[21] I. Chlamtac and S. S. Pinter, "Distributed nodes organization algorithm for channel access in a multihop dynamic radio network," *IEEE Trans. Computers*, vol. C-36, no. 6, pp. 728–737, 1987.

[22] C. R. Lin and J. S. Liu, "QoS routing in ad hoc wireless networks," *IEEE Jour. Select. Areas in Comm.*, vol. 17, pp. 1426–1438, Aug. 1999.

[23] S. Gandham, M. Dawande, and R. Prakash, "Link scheduling in sensor networks: Distributed edge coloring revisted," in *Proc. IEEE INFOCOM*, 2005.

[24] L. Tassiulas and A. Ephremides, "Jointly optimal routing and scheduling in packet radio networks," *IEEE Trans. Infomation Theory*, vol. 38, no. 1, pp. 165–168, Jan. 1992.

[25] C. Joo, X. Lin, and N. Shroff, "Understanding the capacity region of the greedy maximal scheduling algorithm in multi-hop wireless networks," in *Proc. IEEE INFOCOM*, 2008.

[26] M. Kodialam and T. Nandagopal, "Charaterizing achievable rates in multi-hop wireless newtorks: The joint routing and scheduling problem," in *Proc. ACM MOBICOM*, Sep. 2003.

[27] P. Chaporkar, K. Kar, and S. Sarkar, "Throughput and fairness guarantees through maximal scheduling in wireless networks," *IEEE Trans. Infomation Theory*, vol. 54, no. 2, pp. 572–594, Feb. 2008.

[28] A. Gupta, X. Lin, and R. Srikant, "Low-complexity distributed scheduling algorithms for wireless networks," *IEEE/ACM Trans. Networking.*, vol. 17, no. 6, p. 1846C1859, Dec. 2009.

[29] M. Leconte, J. Ni, and R. Srikant, "Improved bounds on the throughput efficiency of greedy maximal scheduling in wireless networks," in *Proc. ACM MOBIHOC*, 2009.

[30] I. Rhee, A. Warrier, J. Min, and L. Xu, "DRAND: distributed randomized TDMA scheduling for wireless ad-hoc networks," in *Proc. ACM MOBIHOC*, 2006.

[31] V. Kumar, M. Marathe, S. Parthasarathy, and A. Srinivasan, "End-to-end packet-scheduling in wireless ad-hoc networks," in *Proceedings of the 15th Symposium on Discrete Algorithms (SODA)*, 2004.

[32] L. B. Jiang and S. C. Liew, "Hidden-node removal and its application in cellular WiFi networks," *IEEE Trans. Veh. Technol.*, vol. 56, no. 5, pp. 2641 – 2654, Sep. 2007.

[33] P. C. Ng and S. C. Liew, "Throughput analysis of IEEE 802.11 multihop ad hoc networks," *IEEE/ACM Trans. Networking.*, vol. 15, no. 2, pp. 309–322, Apr. 2007.

[34] L. B. Jiang and S. C. Liew, "Improving throughput and fairness by reducing exposed and hidden nodes in 802.11 networks," *IEEE Trans. Mobile Computing*, vol. 7, no. 1, pp. 34–49, Jan. 2008.

[35] I. Rhee, A. Warrier, M. Aia, J. Min, and M. L. Sichitiu, "Z-MAC: A hybrid MAC for wireless sensor networks," *IEEE/ACM Trans. Networking.*, vol. 16, no. 3, p. 511C524, Jun. 2008.

[36] J. Gr'onkvist and A. Hansson, "Comparison between graph-based and interference-based STDMA scheduling," in *Proc. ACM MOBIHOC*, 2001.

[37] J. Gr'onkvist, *Interference-Based Scheduling in Spatial Reuse TDMA*. PhD thesis, Royal Institute of Technology, Stockholm, Sweden, 2005.

[38] A. Behzad and I. Rubin, "On the performance of graph-based scheduling algorithms for packet radio network," in *Proc. IEEE Glob. Telecom. Conf.*, 2003.

[39] T. Moscibroda, R. Wattenhofer, and Y. Weber, "Protocol design beyond graph-based models," in *Proc. ACM SIGCOMM Workshop on Hot Topics in Networks (HotNets)*, 2006.

[40] P. Gupta and P. Kumar, "The capacity of wireless networks," *IEEE Trans. Infomation Theory*, vol. 46, no. 2, pp. 388–404, Mar. 2000.

[41] S. A. Borbash and A. Ephremides, "Wireless link scheduling with power control and SINR constraints," *IEEE Trans. Infomation Theory*, vol. 52, no. 11, pp. 5106–5111, Nov. 2006.

[42] O. Goussevskaia, Y. Oswald, and R. Wattenhofer, "Complexity in geometric SINR," in *Proc. ACM MOBIHOC*, 2007.

[43] S. A. Borbash and A. Ephremides, "The feasibility of matchings in a wireless network," *IEEE Trans. Infomation Theory*, vol. 52, no. 6, pp. 2749–2755, Nov. 2006.

[44] J. Chen, K. Sivalingam, P. Agrawal, and R. Acharya, "Scheduling multimedia services in a low-power MAC for wireless and mobile ATM networks," *IEEE Trans. Multimedia*, vol. 1, no. 2, pp. 187–201, Jun. 1999.

[45] *IEEE Standard for Local and Metropolitan Area Networks—Part 16: Air Interface for Fixed Broadband Wireless Access Systems*, IEEE Std. 802.16-2004, Oct. 2004.

[46] T. S. Rappaport, *Wireless Communications: Principles and practice*, 2nd ed. Prentice Hall PTR, 2002.

[47] T. Moscibroda and R. Wattenhofer, "The complexity of connectivity in wireless networks," in *Proc. IEEE INFOCOM*, 2005.

[48] T. Moscibroda, Y. A. Oswald, and R. Wattenhofer, "How optimal are wireless scheduling protocols?" in *Proc. IEEE INFOCOM*, Anchorage, Alaska, USA, May 2007.

[49] S. A. Grandhi, R. Vijayan, D. J. Goodman, and J. Zander, "Centralized power control in cellular radio systems," *IEEE Trans. Veh. Technol.*, vol. 42, no. 6, pp. 466–468, Nov. 1993.

[50] R. A. Horn and C. R. Johnson, *Matrix Analysis.* New York: Cambridge Univ. Press, 1991.

[51] D. Mitra, "An asynchronous distributed algorithm for power control in cellular radio systems," in *Proc. 4th WINLAB Workshop*, Rutgers University, New Brunswick, NJ, 1993.

[52] N. Bambos, C. Chen, and G. Pottie, "Channel access algorithms with active link protection for wireless communication networks with power control," *IEEE/ACM Trans. Networking.*, vol. 8, no. 5, pp. 583–597, Oct. 2000.

[53] M. R. Garey and D. S. Johnson, *Computers and Intractability, A Guide to the Theory of NP-Completeness.* San Francisco, CA: Freeman, 1979.

[54] M. Johansson and L. Xiao, "Cross-layer optimization of wireless networks using nonlinear column generation," *IEEE Trans. Wireless Commun.*, vol. 5, no. 2, pp. 435–445, Feb. 2006.

[55] A. Capone and G. Carello, "Scheduling optimization in wireless mesh networks with power control and rate adaptation," in *Proc. IEEE SECON*, 2006.

[56] S. Kompella, J. E. Wieselthier, and A. Ephremides, "Revisiting the optimal scheduling problem," in *Proc. Conference on Information Sciences and Systems (CISS)*, Mar. 2008.

[57] J. Zander, "Performance of optimum transmitter power control in cellular radio systems," *IEEE Trans. Veh. Technol.*, vol. 41, no. 1, pp. 57–62, Nov. 1992.

[58] A. Behzad and I. Rubin, "Optimum integrated link scheduling and power control for multihop wireless networks," *IEEE Trans. Veh. Technol.*, vol. 56, no. 1, pp. 194–205, Jan. 2007.

[59] M. E. Lubbecke and J. Desrosiers, "Selected topics in column generation," *Operations Research*, vol. 53, no. 6, 2005.

[60] D. Bertsimas and J. Tsitsiklis, *Introduction to Linear Optimization.* Athena Scientific, 1997.

[61] C. Barnhart, E. L. Johnson, G. L. Nemhauser, M. W. Savelsbergh, and P. H. Vance, "Branch-and-price: Column generation for solving huge integer programs," *Operations Research*, vol. 46, pp. 316–329, 1998.

[62] J. Löfberg, "YALMIP : A toolbox for modeling and optimization in MATLAB," in *Proceedings of the CACSD Conference*, Taipei, Taiwan, 2004. [Online]. Available: http://control.ee.ethz.ch/~joloef/yalmip.php

[63] G. Brar, D. M. Blough, and P. Santi, "Computationally efficient scheduling with the physical interference model for throughput improvement in wireless mesh networks," in *Proc. ACM MOBICOM*, 2006.

[64] D. Chafekar, V. Kumar, M. Marathe, S. Parthasarathy, and A. Srinivasan, "Approximation algorithms for computing capacity of wireless networks with SINR constraints," in *Proc. IEEE INFOCOM*, 2008.

[65] T. Elbatt and A. Ephremides, "Joint scheduling and power control for wireless ad hoc networks," *IEEE Trans. Wireless Commun.*, vol. 3, pp. 74–85, Jan. 2004.

[66] A. K. Das, R. J. Marks, P. Arabshahi, and A. Gray, "Power controlled minimum frame length scheduling in TDMA wireless networks with sectored antennas," in *Proc. IEEE INFOCOM*, 2005.

[67] J. Tang, G. L. Xue, C. Chandler, and W. Zhang, "Link scheduling with power control for throughput enhancement in multihop wireless networks," *IEEE Trans. Veh. Technol.*, vol. 55, no. 3, pp. 733–742, May 2006.

[68] R. L. Cruz and A. V. Santhanam, "Optimal routing, link scheduling and power control in multi-hop wireless networks," in *Proc. IEEE INFOCOM*, 2003.

[69] V. V. Vazirani, *Approximation Algorithms.* Springer, 2003.

[70] D. S. Hochbaum, *Approximation Algorithm for NP-hard problems.* PWS, Boston, 1997.

[71] N. Oler, "A finite packing problem," *Canad. Math. Bull.*, vol. 4, no. 2, May 1961.

[72] T. Moscibroda, R. Wattenhofer, and A. Zollinger, "Topology control meets SINR: The scheduling complexity of arbitrary topologies," in *Proc. ACM MOBIHOC*, 2006.

[73] B. Hajek and G. Sasaki, "Link scheduling in polynomial time," *IEEE Trans. Infomation Theory*, vol. 34, no. 5, pp. 910–917, Sep. 1988.

[74] K. Jain, J. Padhye, V. Padmanabhan, and L. Qiu, "Impact of interference on multi-hop wireless network performance," in *Proc. ACM MOBICOM*, 2003.

[75] W. Wang, Y. Wang, X. Y. Li, W. Z. Song, and O. Frieder, "Efficient interference-aware TDMA link scheduling for static wireless networks," in *Proc. ACM MOBICOM*, 2006.

[76] A. Behzad, I. Rubin, and P. Chakravarty, "Optimum integrated link scheduling and power control for ad hoc wireless networks," in *Proc. IEEE WiMob*, Aug. 2005.

[77] U. C. Kozat, I. Koutsopoulos, and L. Tassiulas, "Cross-layer design for power efficiency and QoS provisioning in multi-hop wireless networks," *IEEE Trans. Wireless Commun.*, vol. 5, no. 11, pp. 3306–3315, Nov. 2006.

[78] A. Ephremedis and T. Truong, "Traffic controlled spatial reuse TDMA in multi-hop radio networks," in *Proc. Int'l. Symp. on Personal, Indoor, and Mobile Radio Communications*, 1988.

[79] J. N. J. Gronkvist and D. Yuan, "Throughput of optimal spatial reuse TDMA for wireless ad-hoc networks," in *Proc. IEEE Veh. Technol. Conf.*, 2004.

[80] L. Xiao, M. Johansson, and S. Boyd, "Simultaneous routing and resource allocation via dual decomposition," *IEEE Trans. Communications*, vol. 52, no. 7, pp. 1136–1144, July 2004.

[81] X. Lin and N. B. Shroff, "The impact of imperfect scheduling on cross-layer rate control in multi-hop wireless networks," in *Proc. IEEE INFOCOM*, Mar. 2005.

[82] K. Wang, C. Chiasserini, R. Rao, and J. Proakis, "A joint solution to scheduling and power control for multicasting in wireless ad hoc networks," *EURASIP Journal on Applied Signal Processing*, 2005.

[83] X. Lin, N. B. Shroff, and R. Srikant, "A tutorial on cross-layer optimization in wireless networks," *IEEE Jour. Select. Areas in Comm.*, vol. 24, no. 8, p. 1452C1463, Aug. 2006.

[84] D. Chafekar, V. Kumar, M. Marathe, S. Parthasarathy, and A. Srinivasan, "Cross-layer latency minimization in wireless networks with SINR constraints," in *Proc. ACM MOBIHOC*, 2007.

[85] K. Xu, M. Gerla, and S. Bae, "How effective is the IEEE 802.11 RTS/CTS handshake in ad hoc networks?" in *Proc. IEEE Glob. Telecom. Conf.*, Nov. 2002.

[86] S. Xu and T. Saadawi, "Does the IEEE 802.11 MAC protocol work well in multihop wireless ad hoc networks?" *IEEE Comm. Mag.*, vol. 39, no. 6, pp. 130–137, Jun. 2001.

[87] A. Vasan, R. Ramjee, and T. Woo, "ECHOS–enhanced capacity 802.11 hotspots," in *Proc. IEEE INFOCOM*, Mar 2005.

[88] C. K. Chau, M. Chen, and S. C. Liew, "Capacity of large-scale CSMA wireless networks," in *Proc. ACM MOBICOM*, 2009.

[89] T. S. Kim, H. Lim, and J. C. Hou, "Improving spatial reuse through tuning transmit power, carrier sense threshold, and data rate in multihop wireless networks," in *Proc. ACM MOBICOM*, 2006.

[90] T. Y. Lin and J. C. Hou, "Interplay of spatial reuse and SINR-determined data rates in CSMA/CA-based, multi-hop, multi-rate wireless networks," in *Proc. IEEE INFOCOM*, 2007.

[91] [Online]. Available: http://huizen.deds.nl/~pa0hoo/helix_wifi/linkbudgetcalc/wlan_budgetcalc.html

[92] K. Jamieson, B. Hull, A. Miu, and H. Balakrishnan, "Understanding the real-world performance of carrier sense," in *ACM SIGCOMM Workshops*, 2005.

[93] M. S. Gast, *802.11 Wireless Networks: The Definitive Guide*, 2nd ed. O'Reilly Media Inc., 2005.

[94] J. Zhang, S. C. Liew, and L. Fu, "On fast optimal STDMA scheduling over fading wireless channels," in *Proc. IEEE INFOCOM*, 2009.